RECOVERY OF RARE EARTH ELEMENTS FROM FLUORESCENT LAMP PHOSPHORS

by
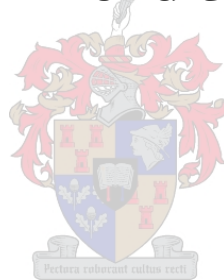
Levie Bumhira

Thesis presented in partial fulfilment
of the requirements for the Degree

of

MASTER OF ENGINEERING

(EXTRACTIVE METALLURGICAL ENGINEERING)

in the Faculty of Engineering
at Stellenbosch University

Supervisor

Prof C. Dorfling

Co-Supervisor

Prof G. Akdogan

April 2019

Declaration

By submitting this thesis electronically, I declare that the entirety of the work contained therein is my own, original work, that I am the sole author thereof (save to the extent explicitly otherwise stated), that reproduction and publication thereof by Stellenbosch University will not infringe any third party rights and that I have not previously in its entirety or in part submitted it for obtaining any qualification.

Date: April 2019

i

Plagiarism Declaration

1. Plagiarism is the use of ideas, material and other intellectual property of another's work and to present is as my own.

2. I agree that plagiarism is a punishable offence because it constitutes theft.

3. I also understand that direct translations are plagiarism.

4. Accordingly, all quotations and contributions from any source whatsoever (including the internet) have been cited fully. I understand that the reproduction of text without quotation marks (even when the source is cited) is plagiarism.

5. I declare that the work contained in this assignment, except where otherwise stated, is my original work and that I have not previously (in its entirety or in part) submitted it for grading in this module/assignment or another module/assignment.

Student number: 21519552

Initials and surname: L Bumhira

Signature: ………………….

Date: 15 February 2019

ii

Abstract

In recent decades, the production and usage of fluorescent lamps has rapidly increased. This is attributed to several benefits they offer in comparison to incandescent bulbs. The lamps are known to have lower energy consumption (about 75 % less than incandescent bulbs) and longer life expectancy. The rapid growth in production and usage has resulted in large volumes of waste fluorescent lamps being discarded every year. Recycling of spent fluorescent lamps offers a number of economic benefits apart from the well-known environmental benefits.

The primary objective of this study is to identify a viable process for rare earths recovery from end of life fluorescent powders in the South African context. The study focused on the use of hydrometallurgical unit operations in the recovery of four rare earth metals namely yttrium (Y), europium (Eu), cerium (Ce) and terbium (Tb). A two-staged leaching process was employed followed by solvent extraction to recover the metals from solution.

Leaching tests indicated that the red phosphor component (Y_2O_3:Eu^{3+}) could be easily dissolved into solution during the first step of acid leaching. Over 98 % Y and 89 % Eu recoveries were achieved using sulphuric acid as the lixiviant. Ce and Tb were not leached at this stage. The effect of ultrasound and alkali fusion on Tb and Ce leaching was then investigated. Alkali fusion followed by acid leaching produced the best recoveries with Ce and Tb recoveries exceeding 96 % and 99 % respectively. Poor recoveries of the rare earths (<10 %) were obtained using ultrasound assisted digestion.

Solvent extraction tests showed that DEHPA could be used to recover rare earths from aqueous solutions obtained after the first and second leaching stages. The results showed that about 11 countercurrent equilibrium stages are required to achieve more than 95 % yttrium extraction at pH -0.25, O/A ratio of 1 and a temperature of 25 ℃. Eu and residual Y could only be extracted after pH adjustment to 0.5 using 5 M sodium hydroxide. More than 92 % Eu and 99 % Y extraction was achieved using an O/A ratio of 1.5 and 1 M extractant concentration. A multiple stage stripping process can then be used to recover more than 95 % of the rare earths from the organic phase prior to precipitation and calcination. Ce and Tb solvent extraction results showed that all the targeted rare earths could only be recovered as a mixed product at this stage. A mixed rare earth product was produced using 1 M DEHPA, a pH of 0.5, O/A ratio of 1 and a temperature of 25 °C. Complete extraction of Y and Eu was

assumed at these conditions since both rare earths could not be detected in the remaining aqueous solution. More than 95 % Ce and 98 % Tb were extracted in a single stage solvent extraction process. The rare earths can undergo stripping using 5 M sulphuric acid prior to precipitation and calcination to recover the metals as rare earth oxides.

Opsomming

In onlangse dekades het die produksie en gebruik van fluoresseerlampe spoedig verhoog. Dit word toegeskryf aan die verskeie voordele wat dit inhou in vergelyking met gloeilampe. Die lampe is bekend dat dit laer energie verbruik (omtrent 75 % minder as gloeilampe) en 'n langer lewensduur het. Die spoedige groei in produksie en gebruik het tot groot volumes fluoresseerlampafval gelei, wat elke jaar weggegooi word. Herwinning van gebruikte fluoresseeerlampe bied 'n aantal ekonomiese voordele, bo en behalwe die welbekende omgewingsvoordele.

Die hoofdoel van hierdie studie was om 'n lewensvatbare proses vir seldsame aardelementherwinning uit einde van lewe fluoresseerpoeiers in die Suid-Afrikaanse konteks te identifiseer. Die studie het gefokus op die gebruik van hidrometallurgiese eenheid bedrywighede in die herwinning van vier seldsame aardelemente naamlik yttrium (Y), europium (Eu), seriuim (Ce) en terbium (Tb). 'n Twee-fase logingsproses is gebruik gevolg deur oplossingekstraksie om die metale uit die oplossing te herwin.

Logingstoetse het aangedui dat die rooi fosfor komponent ($Y_2O_3^-Eu^{3+}$) maklik in die oplossing kon oplos gedurende die eerste fase van suurloging. Meer as 98 % Y en 89 % Eu herwinning is bereik deur swaelsuur as logingsmiddel te gebruik. Ce en Tb is nie geloog in hierdie fase nie. Die effek van ultraklank en loogsoutsmelting op Tb- en Ce-loging is toe ondersoek. loogsoutsmelting gevolg deur suurloging het die beste herwinning opgelewer met Ce- en Tb-herwinning wat 96 % en 99 %, onderskeidelik, oorskry. Swak herwinning van die seldsame aardelemente (<10 %) is verkry deur ultraklank ondersteunde vertering te gebruik.

Oplossingekstraksietoetse het gewys dat DEHPA gebruik kan word om seldsame aardelemente uit waterige oplossings te herwin na die eerste en tweede loogfases. Die resultate het gewys dat omtrent 11 teenstroomewewigfases nodig is om meer as 95 % yttriumekstraksie by pH -0.25, O/A verhouding van 1 en 'n temperatuur van 25 °C, te behaal. Eu en residuele Y kon slegs geëkstraheer word na 'n pH aanpassing na 0.5 deur 5 M natriumhidroksied te gebruik. Meer as 92 % Eu en 99 % Y ekstraksie is bereik deur O/A verhouding van 1.5 en 1 M ekstraheermiddelkonsentrasie. 'n Meervoudige-fase stropingproses kan dan gebruik word om meer as 95 % van die seldsame aardelemente uit die organiese fase voor presipitasie en kalsinering te herwin. Ce en Tb oplossingekstraksieresultate het gewys dat al die geteikende seldsame aardelemente slegs herwin kon word as 'n gemengde produk in hierdie fase. 'n Gemengde seldsame aardelement produk is vervaardig deur 1 M DEHPA, 'n pH van 0.5, O/A

verhouding van 1 en 'n temperatuur van 25 °C te gebruik. Algehele ekstraksie van Y en Eu is aangeneem by hierdie toestande aangesien beide seldsame aardelemente nie in die oorblywende waterige oplossing waargeneem kon word nie. Meer as 95 % Ce en 98 % Tb is geëkstraheer in 'n enkel-fase oplossingekstraksieproses. Die seldsame aardelemente kan stroping ondergaan deur 5 M swaelsuur te gebruik voor presipitasie en kalsinering om die metale as seldsame aardoksiedes te herwin.

Acknowledgements

I would like to take this opportunity to express my sincere gratitude to my supervisors Prof. Christie Dorfling and Prof. Guven Akdogan for their guidance, support and patience throughout the course of this project.

I would also like to thank the technical and administrative staff in the Department of Process Engineering for their contribution towards the completion of this project.

Gratitude also goes to the Council for Scientific and Industrial Research (CSIR) for their financial support.

I wish also to thank my mum Mollen, sister Lyn and brother Sympathy for their undivided support, inspiration, and encouragement.

Finally, I would like to thank the Almighty who granted me the gift of life and strength to complete this project.

Table of Contents

List of Tables

List of Figures

xviii

Nomenclature

REEs	Rare earth elements
XRD	X-ray diffraction
DHA	Dual Dissolution by Hydrochloric acid
ICP-OES	Inductively coupled plasma optical emission spectrometry
AAS	Atomic absorption spectroscopy
CFLs	Compact fluorescent lamps
PLS	Pregnant leach solution
ETP	Effluent treatment plant

1. Introduction

1.1 Background and Problem Statement

Recycling is an integral part in circular economies. The growing demand for raw materials by manufacturing industries is an issue that requires immediate attention. Rare earth elements (REEs) have become more significant in the evolution to a green, low-carbon economy. The growing popularity of compact fluorescent lamps, hybrid cars and wind turbines has caused an increased demand and price of REEs. Rare earth containing deposits seldom exist in concentrated forms making their exploitation challenging (Gupta and Krishnamurthy, 2005). The concentrations are commercially non-viable resulting in a declaration by the European Commission in 2010 and 2014 that they are the most critical raw materials with the greatest supply risk among other raw materials (European Commission, 2010, 2014).

Kilbourn (1994) reported that rare earth deposits contain radioactive uranium and thorium causing radiotoxicity challenges during processing. Furthermore, REEs are known to exhibit similar chemical properties making separation and refinement difficult. REEs processing is regularly associated with large amounts of effluent from several hydrometallurgical separation steps desired to attain rare earths of high purity (Tunsu, 2016). Recycling of spent products can have a positive impact on the above-mentioned problems by offering both environmental and economic benefits.Spent permanent magnets in hard drive disks (HDDs), nickel-metal hydride (NiMH) batteries and fluorescent lamps are relatively abundant nowadays and have high REE content. As a result, these products are most often targeted for recycling (Tunsu, 2016).

Fluorescent lighting mainly relies on six REEs: yttrium, lanthanum, europium, cerium, terbium, and gadolinium. Fluorescent lamps boast higher luminous intensity and better colour purity compared to incandescent bulbs. The production of fluorescent lamps has gradually increased in recent decades hence recovery of rare earths from waste lamp powders has become an issue of utmost importance. A standard 40 W fluorescent lamp constitutes 4 to 6 g of phosphor powder representing almost 2 % of its total mass (Raposo, Windmoller and Junior, 2003). Zhang (2012) and Wang and Zheng (2010) stated that almost 4 800 million fluorescent lamps were discarded in the year 2011. By December 2011, the market price of REEs contained in the spent lamps exceeded 1 600 million dollars with reference to the

domestic market price of rare earths (Wu *et al.*, 2014). These figures have since increased due to increasing popularity of fluorescent lamps over the years. High demand for REEs, decrease in mineral ore reserves each year and geo-political factors have triggered an increased interest in recycling these metals from secondary sources. The development of efficient, environmentally friendly and fully integrated recycling routes is therefore a strategic necessity. Currently, South African fluorescent lamp recyclers focus only on dismantling and physical separation of the different components such as glass, phosphor powders and end caps but no processing capacity exists for value recovery from the phosphor powders. Hydrometallurgical processes such as leaching, liquid-liquid extraction and precipitation have been under investigation as possible recycling operations for REEs recovery. Despite the vast research in waste fluorescent powder recycling, commercial recycling of rare earths is still very low globally (Binnemans and Jones, 2014). A drastic development in spent fluorescent lamps recycling is a strategic need even more so in countries like South Africa having few rare earth deposits. This is only possible if sustainable, economical and effective fully combined recycling routes are developed.

1.2 Project Motivation

The driving forces for the project are grouped into three categories namely environmental, raw material supply, and economic benefits. Environmentally, recycling reduces the spreading of radioactive isotopes such as uranium and thorium during exploitation of REE ores. It also lessens landfill areas for mining tailings and disposal of spent fluorescent lamps. Another environmental benefit is the conservation of mineral deposits due to reduced mining. In terms of raw material supply, REEs can be recycled for similar or other uses in manufacturing industries. The concentrations of REE are higher in end-of-life lamp phosphors compared to most ore bodies hence raw material supply can also be boosted. Economically, recycling provides an additional supply of REE hence reduced raw materials prices. It also allows a country where there is no primary resources to produce some REE that would allow associated products to be manufactured.

1.3 Aim and Objectives

The aim of the project is to evaluate and compare different processes that could be used for REE recovery from waste phosphor powders present in spent fluorescent lamps, and to make a recommendation as to the most suitable process for the South African market.

The following research objectives are set:

- Perform a comprehensive literature review on the current best practices in phosphor powder recycling, specifically focusing on recovery of Y, Eu, Ce and Tb.

- Determine appropriate operating conditions for unit operations used in the recovery of REEs from end-of-life fluorescent lamps.

- Based on experimental work, propose a conceptual flowsheet and perform corresponding mass balances to evaluate metal recovery efficiency and effluent production.

1.4 Document Outline

Section 2 contains an overview of different processes that are used in the recovery of REEs from waste fluorescent phosphor powders. Results from previous studies are also described and these were used in determining the test parameters investigated experimentally. The experimental strategy, equipment, materials and procedure are described in section 3. Results discussion then follows in section 4 while recommendations and conclusions are given in section 5.Supplementary material is included in the Appendix section.

2. Literature Review

2.1 Introduction

In recent decades, management of end-of-life electronic waste products has become an issue of paramount importance. The increasing application of REEs has resulted in vast amounts of rare earths containing spent products. Amongst the rich rare earths containing spent products are waste fluorescent lamps. In previous decades, treatment of the spent fluorescent lamps mainly focused on hazardous mercury management (Jang, Hong and Park, 2005; Chang and Yen, 2006) and recycling of glass, copper, and aluminum parts (Rabah, 2004). However, recycling of waste phosphor is still very low and no effective way of recycling has been established (Yang *et al.*, 2013). Waste phosphor powders contain valuable REEs such as Y, Eu, Tb, Ce, La and Gd. These metals have various applications shown in Table 2.1.

Table 2.1: Some applications of REEs (adapted from: Haxel, Hedrick and Orris, 2002; Diana et al., 2011; USEPA, 2012)

Element	Applications
Yttrium	lamp phosphors, light emitting diodes, metal alloys, catalysts, spark plugs electrodes, lasers, temperature sensors, ceramics
Lanthanum	Automotive catalysts, carbon arc lamps , optical glasses, lamp phosphors, high quality lenses
Cerium	Phosphors, additive in glass and ceramics, cerium lasers, abrasives
Europium	Phosphors, lasers, nuclear reactors control rods, polishing powders
Gadolinium	Phosphors, glass additives, gadolinium yttrium garnets, alloys
Terbium	Phosphors, magnets, control systems

The production and usage of fluorescent lamps has greatly increased in recent decades. Fluorescent lamps offer several advantages compared to incandescent bulbs. The US Department of Energy (2010) reported that the lamps have up to ten times longer life expectancy compared to incandescent bulbs and use almost 75% less energy to give similar light output. Figure 2.1 shows a typical fluorescent lamp.

4
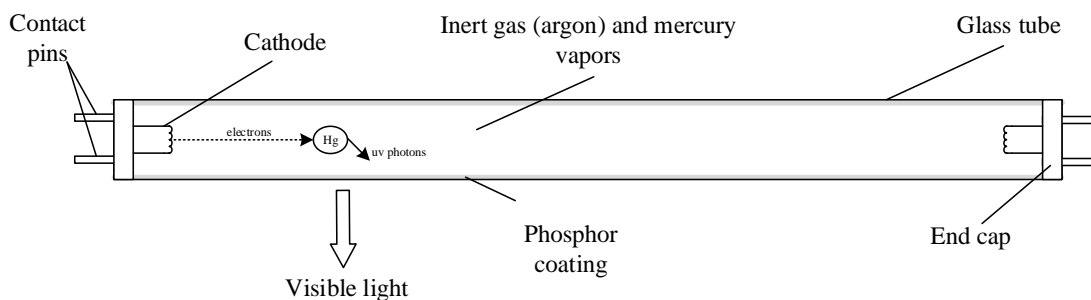
Figure 2.1: Typical fluorescent lamp (redrawn from (Tunsu, 2016))

The lamp consists of a glass tube, which can vary in size and shape. The glass tube is filled with an inert gas such as argon. A thin layer of phosphor powder which provides luminescence coats the interior of the glass tube. Mercury is also present in the glass tubes in elemental form. When the mercury atoms collide with electrons emitted by the cathode, invisible ultraviolet photons are produced. The photons are then absorbed by the phosphor powder thereby emitting visible light. End-of-life fluorescent lamps also contain alumina (Al_2O_3) and silica (SiO_2). SiO_2 is used in the barrier layer between the glass tube and the tricolour phosphor powder layer. The barrier layer shields the glass envelope from attack by mercury vapour thereby inhibiting mercury depletion. It also improves the efficiency of the lamp when it reflects back UV light passing to the glass layer through the phosphor layer (Binnemans *et al*., 2013). Regardless of vast research, commercial recycling of REEs from spent fluorescent lamps is quite low and therefore the development of sustainable and environmentally friendly recycling technologies is a necessity.

2.2 Composition of End-of-life Fluorescent Lamp Phosphor

Fluorescent lamps are often referred to tri-phosphors or tri-band lamps. This is because they contain the red, green and blue REE-containing phosphors. Tricolour phosphors are categorised into phosphate, aluminate, borate and silicate systems (Jüstel, Nikol and Ronda, 1998). Borate and silicate system are still under development while phosphate and aluminate systems are mostly in use either alone or mixed. The phosphate system is known to have poor stability under high voltage and poor colour rendering property (Wu *et al.*, 2014). This has given an edge to the aluminate system hence it has become the most widely used in the world. It offers the following advantages stated by Wu *et al.* (2014):

- high luminous efficiency
- anti-ultraviolet aging

5

- high intensity of ultraviolet irradiation
- Stability under high temperatures

Table 2.2 shows some of the existing REE based phosphors used in fluorescent lamps.

Table2.2: Some of the existing rare earth element based phosphors

Phosphor	Chemical Formula	Composition	Reference
Red	Y_2O_3:Eu^{3+} (YOX)*	55 % (mostly Y and about 4-10 % Eu)	(Jüstel, Nikol and Ronda, 1998; Wu *et al.*, 2014)
Blue	$BaMgAl_{10}O_{17}$:Eu^{2+} (BAM) $Ca_2B_5O_8Cl$:Eu^{2+} $BaZrSi_3O_9$:Eu^{2+} $(Sr,Ca,Ba)_5(PO_4)_3Cl$:Eu^{2+}	10 % (contains less than 5 % Eu)	(Cuif *et al.*, 2005; Wu *et al.*, 2014)
Green	$CeMgAl_{11}O_{19}$:Tb^{3+} (CAT) $(Ce,Gd,Tb)MgB_5O_{10}$ Y_2SiO_3:Ce^{3+},Tb^{3+} $LaPO_4$:Ce^{3+},Tb^{3+} (LAP)	35 % (contains approx. 10 % terbium)	(Ronda, Jüstel and Nikol, 1998; Song, Chang and Pecht, 2013; Wu *et al.*, 2014)

2.3 Recycling Processes Overview

A number of methods are employed in the recycling of spent fluorescent lamps. After collection, end-of-life fluorescent lamps are processed to recycle glass, metal (aluminium caps, electrodes, and filaments), plastics (insulators, caps), mercury and lamp powder. A typical recycling process is shown in Figure 2.2.

6
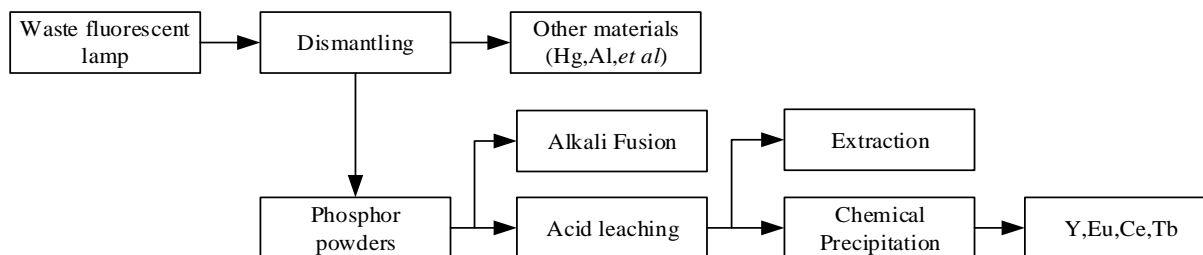
Figure 2.2: Typical recycling process flowsheet for spent fluorescent lamps (redrawn from (Wu et al., 2014)

The first step of the recycling process is dismantling. This is achieved by the end cut/air push method (Li, 2008). In this method, metal caps (aluminium) at the ends of the tube are cut off before the phosphor powders and mercury are collected by blowing air at high pressure in the tubes. Aluminium caps are usually crushed to recover metals whilst hazardous mercury is recovered when the blown gas passes through active carbon (Wu *et al.*, 2014). The clear advantage of the end cut/air push method is the reclamation of tricolour phosphors that do not contain fine glass. However, this method is not suitable for handling large numbers of spent lamps within a stipulated time and it is also not suitable for compact fluorescent lamps (CFLs) with nonlinear constructions.

Binnemans *et al.* (2013) reported that recycling of complex nonlinear shapes is more challenging than that of linear shapes. The spent lamps first undergo crushing and shredding before separation of phosphor powder, glass cullet, metallic constituents and hazardous mercury. Crushing is done either wet or dry. Glass fragments are separated from the phosphor by wet or dry sieving. The presence of very fine glass particles generated during crushing makes separation of clean phosphors impossible to achieve. After crushing and sieving, the product can consist of up to 50 wt% of glass fractions (Binnemans and Jones, 2014). This fraction dilutes the REE content hence lowering the intrinsic worth of the powders. Shredded glass particles also make the complete recycling of the phosphors more challenging since alkali fusion at high temperature transforms the glass fragments into soluble silicates which contaminate the feed solutions to downstream processes. After sorting, metallic fragments are taken for metal recycling while plastic fragments are burnt to recover heat. Uncontaminated glass can be recycled and used to produce other glass products. The remaining materials can be utilised as additives in construction materials. 99 % recycling of spent fluorescent lamps can be achieved using this technique (Wu *et al.*, 2014).

The second step mainly involves the recovery of REEs from the collected spent phosphors. This is achieved through a series of unit operations which involve acid digestion, alkali fusion, solvent extraction, precipitation and other hydrometallurgical processes. These processes are explained in detail in the next section.

2.3.1 Hydrometallurgical vs Pyrometallurgical Unit Operations

Rare earths recovery can be accomplished using either hydrometallurgical or pyrometallurgical unit operations. The rare earth content and the nature of stream to be treated defines the potential treatment method. Pyrometallurgy is most suitable for treatment of high-grade material whereas hydrometallurgy is most suitable for low-grade material. Pyrometallurgy is also energy intensive and is not suitable for use in the treatment of small amounts of material. It also results in extra costs on environmental treatment (Yoon *et al.*, 2014). Further processing using hydrometallurgy or electrolysis is required for products obtained pyrometallurgically to produce pure rare earths. Accumulation of rare earths in the slag phase after treatment of end-of-life products using electric arc furnaces is also a major drawback. This makes the economic recovery of the REEs more challenging (Binnemans *et al.*, 2013). Hydrometallurgical unit operations offer several advantages in the recovery and separation of individual rare earths from waste products as compared to Pyrometallurgy. As mentioned earlier, hydrometallurgical processes are suitable for treatment of low-grade material and chemically complex streams containing many contaminants (Tunsu, 2016). Wu *et al*. (2014) reported that recovery of metals from waste phosphors generally involves the following hydrometallurgical steps:

- Acid leaching which involves dissolution of rare earths into solution. Other unwanted constituents present in the material (impurities) can also go into solution.
- Recovery of REEs from solution using precipitation or solvent extraction.

2.4 Leaching

Leaching is a hydrometallurgical process that is widely used in the recovery of REEs from spent phosphors. Water, base, acid or salt solutions are commonly used leaching lixiviants or leaching agents. The reagent of choice is dependent on the solubility of the compound in which the targeted metals exist (Tunsu, 2016). The rate and extent of dissolution is dependent on factors such as temperature, extractant concentration, residence time, agitation rate and solid-to-liquid ratio.

Leaching kinetics are affected by soluble compounds distribution in the material, soluble compounds entrapment, possible adsorption in the matrix and slow rates of reaction between the soluble elements and the leaching agent (Rao, 2006). Fast kinetics are a necessity from an economical point of view. However, for processes such as selective leaching, slower kinetics are at times valuable. Leaching agent selection is of utmost importance since it does not only affect the hydrolysis process but also downstream processes. The nature of the leachate can affect downstream processes by limiting the choice of organic solvents in the case of solvent extraction.

2.4.1 Leaching of Y and Eu from Spent Fluorescent Lamps

Several researchers conducted studies to recover REEs from waste phosphors. In their studies, the dissolution effectiveness of several acids (HCl, H_2SO_4 and HNO_3) and alkalis (NaOH and NH_3) was investigated. De Michelis *et al.* (2011) reported that alkaline solutions such as ammonia are not suitable for rare earths leaching since they give poor recoveries (about 10% Y recovery). However, REEs in phosphor powders can be dissolved into solution by acid leaching (Li, 2010; De Michelis *et al.*, 2011). The chemical reactions for acid leaching can be written according to Equations 1 to 3.

Red phosphor:

$$Y_2O_3{:}Eu^{3+} + 6\,H^+ \;\leftrightarrow\; 2\,Y^{3+} + Eu^{3+} + 3\,H_2O \tag{1}$$

Blue phosphor:

$$BaMgAl_{10}O_{17}{:}Eu^{2+} + 34\,H^+ \;\leftrightarrow\; Ba^{2+} + Mg^{2+} + 10\,Al^{3+} + Eu^{2+} + 17\,H_2O \tag{2}$$

Green phosphor:

$$CeMgAl_{10}O_{17}{:}Tb^{3+} + 34\,H^+ \;\leftrightarrow\; Ce^{2+} + Mg^{2+} + 10\,Al^{3+} + Tb^{3+} + 17\,H_2O \tag{3}$$
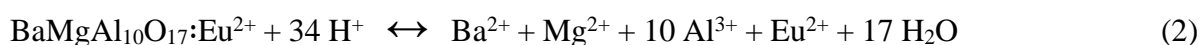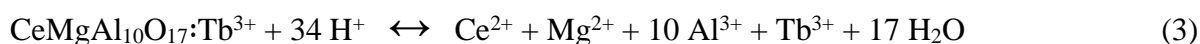
Inorganic acids also digest impurity metals in the stream such as Sr and Ca according to Equation 4.

$$(Sr,Ca)_{10}(PO4)_6(Cl,F)_2{:}Sb^{3+},Mn^{2+}+18H^+ \leftrightarrow 10(Sr,Ca)^{2+}+6H_3PO_4+2(Cl,F)^-+Sb^{3+}+Mn^{2+} \tag{4}$$
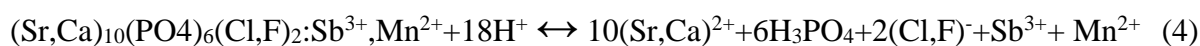
Inorganic acids are effective in the dissolution of Y and Eu present in the red phosphor powders. Y and Eu exist as oxides as shown in Table 2.2. These rare earth oxides are readily soluble in acidic solutions according to Equation 1 (Yang *et al.*, 2013). Inorganic acids are however not effective in direct dissolution of the green and blue emitting phosphors due to stable and complex chemical structures of these powders.

Takahashi *et al.* (2001) recommended H_2SO_4 as the preferred leaching agent in comparison to HCl and HNO_3. In their research, Y and Eu recoveries of 92 % and 98 % were obtained using 1.5 M H_2SO_4 at a temperature of 70 °C. They also found that Tb, Ce and La dissolution could only be achieved using high temperatures using concentrated H_2SO_4.

Leaching results obtained by Li (2010) showed that high rare earth recoveries can be obtained from phosphor sludge using H_2SO_4 compared to HCl and HNO_3. The author reported that leaching extent of REEs was improved by increasing temperature, acid concentration and agitation speed. Highest metal dissolution was obtained using 2 M H_2SO_4, a temperature of 100 °C and residence time 8 hours. Optimal recoveries for Y, Eu, Ce and Tb were 80.4 %, 82.2 %, 81.4 % and 80.0 % respectively.

Yang *et al.* (2013) investigated the effect of acid type on metal recovery. Their findings are shown in Table 2.3.

Table 2.3: Effect of leaching agent on percentage recovery (adapted from (Yang et al., 2013))

	Y	**Eu**	**Ca**
HNO_3	91.6 ± 1.7 %	85.7 ± 1.7 %	83.5 ± 1.7 %
HCl	93.3 ± 2.1 %	89.2 ± 1.8 %	85.1 ± 2.5 %
$H_2 SO_4$	98.4 ± 1.5 %	87.6 ± 1.3 %	37.1 ± 1.6 %

The three inorganic acids could readily dissolve Y and Eu into solution. H_2SO_4 gave the best recoveries for the targeted rare earths. It was also found that H_2SO_4 significantly suppressed the dissolution of Ca which is the main impurity. Yang *et al.* (2013) also investigated the effect of acid concentration, temperature and leaching time on REEs recovery. They found that REEs recoveries from phosphor powders increased with increase in acid concentration

and temperature. Optimal recoveries were found when operating at an acid concentration of 5 M, leaching temperature of 70 °C, residence time of 6 h and solid to liquid ratio of 5 % (w/v).Ce and Tb could not be leached under these conditions therefore were undetected in the leach solutions.

Experiments conducted by (Wang *et al.*, 2011) gave an overall recovery of 89.95 % for all the targeted REEs. 96.28 % Yttrium was recovered. The optimum leaching parameters were found to be a concentration of 4 M HCl solution, 100 g/L solid-liquid ratio, 600 rpm stir intensity, 60 ℃ reaction temperature, 4.4 g/L H_2O_2 and a reaction time of 60 minutes.

De Michelis *et al*. (2011) conducted leaching tests with NH_3, H_2SO_4, HNO_3 and HCl. Although HCl and H_2SO_4 gave almost similar recoveries, the latter significantly suppressed the dissolution of the main impurity calcium. $BaSO_4$ and $PbSO_4$ whose solubilities are very low also precipitate and this is beneficial since it acts as a preliminary purification process to remove impurities that would affect downstream processes. HNO_3 gave the best recoveries but toxic gases such as NO, NO_2 and N_2O were produced during the leaching. The acid was therefore excluded. Leaching with ammonia gave very poor recoveries. An acid concentration of 4 M, 20 % (w/v) S/L ratio and a temperature of 90 ℃ gave optimal recoveries. Yttrium recovery was found to be 85 %.

Rabah (2008) used pressure leaching to recover rare earths from spent phosphors. The lixiviant comprised a mixture of H_2SO_4 and HNO_3. Leaching was conducted for 4 hours in an autoclave at a temperature of 125 °C and pressure of 5 MPa. Y and Eu recovery were 96.4 % and 92.8 %, respectively. However, Ce and Tb recovery remained below 30 %.

Based on the results obtained by the different researchers, it was clear that alkaline solutions are not suitable for rare earths leaching. It is also clear that inorganic acids are effective in the dissolution of the red component of the waste phosphor (Y_2O_3:Eu) in a single stage leaching process. However, a single stage leaching process is not effective in the dissolution of the green and blue emitting phosphors. H_2SO_4 is the preferred lixiviant considering technique costs and environmental protection advantages over HCl and HNO_3. It also suppresses dissolution of impurities such as Ca, Ba, and Pb in the leach solution.

11

2.4.2 Leaching of Ce and Tb from End-of-Life Fluorescent Lamp Phosphors

2.4.2.1 Ultrasound Assisted Digestion

A number of studies recommended the use of ultrasound to recover REEs from spent fluorescent lamp phosphor powders and other recyclable materials (Tanaka, Zhang and Saito, 2002; Yang *et al.*, 2013; Ekberg *et al.*, 2016; Tunsu, 2016;). Ultrasound improves the dissolution of REEs due to the cavitation phenomenon. Cavitation causes localized high temperatures and pressure when formed bubbles collapse. Cavitation happens near the solid surface of the waste phosphors. It results in an asymmetric collapse that produces microjets (about $400 \ ms^{-1}$) which are focused towards the solid surface (Feng *et al.*, 2002). These microjets are responsible for the dissolution effects of ultrasound. They result in phosphor powder surface activation which increases interaction between the leaching agent and the solids (Diehl *et al.*, 2018). Successive cycles of compression and rarefaction result in bubble formation and collapse generating shock waves. These waves provide better diffusion of lixiviant into the solid thereby enhancing mass transfer. The cavitation effect also reduces phosphor powder particle size thereby increasing surface area. This in turn improves rare earth recovery.

Yang *et al*. (2013) investigated the use of ultrasound in acid leaching of the blue and green phosphor components. They reported that about 90 % of Ce and over 98 % of Tb could be leached out with 5 M HNO_3 after 5 minutes of ultrasonic irradiation. Information on the frequency and power used was not provided. Diehl *et al*. (2018) reported that better extraction efficiencies for REEs (82 %) could be obtained using an ultrasound probe operating at a frequency of 20 kHz and amplitude of 40 % ($692 \ Wdm^{-3}$) for 15 minutes.

Tunsu, Ekberg and Retegan (2014) studied the effect of ultrasound and temperature on acid leaching of waste phosphors. Ultrasound assisted digestion was conducted at a temperature of 60 ± 2 °C using 1 M HNO_3. Three samples were digested in a VWR USC200TH ultrasound bath for 6 hours. Ce and Tb recoveries were <40 % respectively. The authors did not provide information on the frequency and power used.

Based on the above-mentioned findings it was considered necessary to conduct preliminary tests to investigate the effect of ultrasound on Ce and Tb leaching using HNO_3 as the preferred lixiviant.

2.4.2.2 Alkali Fusion

Alkali fusion can be defined as the thermal breakdown of insoluble substances with an alkali such as NaOH or $NaCO_3$ to produce soluble substances. $BaMgAl_{10}O_{17}:Eu^{2+}$ (BAM) and $CeMgAl_{11}O_{19}: Tb^{3+}$ (CAT) are composed of spinel structures that are so stable that they can resist chemical attack (Wu and Cormack, 2003; Tang *et al.*, 2006; Wu *et al.*, 2013). BAM is composed of a hexaaluminate structure while CAT consists of a distorted magnetoplumbite structure (Liu *et al.*, 2014) . They both consist of oxygen close-packed spinel blocks that are parted by mirror planes. During alkali fusion with NaOH, the alkali melts to produce ionic liquids in the OH^- environment. Ba and Eu present in the blue phosphor powder (BAM) are substituted by Na in the mirror planes before transformation of the spinel blocks $MgAl_{10}O_{16}$ into MgO and $NaAlO_2$.

For the green phosphor powder (CAT), terbium and cerium are substituted by Na in the mirror planes prior to transformation of spinel blocks of $MgAl_{11}O_{19}$ into $NaAlO_2$ and MgO. BAM and CAT then decompose into soluble REO, CaO, $NaAlO_2$, MgO and $BaCO_3$ to keep the unit cell charge neutral. Equation 5 and 6 show the reactions that occur between BAM, CAT and NaOH during alkali fusion at high temperatures.

$$BAM + NaOH + CO_2 \rightarrow NaAlO_2 + MgO + BaCO_3 + Eu_2O_3 + H_2O \qquad (5)$$

$$CAT + NaOH \rightarrow NaAlO_2 + MgO + CeO_2 + Tb_2O_3 + H_2O \qquad (6)$$
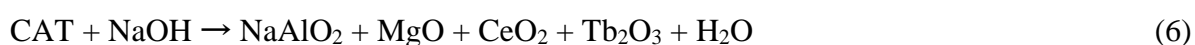
The reactions can destroy the spinel structure and convert the rare earth metals into oxides or partial acid salts which can be easily digested by inorganic acid (Wu *et al.*, 2014). The main component in the products is the water soluble $NaAlO_2$, and minor products are REOs, MgO and BaO as shown by Equations 5 and 6. One of the potential drawbacks with the alkali fusion method is the solubilisation of silica originating from the glass impurity fractions. At high temperatures, the glass fraction produces slag which traps some of the REEs. In this case, some of the valuable metals will be lost in the slag phase. The silicate from the glass phase

13

also makes the leaching solution viscous thereby inhibiting efficient mass transfer (Tan, Li and Zeng, 2015)

Zhang *et al.* (2013) investigated the effect of using either NaOH or Na_2CO_3 as the alkali during alkali fusion. Alkali fusion was conducted using residue from the first stage leaching where Y and Eu were recovered using 3 M HCl, a temperature of 60 ºC and a residence time of 4 hours. The best recoveries were achieved after acid leaching of the alkali fusion product obtained using NaOH compared to Na_2CO_3. HCl leaching was conducted for 3 hours at 60 °C and a S/L ratio of 1:3 w/v. The leaching recoveries of Tb and Ce were 97.99 % and 98.97 % respectively when NaOH was used. However, only 8.36 % and 26.62 % Ce and Tb could be recovered when Na_2CO_3 was used. Alkali fusion with NaOH produces acid soluble Eu_2O_3, CeO_2, and Tb_4O_7 or Tb_2O_3. However, alkali fusion with Na_2CO_3 produces Eu_2O_3, CeO_2 and in addition $Ce_{0.6}Tb_{0.4}O_{2-x}$ which has a very low solubility in inorganic acids hence the poor recoveries. Zhang *et al*. (2013) recommended the following conditions for the alkali fusion process: a temperature of 800 ºC, leach residue to NaOH ratio of 1:1.5 (mass ratio) and 2 hours of fusion time.

Liu *et al.* (2014) compared the traditional and dual dissolution by HCl (DHA) methods for the recovery of rare earths from spent phosphor powders. In the traditional method, the waste phosphor was mixed with sodium hydroxide in the ratio 1:1.5 (by mass). The mixture was fused in a furnace at a temperature of 800 ± 10 ºC for 120 minutes. The fusion product was washed with water at a temperature of 60 °C before the insoluble material was filtered and dried. Leaching was conducted with 5 M HCl for 2 hours with stirring (250 rpm) at 60 ºC. In the DHA method, Y_2O_3:Eu (red phosphor) was dissolved first while BAM and CAT (present in the first leach residue) were mixed with caustic soda prior to sintering at 800 ºC for 2 hours. Excess NaOH and $NaAlO_2$ were water washed before filtration and drying. Acid digestion was then performed on the alkali fusion product. 94.6 % and 42.08 % total rare earth recoveries were obtained by the DHA and traditional methods respectively. Recoveries of Y, Eu, Ce and Tb reached 94.6 %, 99.1 %, 71.5 %, and 76.2 %, respectively. The DHA method offers advantages of less chemicals and energy consumption.

An efficient recovery process for REE recovery using alkali fusion was reported by Wu *et al.* (2013). Alkali fusion was performed using a reaction temperature, time and Na_2O_2 to waste

14

phosphor ratio of 650 ℃, 15 minutes and 2:1 respectively. After calcination, the alkali fusion product was leached with HCl and H_2O_2. The rare earth recoveries were 99.7 % Y, 99.4 % Eu, 98.6 % Ce and 99.8 % Tb.

Porob *et al.* (2012) proposed alkali fusion as a suitable method for the destruction of the spinel structure in the blue and green phosphors. They suggested that LAP, BAM and CAT phosphors could be decomposed by molten Na_2CO_3 at a temperature of 1000 ℃. However, the use of Na_2CO_3 gave poor recoveries since it could not completely decompose the spinel structure.

Based on these findings, it was found that NaOH is the best alkali to use in the alkali fusion process. The recommended conditions for the alkali fusion process are a temperature of 800 ℃, residence time of 2 hours and a residue-to-NaOH ratio of 1:1.5 (Liu *et al.*, 2014; Zhang *et al.*, 2013).

2.4.3 Thermodynamics of REE Leaching

The author did thermodynamic modelling presented in this section which mainly focused on yttrium, europium, cerium and terbium leaching since they were the targeted rare earths in this study. Efficient recovery of these valuable rare earth elements therefore ensures maximum profitability. HSC Chemistry 9.0.6 was used to evaluate the thermodynamics of the leaching reactions. The proposed chemical reactions for the process are shown below:

$$Y_2O_{3(s)} + 6\ H^+_{(aq)} + 6\ SO_4^{2-}_{(aq)} \rightarrow 2Y^{3+}_{(aq)} + 6\ SO_4^{2-}_{(aq)} + 3\ H_2O_{(l)} \tag{7}$$

$$Eu_2O_{3(s)} + 6\ H^+_{(aq)} + 6\ SO_4^{2-}_{(aq)} \rightarrow 2\ Eu^{3+}_{(aq)} + 6\ SO_4^{2-}_{(aq)} + 3\ H_2O_{(l)} \tag{8}$$

$$CeO_{2(s)} + 4\ H^+_{(aq)} + 4\ Cl^-_{(aq)} \rightarrow Ce^{4+}_{(aq)} + 4\ Cl^-_{(aq)} + 2\ H_2O_{(l)} \tag{9}$$

$$Tb_2O_{3(s)} + 6\ H^+_{(aq)} + 6\ Cl^-_{(aq)} \rightarrow 2\ Tb^{3+}_{(aq)} + 6\ Cl^-_{(aq)} + 3\ H_2O_{(l)} \tag{10}$$
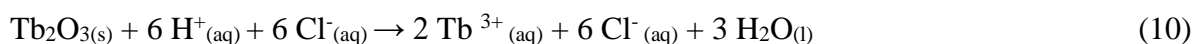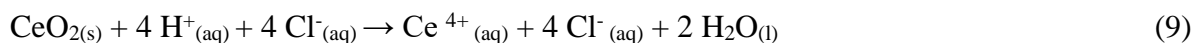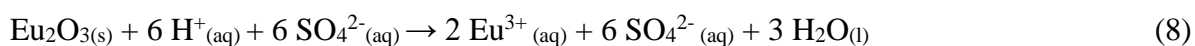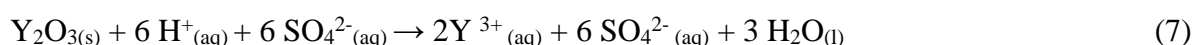
Tables 2.4 to 2.7 show the predicted thermodynamic properties of Y, Eu, Ce and Tb leaching with H_2SO_4

Table 2.4: Thermodynamic properties for leaching of yttrium with H_2SO_4 (Equation 7)

T [°C]	ΔH [kJ]	ΔS [J/K]	ΔG [kJ]	k
30	-382.459	-391.037	-263.927	3.03E+045
60	-381.664	-388.484	-252.253	3.57E+039
90	-381.497	-387.982	-240.622	4.08E+034

Table 2.5: Thermodynamic properties for leaching of europium with H_2SO_4 (Equation 8)

T [°C]	ΔH [kJ]	ΔS [J/K]	ΔG [kJ]	k
30	-406.81	-374.845	-293.173	3.30E+050
60	-411.58	-389.949	-281.667	1.47E+044
90	-416.266	-403.296	-269.784	6.43E+038

Table 2.6: Thermodynamic properties for leaching of cerium with HCl (Equation 9)

T [°C]	ΔH [kJ]	ΔS [J/K]	ΔG [kJ]	k
30	-56.9442	-339.699	46.024	1.17E-008
60	-54.5175	-332.042	56.10744	1.59E-009
90	-52.9276	-327.482	65.98168	3.21E-010

Table 2.7: Thermodynamic properties for leaching of terbium with HCl (Equation 10)

T [°C]	ΔH [kJ]	ΔS [J/K]	ΔG [kJ]	k
30	-392.919	-405.43	-269.994	3.37E+046
60	-398.066	-421.705	-257.609	2.46E+040
90	-403.087	-436.098	-244.722	1.60E+035

Tables 2.4 to 2.7 show that all the reactions given by Equations 7 to 10 are thermodynamically favourable for Y, Eu and Tb oxides at 30 ,60 and 90 ℃ temperature range. This is due to the large negative Gibb's free energy values (ΔG) and large positive equilibrium constant values (k) for all the three reactions. For the cerium reaction in Equation 10, the equilibrium constant (k) values are very small (Table 2.6). This means that the backward reaction is favoured with an increase in temperature and therefore there will be low concentration of Ce^{4+} in solution. The small k value also suggests that the solubility of cerium chlorides in HCl is lower compared to that of terbium. The enthalpies of reaction are negative for all reactions meaning that all the three reactions will be exothermic (Table 2.4 to 2.7). Thermodynamic properties for leaching from 0 to 100 ℃ are given in Appendix D.

2.4.4 Eh-pH Diagrams for REE Systems

Pourbaix diagrams were generated using HSC Chemistry version 9.0.6 to test the feasibility of rare earth metals dissolution with inorganic acids. The diagrams illustrate the most thermodynamically stable phases of a system at equilibrium at a particular redox potential (Eh) and pH. A major drawback of these Eh-pH diagrams is that reaction kinetics of the respective reactions are not shown. The Pourbaix diagrams were generated using a molarity of 1 mole of the reacting species per kg of water and a pressure of 1 bar. A temperature of 70 ℃ which gave the optimal recoveries in studies conducted by Takahashi *et al.* (2001) and Yang *et al*. (2013). Sulphuric acid and hydrochloric acid were used as lixiviants of choice for the first stage and second stage leaching respectively. The redox state of a metal and ligands that may complex it greatly affects its solubility.
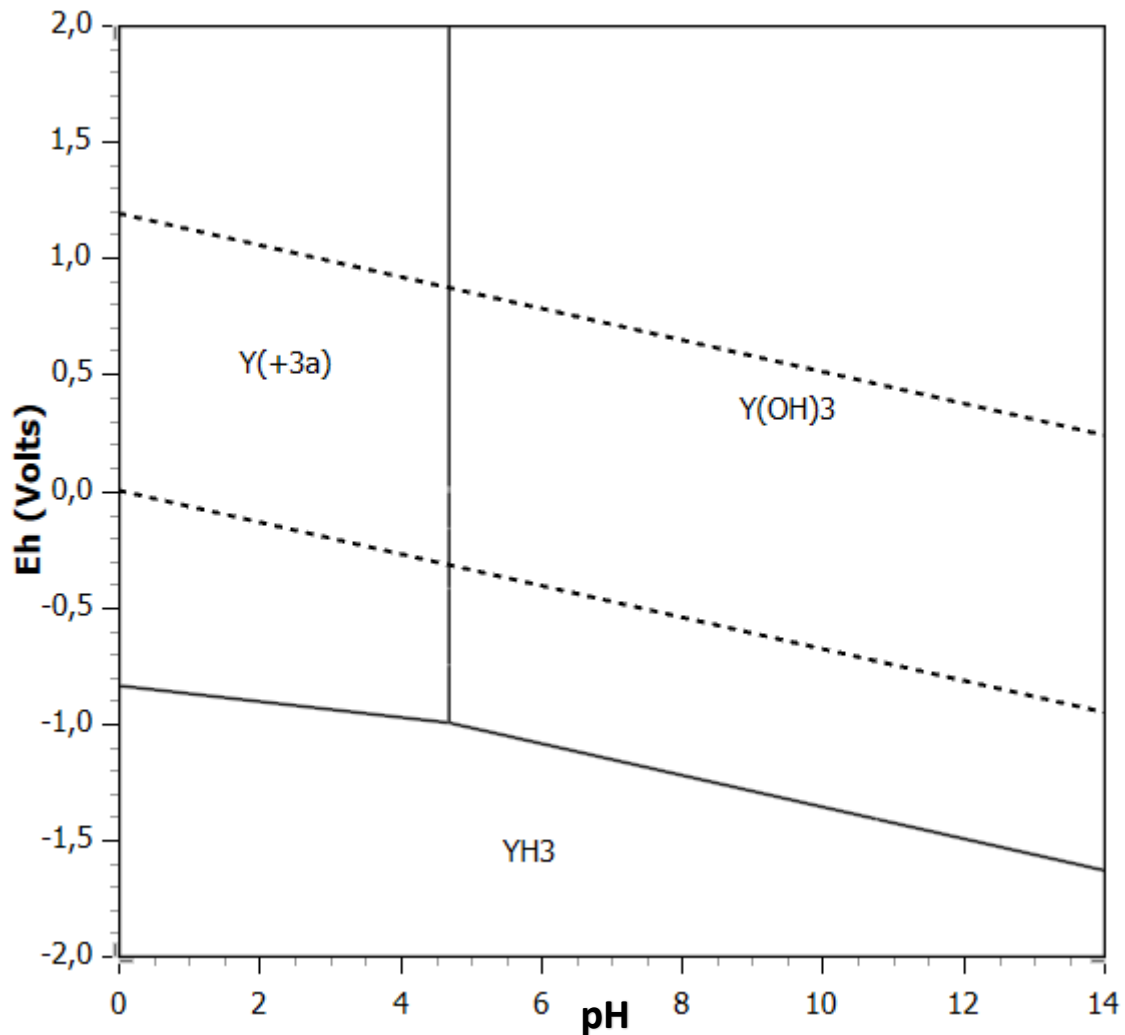
Figure 2.3: Pourbaix diagram for a Y-Eu-S system at 70 °C

Figure 2.3 shows the Pourbaix diagram for a Y-Eu-S system at 70 °C. The diagram illustrates that it is thermodynamically feasible to dissolve yttrium into solution using H_2SO_4 acid. The diagram indicates that yttrium only dissolves in H_2SO_4 at pH less than 4.6 and Eh above -0.8 V to give Y^{3+} ions. It is also shown that yttrium dissolves significantly at higher or positive Eh values. The Pourbaix diagram illustrates that above a pH of 4.6, yttrium forms $Y(OH)_{3(s)}$ which is sparingly soluble in strongly oxidising solutions. Yttrium dissolution is therefore favoured in oxidising acidic environments.
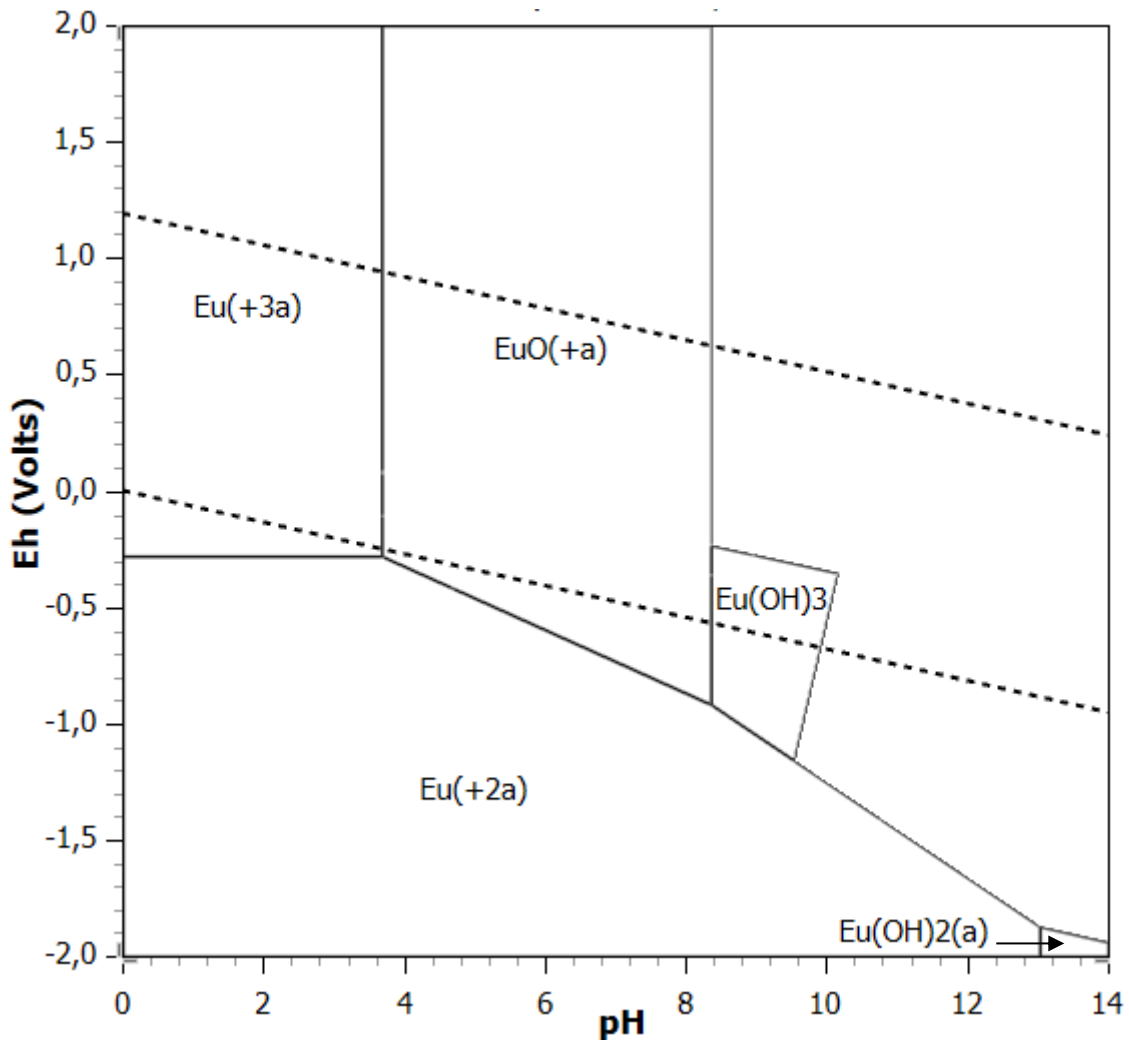
Figure 2.4: Pourbaix diagram for a Eu-Y-S system at 70 °C

The Pourbaix diagram for a Eu-Y-S system at 70 °C is shown in Figure 2.4. The Eh-pH diagram shows that it is thermodynamically feasible to get europium into solution in an aqueous phase. Eu dissolves in H_2SO_4 at pH less than 4 and Eh above -0.3 V to give Eu^{3+} ions. The diagram also shows that Eu dissolves significantly at higher or positive Eh values. This shows that oxidative dissolution of the waste phosphor powder is required to dissolve Eu into solution. At higher pH (above 8.4) Eu forms $Eu(OH)_{3(s)}$ which is sparingly soluble in oxidising environments .
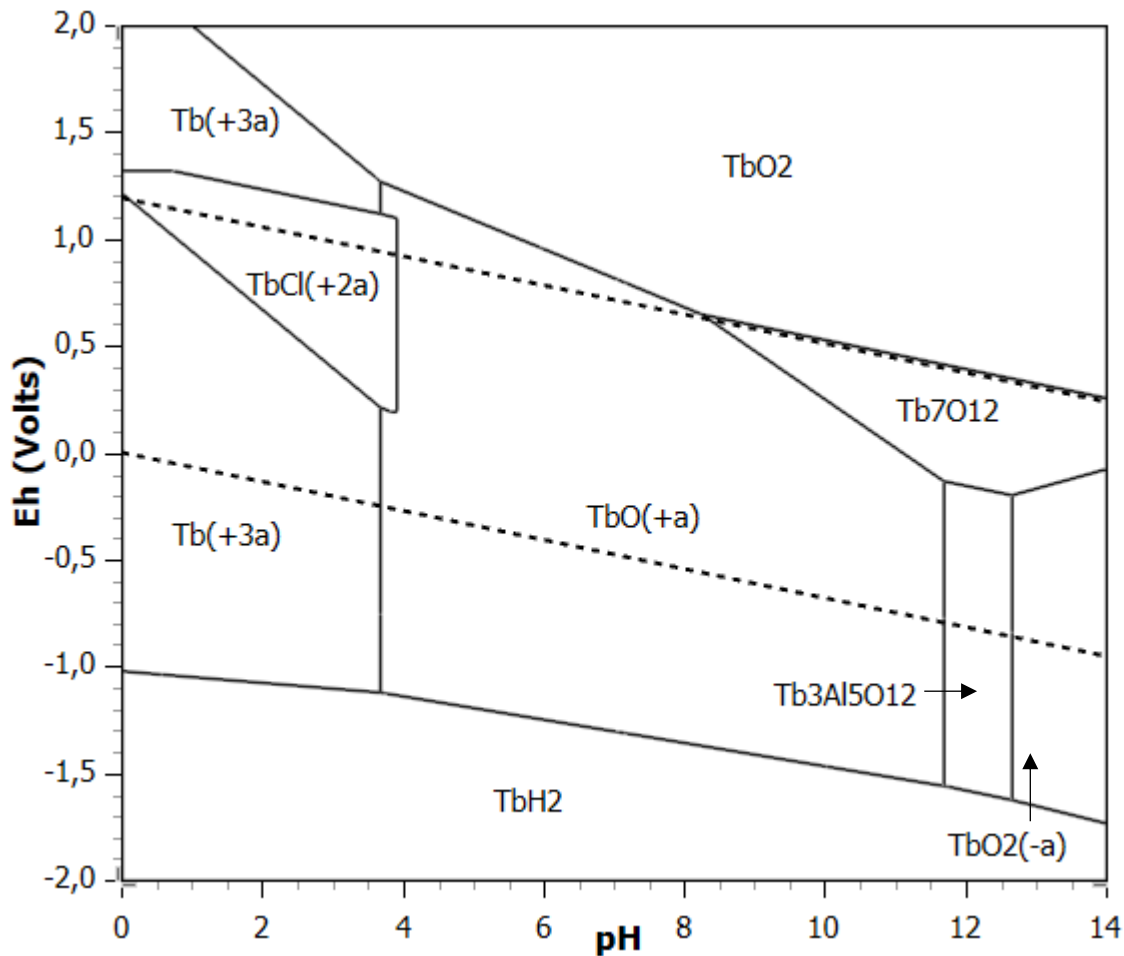
Figure 2.5: Pourbaix diagram for a Tb-Mg-Cl-Ce-Al system at 70 °C

The Pourbaix diagram for a Tb-Mg-Cl-Ce-Al system at 70 °C is shown in Figure 2.5. The aluminate system was used to generate this diagram since it is the one that is mostly used as discussed in section 2.2. The Pourbaix diagram shows that Tb solubilises to Tb^{3+} below a pH of 3.7 and between Eh values of -1 to 1.2 V. The diagram also shows that dissolution to Tb^{3+} is also possible beyond 1.4 V. It is therefore possible to leach terbium in highly reducing and highly oxidising environments.

Figure 2.6 shows the Pourbaix diagram for a Ce-Tb-Mg-Cl-Al system at 70 °C. Ce is only soluble at negative Eh values (-1.1 to -0.4 V) and pH below 4. This suggests that cerium only solubilises in highly reducing environments. The Pourbaix diagram also shows that at pH beyond 10, there is formation of insoluble $Ce(OH)_{3(s)}$. This property can be useful in extracting cerium by first precipitating it to a hydroxide prior to dissolution with an acid.

20
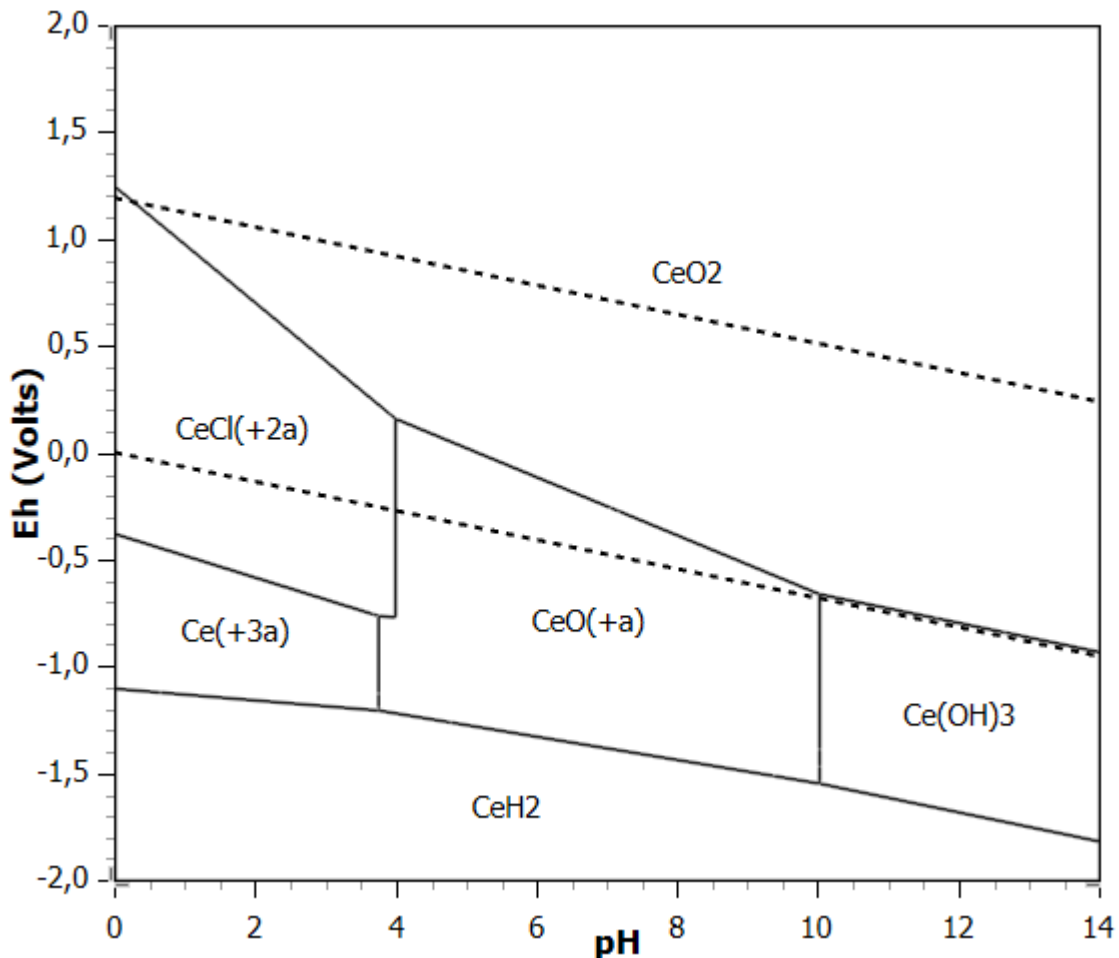
Figure 2.6: Pourbaix diagram for a Ce-Tb-Mg-Cl-Al system at 70 °C

2.5 Solvent Extraction

Solvent extraction is a process where a solute of interest is partitioned between two immiscible liquid phases, which are in contact (Rydberg *et al*., 2004). The aqueous phase constitutes mainly water while the organic phase comprises an extractant and a diluent to make up the rest of the volume. Figure 2.7 shows a typical representation of a solvent extraction process.
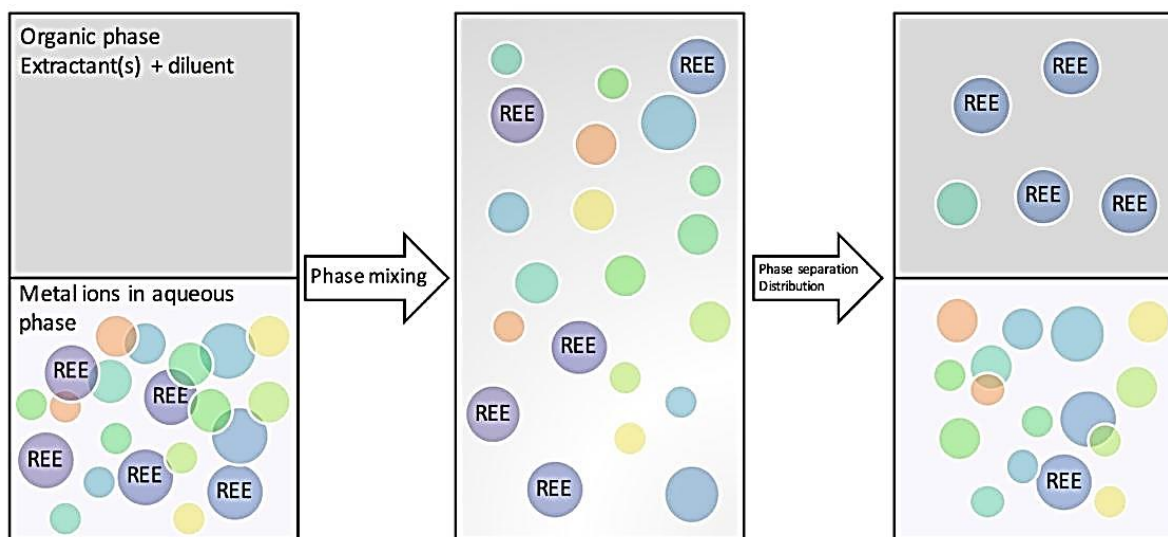
Figure 2.7: Typical solvent extraction process for rare earths recovery (adapted from (Tunsu, 2016))

The REEs are initially present as soluble ions in the aqueous phase. The ions are then extracted into the organic phase during phase mixing and phase separation. Unwanted elements (impurities) are also extracted depending on the operating conditions.Individual separation of REEs is challenging due to small differences in ionic radius between the elements. Ion exchange and solvent extraction technologies were developed to produce REEs of high purity. Ion exchange was the only separation technique used in the separation of REEs before the introduction of large scale solvent extraction (Jamrack, 1963; Kumar, 1994; Reddy, Kumar and Radhika, 2009). Currently, ion exchange is mostly employed to attain small amounts of highly pure REEs (Taniguchi, Doty and Byers, 1988), whereas solvent extraction has become the most suitable industrial technology for separating REEs when handling large volumes of leach solutions (Xie *et al.*, 2014).

Since fluorescent powders are chemically complex, REEs and other metals (impurities) are leached into solution. These metal impurities include Al, B, Ca, Ba, Fe, Mg, Mn and others (Tunsu *et al.*, 2014). The REEs can be co-extracted prior to further purification to get individual elements (Tunsu *et al*., 2014). In this case, unwanted metal elements remain in the aqueous phase.

Solvent extraction mainly relies on the reduction in ionic radius across the lanthanide series. This phenomenon is known as the lanthanide contraction (Rydberg *et al.*, 2004). Going

22

across the lanthanide series, there is a steady decrease in atomic size, which brings about an increase in the acidity of the element with increase in atomic number. This results in a difference in formation coefficient of the rare earth-extractant complex, thereby permitting preferential extraction of the complex into the organic phase (Rydberg *et al.*, 2004). Heavy elements of the lanthanide series form stronger bounds with extractant molecules than lighter members (Nash, 1993). This then allows preferential extraction of these rare earths compared to the lighter ones. The properties of the targeted rare earths are given in Table 2.8 and it is shown that the ionic radius follows the sequence: Y<Tb<Eu<Ce.

Table 2.8: Properties of Lanthanides elements (adapted from (Rydberg et al., 2004))

Element	Atomic number	Atomic mass	Ionic radius (Ln^{3+}) $(\mathring{A})$
Yttrium	39	88.8	0.880
Terbium	65	158.9	0.923
Europium	63	152.0	0.950
Cerium	58	138.9	1.061

The selectivity order for REE extraction follows the sequence Lu > Yb > Tm > Tb > Eu > Pm > Pr > Ce > La (Peppard and Wason, 1961; Wang *et al.*, 2002) .If physical properties were plotted against proton number, Y would have an apparent number between 64.5 to 67.5 (Hampel, 1968). Yttrium extraction occurs between terbium and thulium corresponding to an artificial atomic number of 67.6 (Xie *et al.*, 2014).

2.5.1 Extracting Reagents

There are three main classes of organic solvents that have been used to produce rare earths of high purity. These are cation exchangers also known as acidic extractants, solvation extractants also known as neutral extractants, and anion exchangers also known as basic extractants (Xie *et al.*, 2014).The distribution coefficient, percentage extraction and separation factor help in understanding and quantifying the performance of various extractants (Habashi, 1999). The ratio between the concentration of the targeted solute in the extractant and the aqueous phase at equilibrium is known as the distribution ratio (D).

$$D = \frac{[A]_{org}}{[A]_{aq}} \qquad (11)$$

The percentage of metal ions extracted can be determined from the distribution ratio according to Equation 12.

$$\%E = \frac{100 \times D}{\dfrac{V_{aq}}{V_{org}} + D} \qquad (12)$$

Where V_{org} is the organic phase volume and $V_{aq\ is}$ the aqueous phase volume.

The separation factor showing the extent of separation between solutes A and B is given by Equation 13.

$$\alpha_{\frac{A}{B}} = \frac{D_A}{D_B} \qquad (13)$$

Separation between solute A and B is only possible if $\alpha_{\frac{A}{B}}$ is larger or smaller than unity (Gupta and Krishnamurthy, 2005). Separation is impossible if the separation factor is unity.
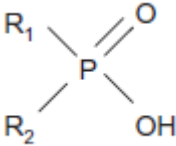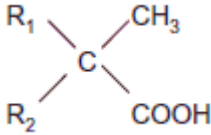
2.5.1.1 Cation exchangers

The extraction of REEs by cationic exchange from aqueous solutions is given by Equation 14 (Morais and Ciminelli, 2004; Gupta and Krishnamurthy, 2005).

$$RE^{3+}_{\ aq} + 3H_2A_{2\ (org)} \rightarrow RE\ (HA_2)_{3(org)} + 3H^+_{\ aq} \qquad (14)$$
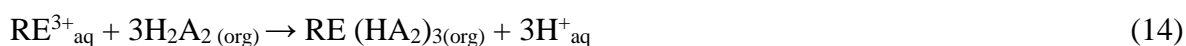
Where RE and H_2A_2 denote the trivalent rare earth and the dimeric form of the organic acid respectively. Equation 14 shows that REEs extraction increases with increase in aqueous phase pH. Stripping (reverse reaction) is promoted by decreasing the pH. There are two classes of cationic exchangers which are carboxylic acids and organic derivatives of phosphorous acids (Xie *et al.*, 2014). Some of the most commonly used cationic exchangers in REEs extraction are shown in Table 2.9 below.

Table 2.9: Some of the most commonly used cationic exchangers (adapted from (Rydberg et al., 2004))

Type	Structure	Extractant
Phosphorous acids		DEHPA: R1=R2=$C_4H_9CH(C_2H_5)CH_2O$- (Bis(2-ethylhexyl) hydrogen phosphate) HEHEHP/PC88A:R_1=$C_4H_9CH(C_2H_5)CH_2O$, R_2=$C_4H_9CH(C_2H_5)CH_2$–(2-ethylhexylphosphonic acid mono -2-ethylhexyl ester) Cyanex 272: R_1=R_2 = $CH_3(CH_2)_3CH_2CH(CH_3)CH_2$–, (di-2,4,4-trimethylpentylphosphinic acid)
Carboxylic acids		Versatic acids: R1 + R2 = C7, Versatic 10; R1 + R2 = C6–C8, Versatic 911

2.5.1.2 Solvating Extractants
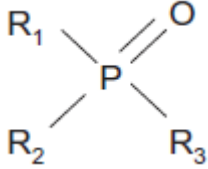
Solvating extractants comprise of electron-rich oxygen or sulphur atoms that can coordinate rare earth cations making them hydrophobic. Extraction of metal ions by solvating extractants occurs according to reaction Equation 15 (Rydberg *et al.*, 2004).

$$M^{n+}_{(aq)} + n\, X^-_{(aq)} + b\, B_{(org)} \leftrightarrow MX_n B_{b\ (org)} \tag{15}$$

According to Equation 15, the metal ions (M^{n+}) first form complexes with counter ions (X^-). Water molecules occupy the remainder of the coordination sites resulting in the complexes having very low distribution coefficients (Tunsu, 2016). However, on addition of a neutral or solvating extractant, the water molecules are substituted by the extractant molecules. Examples of solvating extractants are tri-n-octylphosphine oxide (CYANEX 921),

dibutylbutylphosphonate (DBBP) and tri-n-butyl-phosphate (TBP). These are shown in Table 2.10.

Table 2.10: Some of the most commonly used solvating extractants (adapted from: Ritcey and Ashbrook, 1984; Rydberg et al., 2004)

Type	Structure	Extractant
Solvating Extractants		TBP: $R_1 = R_2 = R_3 = CH_2(CH_2)_2CH_2O–$, DBBP : $R_1 = R_2 = CH_2(CH_2)_2CH_2O–$, $R_3 = CH_2(CH_2)_2CH_2–$ TOPO/Cyanex 921 $R_1 = R_2 = R_3 = CH_2(CH_2)_6CH_2–$

Equation 16 shows the extraction of rare earth ions with an oxidation state of +4 from sulphuric solutions using a solvating extractant (Jun *et al.*, 1998):

$$M_{aq}^{4+}+SO_4{}^{2-}{}_{aq}+ 2HSO^{4-}{}_{aq}+2X_{org} \rightarrow M(SO_4)(HSO_4)_2.2X_{org} \tag{16}$$
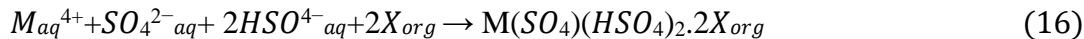
Where M represents the rare earth and X denotes the extractant.

2.5.1.3 Chelating agents

Chelating agents extract metal ions in a similar way to cationic exchangers as shown by reaction equation 14. However, for chelating agents, extraction happens at higher pH and lower acid concentrations are required for stripping (Tunsu, 2016). Another difference is that, organic complexes that are formed are stabilised by the organic anion coordinating the central cation in two or more positions (Hudson, 1982). Examples of chelating agents used for rare earth extraction are Cyanex 572 and LIX 54. Cyanex 572 composition has not been exposed but it is said to contain phosphinic and phosphonic acids (Cytec, 2014). The structure of LIX 54 is shown in Table 2.11.

Table 2.11: Structure of LIX 54 (adapted from (Rydberg et al., 2004))

Type	Structure	Extractant
Chelating Extractants		LIX 54: R1 = R-C_6H_5, R2 = $CH_3(CH_2)_5-$, R: unknown side alkyl

2.5.1.4 Anionic exchangers

Anionic exchangers perform well when there exist strong anionic ligands since they extract metal ions as anionic complexes (Xie *et al.*, 2014). Reactions 17 and 18 were suggest by EL-Yamani & Shabana (1985) when extracting trivalent lanthanides from sulphate solution using Primene JMT as the extractant:

$$2RNH_{2,org} + H_2SO_{4,aq} \rightarrow (RNH_3)_2SO_{4,org} \tag{17}$$

$$2M(SO_4)_{3,aq}^{3-} + 3(RNH_3)_2SO_{4,org} \rightarrow 2(RNH_3)3M(SO_4)_{3,org} + 3SO_{4,aq}^{2-} \tag{18}$$
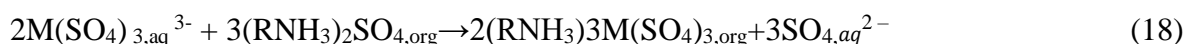
Where RNH_2 represents the Primene JMT in the organic phase. An example of an anionic exchanger is tri-octyl methylammonium nitrate. Reaction 19 represents extraction using this quaternary ammonium salt.

$$Ln^{3+} + 3NO_3^- + x(R_4N^+NO_3^-)_n \longrightarrow LnNO_3.R_4N^+NO_3^- \tag{19}$$

Where Ln represents the rare earth ion and $R_4N^+NO_3^-$ the quaternary ammonium nitrate salt. Table 2.12 shows some of the commonly used anionic exchangers.

Table 2.12: Some of the commonly used anionic exchangers (adapted from (Rydberg et al., 2004))

Type	Structure	Extractant
Anion Exchanger	RNH_2 ... $R_1, R_2, R_3, N, CH_3\,Cl$	Primene JMT: $R = (CH_3)_3C(CH)_2C(CH_3)_2)_4$ Aliquat 336: R1 = R2 = R3 = C8–C10

2.5.2 Diluents

Extractants are not often used in pure form. They are normally mixed with organic solvents which are also immiscible with the aqueous phase. The organic solvents are mostly referred to as diluents. Long chain alcohols, aliphatic and aromatic diluents are in existence. Some of the most widely used diluents are shown in Table 2.13.

Table 2.13: Some of the commonly used diluents (adapted from (Tunsu, 2016))

Diluent category	Commercial name
Aliphatic	Solvent 70
	TetraPropyleneHydrogenated (TPH)
	Isopar L
	Escaid 120
	Kerosene
Aromatic	Toluene
	Nitrobenzene
	Solvesso 150
	Tertbutylbenzene
Alcohols	1-octanol

Diluents often improve physical properties of the extractant such as viscosity. However, Habashi (1999) stated that diluents may affect the extracting ability of the extractant. This is caused by interactions such as dipole-dipole interactions, pi-electron interaction, hydrogen

28

bonding and cavity formation (Olivier, 2011). Polymerisation of the organic phase may also occur making the cation exchange process more difficult (Mohapatra *et al.*, 2007). Kerosene has been widely used as a diluent in cationic exchangers such as DEHPA (EL-Yamani and Shabana, 1985; Doyle *et al.*, 2000; Gupta and Krishnamurthy, 2005; Kraikaew, Srinuttrakul and Chayavadhanakur, 2005; Wang *et al.*, 2010; Abreu and Morais, 2014; Takip, Markom and Sulaiman, 2015). It is cheap and is widely used on industrial scale. It was therefore the diluent of choice in this study.

2.5.3 Extraction of REEs

Abreu and Morais (2014) investigated the use of different organophosphorous acids (DEHPA, CYANEX 272 and IONQUEST 801/PC-88A) and amines (ALIQUAT 336, ALAMINE 336 and PRIMENE JM-T) in the extraction of REEs from sulphate and hydrochloric solutions. Tests were only conducted in sulphuric acid medium for amines since amines only extract neutral and anionic species. These species do not form in hydrochloric solutions (Morais and Ciminelli, 2007).The obtained results are shown in Table 2.14.

Table 2.14: Effect of extractant type on percentage extraction of REEs (adapted from (Abreu and Morais, 2014))

Extractant	Extraction (%)			
	Hydrochloric medium		Sulphuric medium	
	Tb	Y	Tb	Y
DEHPA	41.4	81.3	55.4	90.7
IONQUEST 801	14.3	58.6	15.4	62.5
CYANEX 272	4.01	10.3	4.21	7.70
ALAMINE 336	–	–	<0.01	<0.01
ALIQUAT 336	–	–	<0.01	<0.01
PRIMENE JM-T	–	–	77.7	64.1

According to the found results, CYANEX 272 was the least effective of the three cationic exchangers. DEHPA gave the highest extraction in both mediums. DEHPA concentration of 1 M and an aqueous solution pH of 0.3 was used. Rare earth extraction was only possible using PRIMENE JM-T in the sulphuric medium.

DEHPA and HEHEHP have been widely employed in rare earth extraction from leach solutions (Xie *et al.*, 2014). Although DEHPA is the most commonly used extractant in REEs extraction industries, HEHEHP is known to give higher separation factors for REEs separation. HEHEHP also has an additional advantage that it requires less acid in the aqueous phase during stripping (Song *et al.*, 2009). A major drawback in the use of HEHEHP is that, extraction efficiency decreases when the viscosity of the organic phase increases. Higher extraction efficiencies can be obtained when DEHPA is used as the extractant (Song *et al.*, 2009; Abreu and Morais, 2014). DEHPA is also relatively cheap compared to HEHEHP (Huang *et al.*, 2008). The lower selectivity for some adjacent rare earth pairs such as Nd/Pr, Gd/Eu, Er/Y, Lu/Yb has resulted in the extractant being limitedly utilised (Song *et al.*, 2009). In this regard HEHEHP has often been mixed with other extractants such as DEHPA (Huang *et al.*, 2008) and 8-hydroxyquinoline (Wu, Bao and Zhang, 2007) for synergistic extraction of REEs. HEHEHP in kerosene was used to extract Eu, Tb, and Y from nitric acid leachates (Nakamura, Nishihama and Yoshizuka, 2007). They reported 97.8 % Y, 58.1 % Tb, and 52.8% Eu recoveries respectively.

Shimizu *et al.* (2005) compared the extraction of rare earths using tri-n-butyl phosphate (TBP) complexes with nitric acid and water at atmospheric pressure and under supercritical carbon dioxide (SF-CO$_2$). 37.4 % Y and 36.8 % Eu extraction was achieved at atmospheric pressure. Less than 3% La, Tb and Ce were extracted. Y and Eu extraction was >99 % under supercritical conditions. However, for La, Ce and Tb the recovery remained below 7 %.

Solvent extraction of REEs with ionic liquids was investigated by (Yang *et al.*, 2013). N,N-dioctyldiglycol amic acid (DODGAA) in the ionic liquid [C4mim][Tf2N] (1-butyl-3-methylimidazolium bis(trifluoromethylsulfonyl)imide) was used as the extractant. Rare earth extraction from sulphuric and nitric acid-based leach solutions was achieved at an aqueous pH of 3 using 5 mM DODGAA. 100 ppm Y and 8 ppm Eu was extracted to the ionic liquid with 25 mM DODGAA at a pH less than 1.2. Impurities extraction was very low. The leachate containing La, Ce, Pr and Tb (obtained after second stage leaching) was also subjected to extraction using DODGAA in the ionic liquid. Selective separation of rare earths was possible at a pH of 3.0 using 50 mM DODGAA. The authors reported that the extractant showed a higher selectivity for heavier rare earth ions than conventional organic extractants such as PC-88A. Another notable advantage was that ionic liquids compared to organic extractants have low vapour pressure, high heat capacity and can be easily be used after leaching at a relatively

high temperature (Baba *et al.*, 2011). Complete Eu and Y stripping could be achieved using 0.5 M H_2SO_4 and 1 M HNO_3.

Rabah (2008) used trimethyl-benzylammonium chloride to selectively extract Eu and Y from a thiocyanate solution. The rare earth powder was leached from waste phosphor using a sulphuric/nitric acid mixture prior to conversion to thiocyanate. 96.5 % Eu and 98.8 % of Y could be extracted. Stripping from the organic phase was conducted using N-tributylphosphate (TBP) in 1 M nitric acid to produce nitrate salts of Eu and Y. Europium nitrate and yttrium nitrate were then separated by dissolving in ethyl alcohol (TMPA). The separation factor of Y to Eu (given by Equation 3) was found to be 9.4.

In order to address the shortcomings of the conventional single extractant solvent extraction process studies have been conducted on the use of mixtures of reagents as the extractant in solvent extraction processes. It is believed that synergistic extraction effects can be achieved if some of the conventional extractants are used in combination with each other and with alternative reagents. Wang *et al.* (2006) found that heavy rare earth extraction is highest for a mixture of HEHEHP and DEHPA, followed by HEHEHP and Cyanex 301, HEHEHP and HHEOIPP (isopropylphosphonic acid 1-hexyl-4-ethyloctyl ester), HEHEHP and Cyanex 302, and HEHEHP and Cyanex 272, in that order. The HEHEHP and DEHPA mixture achieved the highest separation factors on average. The HEHEHP and DEHPA mixture and the HEHEHP and Cyanex 272 mixtures were the only two that exhibited synergistic extraction effects.

The discussion above shows that better separation factors can be obtained using HEHEHP. It was also found that HEHEHP is relatively easy to strip. However, the extractant suffers poor extraction efficiencies and it is relatively costly compared to other extractants such as DEHPA. In this regard, DEHPA was the extractant of choice.

2.5.4 Operating Variables

2.5.4.1 Effect of pH

The pH of the aqueous solution is an important variable in solvent extraction processes with respect to selective separation. Different metal ions are extracted at different pH so it is of utmost importance to find the optimal pH to selectively extract the targeted metal elements

without impurities. Since DEHPA is the extractant of choice in this study, according to Equation 14, increasing the aqueous solution pH will favour the forward reaction. However, impurities such as calcium and magnesium are also extracted at higher pH compromising the purity of the rare earth product. This is shown in Figure 2.8.
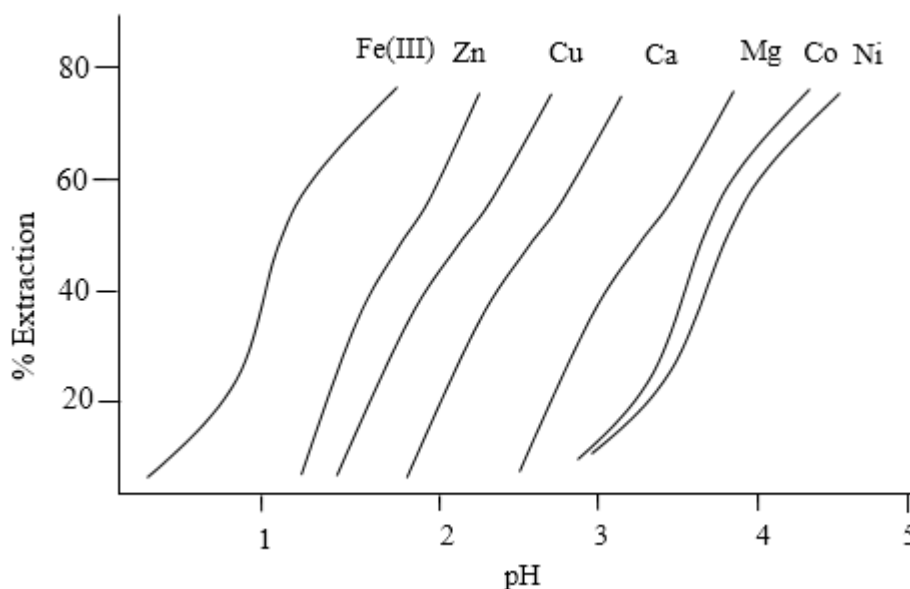
Figure 2.8: Metal extraction from sulphate media using DEHPA (redrawn from (Cox and Flett, 1987))

It is important to make a trade-off between the amount of REEs extracted and the amount of impurities that are acceptable. Another important variable is the pH_{50} value which is the pH where 50 % of the metal species are extracted into the organic phase. A big difference between pH_{50} values of two species (pH_{50}^{Y-Eu}) suggests that selective separation is possible. It is important that the aqueous solution pH remains below the precipitation point of the targeted metal ions (Konishi, Satoh and Takano, 2002). NaOH and NH_4OH are the most common base diluents used for pH adjustments during solvent extraction (Rousseau, 1987; Morais and Ciminelli, 2004; Rydberg *et al.*, 2004; Nakamura, Nishihama and Yoshizuka, 2007; Wu, Bao and Zhang, 2007). However, in most studies, NaOH was the preferred base titrant since NH_4OH was reported to lead to the formation of amine precipitates. In this regard, NaOH will be the preferred diluent.

2.5.4.2 Organic / Aqueous Phase Mixing Ratio (O/A Ratio)

The O/A ratio is the volumetric ratio at which the organic and aqueous phases are mixed. Extraction isotherms are constructed using concentrations of the targeted metals in the organic and aqueous phases at equilibrium. The concentrations are obtained after varying the O/A

ratio at a constant pH and aqueous concentration. A typical extraction isotherm is displayed in Figure 2.9.
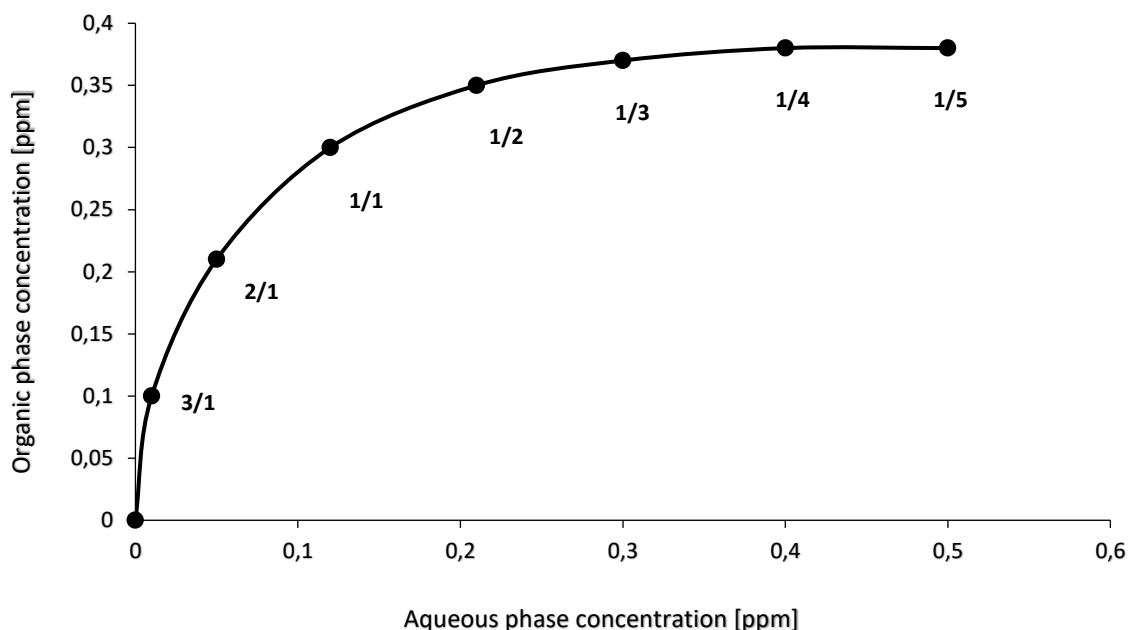
Figure 2.9: A typical extraction isotherm constructed at a constant pH, constant extractant concentration and varying O/A ratio (adapted from (Rydberg et al., 2004))

From Figure 2.9 it is shown that at a low O/A ratio say for instance ¼, most of the targeted metal will be present in the aqueous phase at equilibrium. The high concentration in the organic phase is because the targeted metal was transferred from a larger aqueous phase volume to a smaller organic phase volume. The higher the O/A ratio the higher the metal extraction. Often low O/A ratios and pH values are used. In this case, complete metal extraction in one stage is not achievable. In order to attain complete extraction under such conditions a multiple stage process displayed in Figure 2.10 can be used.
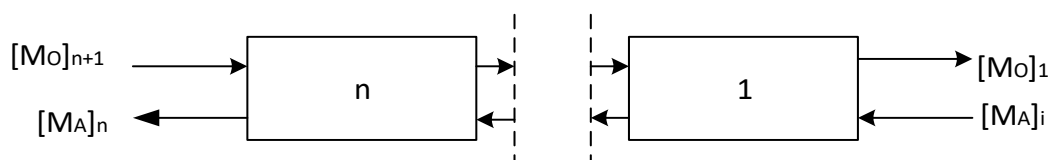
Figure 2.10: Schematic diagram for a simple multiple staged counter-current extraction system (adapted from (Xie et al., 2014))

The organic and aqueous phases are fed in either a counter current (as shown in Figure 2.10) or a co-current manner. The counter current manner is more popular since its regarded as

more effective (Habashi, 1999). The McCabe-Thiele method involves plotting an equilibrium curve and an operating line on the same graph. Equation 20 shows the operating line equation.

$$[M_O]_1 = \frac{A}{O} \left([M_A]_i - [M_A]_{n)} + [M_O]_{n+1}\right)$$

(20)

where $[M_O]_1$ = Metal concentration in the organic phase exiting the system (extract)

$[M_A]_i$ = Metal concentration in aqueous phase entering the system

$[M_A]_n$ = Metal concentration in the aqueous phase exiting the system (raffinate)

$[M_O]_{n+1}$ = Metal concentration in the organic phase entering the system

n = Number of theoretical stages

A/O = Slope of the operating line (ratio with which the aqueous and organic phases are fed to the system in Figure 2.10)

The method is used to find the number of theoretical stages necessary to reduce the targeted metal concentration from $[M_A]_i$ to $[M_A]_n$ thereby increasing the metal concentration in the extractant from $[M_O]_{n+1}$ to $[M_O]_1$ as presented in Figure 2.11.
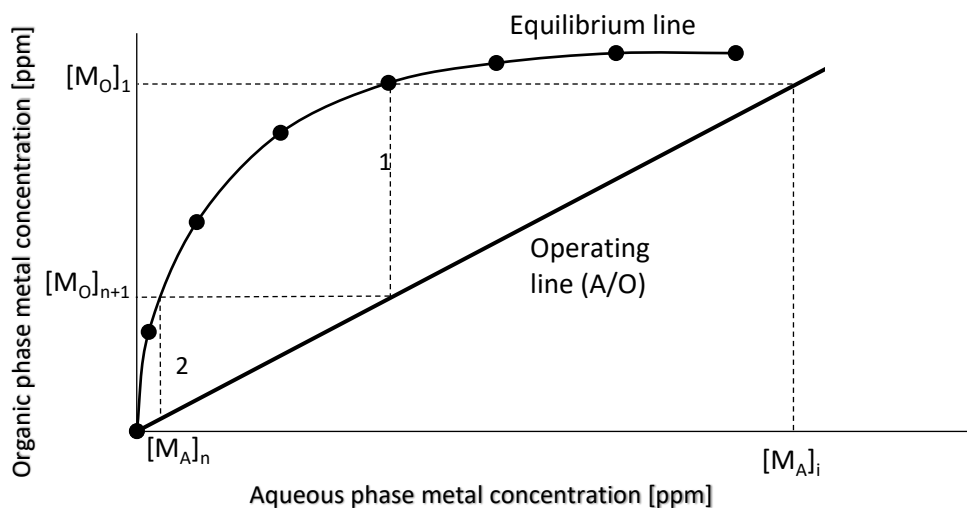
Figure 2.11: Typical McCabe-Thiele Diagram (adapted from (Xie et al., 2014))

In Figure 2.11, the dotted lines clearly show that two theoretical stages are adequate to achieve the targeted extraction. The number of theoretical stages can be reduced by decreasing the

A/O ratio (increasing the volume of the extractant). This results in a decrease in the gradient of the operating line thereby reducing the number of steps.

2.5.4.3 Extractant Concentration

Takip *et al*. (2015) studied the effect of varying DEHPA concentration between 0.1 and 1.0 M on the extraction of light rare earths. All the other parameters were kept constant. They found that percentage extraction increases with increase in DEHPA concentration. More than 99 % extraction for all the four rare earths investigated was obtained at an extractant concentration of 1 M. Abreu and Morais (2014) also investigated the effect of DEHPA concentration on rare earths extraction between 0.5 M and 2 M. They found that the viscosity of DEHPA increases significantly with concentration hence resulting in separation that is more difficult. This causes a decrease in percentage extraction of rare earths. It was therefore decided to investigate the use of 0.5 M and 1 M DEHPA concentrations.

2.5.4.5 Temperature

Temperature is known to influences phase separation. Solubility issues in the organic phase cause third phase formation. In most cases, an increase in temperature causes the disappearance of the third phase (Olivier, 2011). Most studies conducted with regards to solvent extraction of REEs were conducted at room temperature(Kraikaew, Srinuttrakul and Chayavadhanakur, 2005; Wu, Bao and Zhang, 2007; Song *et al.*, 2009; Abreu and Morais, 2014; Takip, Markom and Sulaiman, 2015). It was therefore decided to perform solvent extraction tests at room temperature.

2.6 Stripping

Stripping occurs when metal ions in the organic phase are recovered through contact between the organic phase and a stripping agent. There is limited data on stripping of rare earths from the DEHPA-kerosene extractant system (Alberts, 2011). Similar operations that involve cationic exchangers were therefore considered to act as a basis. A number of stripping agents which include NaOH, NH_4OH, H_2SO_4, HCl, and HNO_3 can be used in the stripping of rare earths from the extractant. The stripping of REEs from the extractant using inorganic acids occurs according to Equation 21.

$$(M)X_3.3HX_{org}+3H_{aq}^+ \longrightarrow (M)_{aq}^{3+}+ 3(HX)_{2(org)} \tag{21}$$
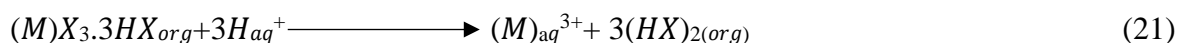
The choice of the stripping agent is dependent on the organic phase and type of salt under consideration (Gupta and Krishnamurthy, 2005; Desouky *et al.*, 2009). Alberts (2011) reported that over 80 % stripping of the rare earths Y and Er could be attained using 5 M HCl concentration and over 90 % Y, Er and Yb stripping could be attained with 5 M sulphuric acid. The author also reported that stripping is not affected much by rare earth content as long $(M)X_3.3HX$ remained the limiting factor. Reducing the O/A ratio also enhances stripping.

Wu, Wang and Li (2007) reported that when using DEHPA as the extractant, higher acidities are essential for stripping compared to other cationic exchangers. Ekberg *et al.* (2016) studied the effect of O/A ratio and acid concentration on yttrium and europium stripping from loaded 50 % Cyanex 923 solution. They found that more than 99 % stripping of Y and Eu could be achieved in one stage at an O/A ratio of 1:4 irrespective of acid concentration and when using an O/A ratio of 1:2, more than 96 % recovery is achievable in a single stage stripping process with 4 M HCl acid. Although the authors found better recoveries using 6 M acid concentration, they noted that at higher O/A ratios, the differences in recoveries become small. The authors also noted that stripping using lower acidic concentrations is possible although several stripping stages will be needed. Even though Cyanex 923 and DEHPA are different extractants which use different extraction mechanisms, Cyanex system results are considered since it is an organophosphorous acid.

Yang *et al.* (2013) reported that stripping behaviour using sulphuric acid is more effective than nitric acid. They found that Y, Eu and Ce are completely stripped from the organic phase using 0.5 M acid solution. No information on the O/A ratio used was provided. Gupta and Krishnamurthy (2005) summarised some of the processes used for rare earth separation from aqueous solutions. According to the Molycorp process, Eu and other REEs were stripped from loaded 10 % DEHPA using 5 M HCl. Sulphuric acid was then used to precipitate Eu as europium sulphate prior to calcination to produce 99.99 % Eu_2O_3. Mintek developed a process to recover REEs from the leachate solutions obtained after leaching sludge produced during phosphoric production (Preston *et al.*, 1996). TBP (40% v/v in Shellsol 2325) was used as the extractant. The pregnant organic phase was stripped using water and a mixed rare earth nitrate solution was produced. The product was treated with NH_3 and $C_2H_2O_4$ to yield a mixed rare earth oxalate. Calcination was performed on the precipitate to produce a mixed rare earth oxide of 89-94% purity. The product consisted mostly Eu, Ga, Nd and Sm.

From the limited literature reviewed, stripping was found to be largely dependent on pH of the stripping agent. Sulphuric acid was considered as the preferred stripping agent due to the strong reliance of the equilibrium constant on H^+ ion concentration. The stripping efficiency is largely reliant on the proton concentration in the stripping solution (Yang *et al.*, 2013). There are relatively more H^+ ions in H_2SO_4 compared to the other inorganic acids. As discussed in section 2.5, lanthanide contraction across the period results in differences in extraction and stripping ability of different REEs relative to each other. In this study, it was anticipated that all the rare earths would strip easier than Y due to their relative atomic numbers. Alberts (2011) recommended H_2SO_4 as the best stripping agent for rare earths followed by HCl and finally HNO_3.

2.7 Chemical Precipitation

Chemical precipitation is carried out to transfer the metal ions in an aqueous solution into insoluble precipitates (Cantrell and Byrne, 1987; Iwata, Imura and Suzuki, 1990) A common method to recover rare earths ions from stripping liquor is precipitation with oxalic acid or oxalate. The precipitates are then calcined to produce rare earth oxides. Equations 22 to 24 show chemical precipitation in nitrate, sulphate and chloride solutions.

$$2RE(NO_3)_3 + 3H_2C_2O_4 + nH_2O \rightarrow RE_2(C_2O_4)_3 \cdot nH2O + 6HNO_3 \qquad (22)$$

$$RE_2(SO_4)_3 + 3H_2C_2O_4 + nH_2O \rightarrow RE_2(C_2O_4)_3 \cdot nH2O + 3H_2SO_4 \qquad (23)$$

$$2RECl_3 + 3H2C_2O_4 + nH2O \rightarrow RE_2(C_2O_4)_3 \cdot nH2O + 6HCl \qquad (24)$$
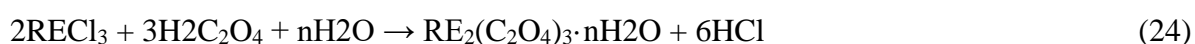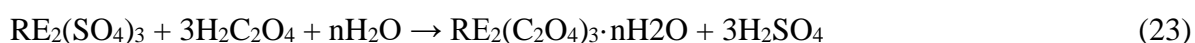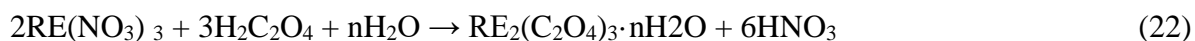
The solubility of rare earth oxalate increases with increase in acidity. In similar acid concentration, the precipitate solubility decreases from HCl, medium, HNO_3, and lastly H_2SO_4. The solubility of rare earth oxalates also decreases with increase in atomic number (Wu *et al.*, 2014). De Michelis *et al.* (2011) investigated the use of oxalic acid in in recovering Y and the impurity Ca from solution. They reported that at least the stoichiometric amount of oxalic acid is needed to obtain a pure yttrium oxalate n-hydrate of 99 % grade. Less than 2 % Ca precipitation occurred within 30 minutes of the precipitation tests. This is therefore a promising route to obtain Y of high purity after solvent extraction and stripping.

3. Experimental

3.1 Experimental Design

The received waste fluorescent powder sample was thoroughly mixed prior to splitting into representative samples using a rotary splitter. Experiments were divided into 3 phases as shown in Figure 3.1. The first phase involved leaching tests to recover Y and Eu from the "as received" waste fluorescent powders. The second phase involved Tb and Ce recovery from the leach residue produced from the first phase experiments. The final phase involved REE recovery from the leach solutions by solvent extraction.
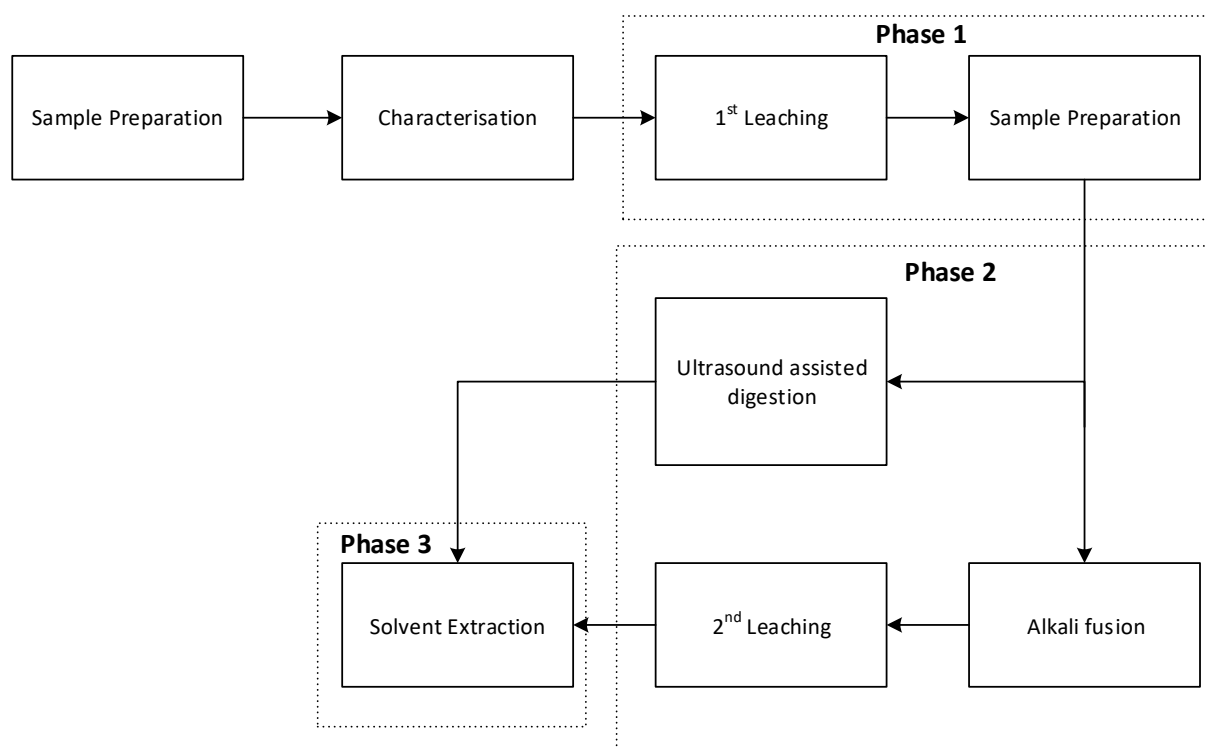
Figure 3.1: Schematic representation of experimental work carried out

3.2 Phosphor Powder Characterisation

The waste fluorescent phosphor powder investigated was obtained from a lamp recycling and mechanical processing facility in South Africa. The received powder was obtained from typical waste fluorescent lamps which were treated to remove hazardous mercury. Particle size characterisation of the received sample was performed using a Saturn DigiSizer 5200. XRD analysis was performed to determine the different phases present in the waste phosphor powder. Dissolution experiments using aqua regia were also performed to estimate the metal content in the waste fluorescent powders. The aqua regia solution was prepared by mixing

38

HCl solution (32 %) and HNO_3 solution (55 %) in a molar ratio of 3:1. Tests were performed in triplicate using 20 g samples. Each sample was digested in aqua regia and the concentration of metals in solution analysed using ICP-OES. The samples were digested in a 500 mL flat-bottomed flask at a temperature of 65 °C and a S/L ratio of 10 % (w/v). Aqua regia digestion results were used as an indication of the amount of metals present in the waste powders.

3.3 Phase 1: Yttrium and Europium Leaching

3.3.1 Experimental Strategy

The targeted rare earths in the first phase of experiments were Y and Eu. Sulphuric acid was the preferred lixiviant since it suppresses the dissolution of calcium the main impurity calcium (De Michelis *et al.*, 2011; Yang *et al.*, 2013). A full factorial experimental design was used with effects of acid concentration and temperature on leaching efficiency being the main factors investigated. The process conditions are shown in Table 3.1 and 3. 2.

Table 3.1: Factors investigated in the leaching tests

Factors		Levels		
		-1	0	1
A	Acid Concentration [M]	2	3.5	5
B	Temperature [°C]	30	60	90

Table 3.2: Full factorial design for performed experiments

Test Run	A	B
1	-1	-1
2	-1	0
3	-1	1
4	0	-1
5	0	0
6	0	1
7	1	-1
8	1	0
9	1	1
10	0	0
11	0	0
12	0	0

The remaining factors were fixed at conditions shown in Table 3.3 and the justification for selecting the conditions is stated.

Table 3.3: Fixed parameters for Y and Eu Leaching

Parameter	Fixed set point	Reason for set point
Agitation speed	600 rpm	Minimum agitation speed to ensure complete suspension of particles.
Solid to liquid ratio	10% w/v	This S/L ratio has commonly been used in previous studies (De Michelis *et al.*, 2011; Tunsu, Ekberg and Retegan, 2014)
Leaching Time	6 hours	Based on literature review discussed in section 2.4. This residence time was found to be adequate to come up with meaningful conclusions regarding leaching performance.

The results providing the highest recoveries for Y and Eu from the first leaching tests were used in the preparation of a bulk leach residue for phase 2 experiments.

3.3.2 Equipment

The leaching setup comprised of a 1.7 L jacketed glass reaction vessel with a working volume of 1 L and a hot plate coupled with a magnetic stirrer. The glass vessel was fitted to a metal stand to provide stability. The vessel had a glass lid which could be secured to the metal stand by means of bolts and stainless-steel ear wing butterfly nuts. The lid consisted of fittings for a condenser, temperature probe, sampling port and a pH probe. The condenser recycled vapours exiting the reaction vessel thereby preserving the reaction volume. A hot plate connected to a temperature probe was used to maintain temperature at the desired level. Figure 3.2 shows the experimental setup used during leaching tests.
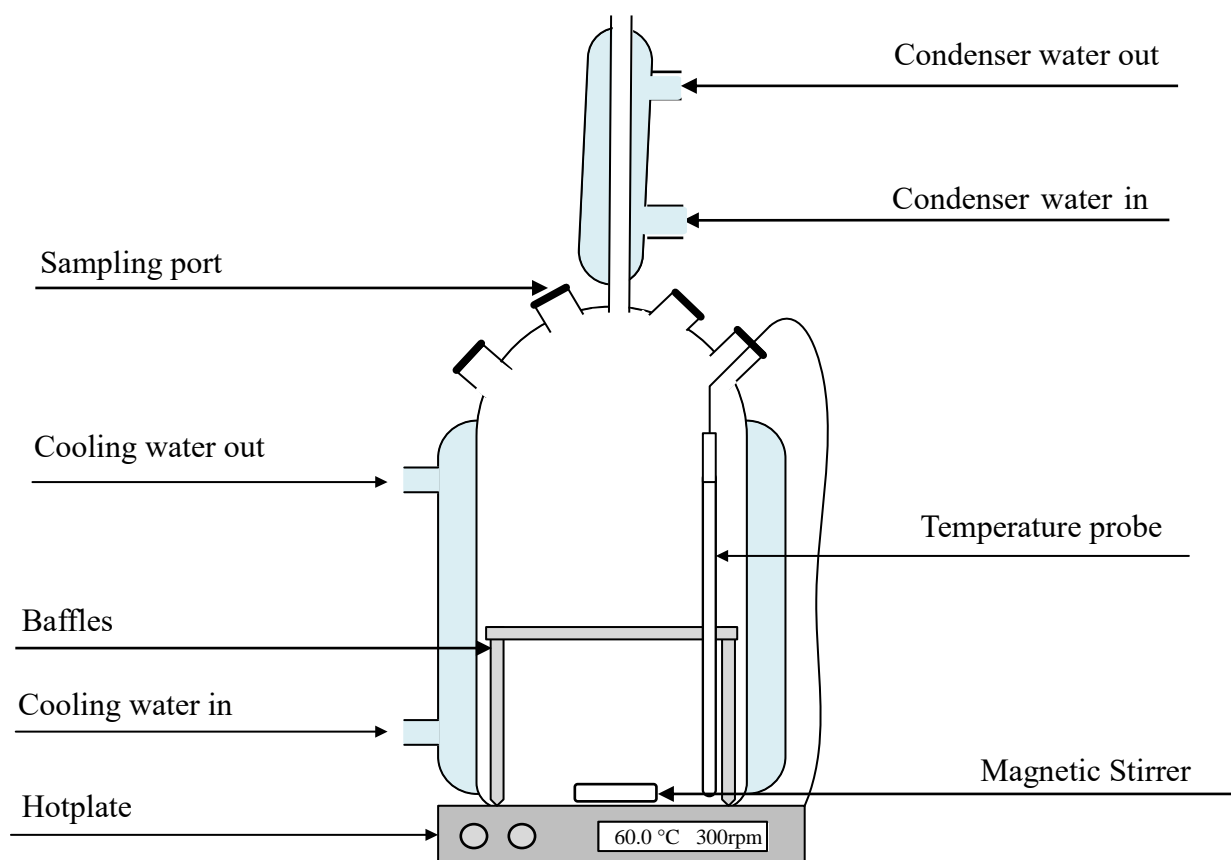
Figure 3.2: Laboratory scale leaching equipment

3.3.3 Materials

Sulphuric acid used in the preparation of the lixiviant for use in the first phase of experiments was supplied by Kimix at 98 wt%. Deionized water was used to dilute the concentrated acid to the desired concentration. The molarity and desired volume needed for each investigation determined the amount of concentrated acid needed based on calculations. The calculations are given in Table A.1 in Appendix A.

41

3.3.4 Experimental Procedure

500 mL of diluted sulphuric acid at the desired concentration was measured and poured into the reaction vessel. The hot plate and magnetic stirrer were switched on and set to the desired levels. Adequate time was allowed for the diluted acid to reach the desired leaching temperature. 50 g of the waste phosphor powder was then added marking the beginning of the experiment.

3 mL samples were taken at 15, 30, 45, 60, 120, 240 and 360 minute intervals. The samples were filtered using 0.22 µm syringe filters soon after sampling and the filtered solutions were stored in 15 mL centrifuge tubes. The solution remaining at the end of each test was filtered from solids using a Buchner funnel, filter paper and vacuum pump. This was performed immediately after stopping the experiment. The residue was washed with demineralised water before drying in an oven at 60 °C for 24 hours. Solution samples were analysed using ICP-OES while the residue was analysed using XRD analysis. A particle size analysis was conducted to determine the particle size distribution of the residue.

3.4 Phase 2: Ce and Tb Leaching

3.4.1 Experimental Strategy

A bulk sample of the first leach residue was prepared using conditions determined to give the highest yttrium and europium leaching recoveries in the first phase of experiments. After drying, wet sieving was performed on the residue to remove glass fragments which would affect downstream processes such as alkali fusion. The residue was wet sieved using a 25 µm prior to drying in an oven for 24 hours at 60 °C. The sample was then pulverised and split into 20 g samples on a rotary splitter.

The second phase of experiments involved Ce and Tb leaching from the blue and green phosphors which could not be leached in the first stage leaching. In this study, two different technologies were investigated. The first involved the use of ultrasound assisted leaching while the other involved alkali fusion prior to HCl leaching.

3.4.1.1 Ultrasound Assisted Digestion

Preliminary tests were performed to investigate the suitability of ultrasound leaching in the recovery of Ce and Tb from waste fluorescent powders as reported by Yang *et al*. (2013) and Tunsu *et al*. (2014). The conditions outlined in Table 3.4 used.

Table 3.4: Ultrasound assisted leaching preliminary tests conditions

Parameter	Fixed set point	Reason for parameter set point
Nitric acid Concentration	5 M	Adequate to ensure metal dissolution (Yang *et al.*, 2013)
Temperature	Not fixed	Temperature is known to increase due to the ultrasound. The temperature reaches about 60 °C after 60 minutes (Tanaka, Zhang and Saito, 2002)
Agitation	None	Solids are well suspended by bubbles due to the ultrasound
S/L Ratio	10 % (w/v)	Adequate to ensure enough mass transfer.
Time	2 hours	Adequate time for the leaching to take place (Tanaka, Zhang and Saito, 2002)
Power	200 W	Maximum power output provided by available device. This is lower compared to 750 W used by Diehl *et al.* (2018)
Frequency	20 kHz	Maximum frequency output provided by available device. This is the same as that used by Diehl *et al.* (2018)

Results from the preliminary test were used to determine if the route was worth investigation. Literature available on this by previous authors was not adequate to clearly conclude if the technology would work hence the preliminary experiments.

3.4.1.2 Alkali fusion and HCl Leaching

The other technology investigated involved the use of alkali fusion prior to HCl leaching to recover Tb and Ce as discussed in section 2.5.2.1. The leaching was performed using HCl as the lixiviant and employing the same experimental set up as that of Y and Eu leaching

discussed in section 3.3.2. A full factorial experimental design was used with acid concentration and temperature being the key variables under investigation. The process conditions are shown in Table 3.5 and 3.6. Parameters that were fixed are given in Table 3.7

Table 3.5: Factors investigated in the leaching tests

Factors		Levels		
		-1	0	1
A	Acid Concentration[M]	1	3	5
B	Temperature[°C]	30	60	90

Table 3.6: Full factorial design with replicated central point

Test Run	A	B
1	-1	-1
2	-1	0
3	-1	1
4	0	-1
5	0	0
6	0	1
7	1	-1
8	1	0
9	1	1
10	0	0
11	0	0
12	0	0

The other parameters were fixed at values stated in Table 3.7. Justification for the selected the values is also provided.

Table 3.7: Fixed parameters for Ce and Tb Leaching

Parameter	Fixed set point	Reason for set point
Agitation speed	300 rpm	Minimum agitation speed to ensure complete suspension of particles
Solid to liquid ratio	5 % (w/v)	This S/L ratio has commonly been used (De Michelis *et al.*, 2011; Tunsu *et al.*, 2014)
Leaching Time	2 hours	This residence time was found to be adequate to come up with meaningful conclusions regarding leaching performance.

3.4.2 Equipment

3.4.2.1 Ultrasound Assisted Digestion

The set up consisted of a 1 L vessel enclosed in a sound protective box. The lid of the sound protective box had a groove drilled inside enabling it to act as the reaction vessel lid also. The lid was fitted with 3 openings; 1 for the ultrasound probe, the second for the condenser and the 3rd acted as a sampling port. A UP200St ultrasonic processor was used as the ultrasound generating device. The frequency and maximum power of the device are 26 kHz and 200 W respectively. The sonic tip dipped into the solution was made from titanium.

3.4.2.2 Alkali Fusion and HCl Leaching Equipment

A Gallenkamp muffle furnace with a nominal temperature of 1100 ℃ was used for alkali fusion experiments. Four 100 mL alumina crucibles were used. The experimental setup used in the leaching of rare earths after alkali fusion was the same as the one used in the first phase of experiments shown in section 3.3 2, Figure 3.1.

3.4.3 Materials

3.4.3.1 Ultrasound Assisted Leaching

Kimix supplied nitric acid used in the preparation of the lixiviant for ultrasound-assisted digestion at 55 wt%. Demineralised water was used to dilute the concentrated acid to the desired concentration. The molarity and desired volume for each investigation determined the amount of concentrated acid needed based on calculations. The calculated volumes are shown in Table A.2 in appendix A.

3.4.3.2 Alkali fusion and HCl Leaching

Hydrochloric acid used in the preparation of the lixiviants for leaching of alkali fusion product was also supplied by Kimmix at 32 wt% respectively. The company also supplied sodium hydroxide pellets used in the alkali fusion process. Demineralised water was used to dilute the concentrated acid to the desired concentration and volume based on calculations. The calculated volumes are presented in Table A.3 Appendix A.

3.4.4 Experimental Procedure

300 mL of 5 M nitric acid was poured into the 500 mL reaction vessel used in ultrasound digestion. 30 g of the leach residue from the 1st phase was then added. The lid and ultrasound probe were secured in position and the probe was switched on to mark the beginning of the experiment. The sonic power and frequency were set at 200 W and 20 kHz. 3 mL samples were taken at 15, 30, 45, 60, 90 and 120-minute intervals. The samples were filtered as described in section 3.3.4. At the end of the experiment the ultrasound device was switched off and the shutdown was as described in section 3.3.4

Alkali fusion was performed in a muffle furnace using 100 mL alumina crucibles. The leach residue and sodium hydroxide were mixed in the ratio 1:1.5 (mass basis). Sintering was performed at a temperature of 800 ± 3 °C for 120 minutes (Liu *et al.*, 2014). The heating rate was set at 50 °C per minute and the sample was inserted after the temperature reached 500 °C. After 120 minutes, the furnace was switched off and the sample was left to cool for 10 minutes before removal from the crucibles. The fusion product was washed under magnetic stirring at 250 rpm for about 30 minutes at 60 °C. This was done in order to remove soluble material such as   sodium aluminate (Liu *et al.*, 2014). 500 mL of demineralised water per 100 g of product was used. The insoluble material was filtered prior to drying in an oven for 24 hours at a temperature of 60 °C. The sample was then pulverised and split into 15 g representative samples for leaching experiments. 300 mL of diluted HCl at the desired concentration was poured into the reaction vessel. The hot plate and magnetic stirrer were switched on before setting the temperature and agitation speed to the desired levels. Adequate time was allowed for the diluted acid to reach the desired temperature. 15 g of the waste phosphor powder was then added and this marked the start of the experiment. 3 mL samples were taken at 15, 30, 45, 60, 90 and 120-minute intervals. The samples were filtered using 0.22 µm syringe filters soon after sampling and the filtered solutions were put into 15 mL centrifuge tubes. The aqueous samples were then diluted with demineralised water as described in section 3.5 prior

to analysis. The remaining solution and solids were filtered immediately after switching off the hotplate and a Buchner funnel, filter paper and vacuum pump were used to separate the residue from the solution before drying it in an oven for 24 hours at 60 °C.

3.5 Analysis

Metal content in the obtained liquid samples was mostly determined using inductively coupled plasma optical emission spectrometry (ICP-OES) in the Process Engineering Analytical laboratory. Some samples were however sent for analysis by inductively coupled plasma mass spectrometry (ICP-MS) at the Central Analytical Facilities situated at the Geology Department. ICP-MS was used in the validation of ICP-OES results.

Soon after collection of 3 mL samples at regular intervals, a micropipette was used to draw a sample for dilution. This was done to ensure non-formation of precipitates in the collected sample before dilution. The samples were diluted with demineralised water before they were sent for analysis. The elements analysed included but were not limited to Eu, Y, Tb, Ce, Ca and Al.

3.6 Phase 3: Rare Earth Recovery by Solvent Extraction

3.6.1 Yttrium and Europium Solvent Extraction

3.6.1.1 Experimental Strategy

Two leaching experiments were performed to produce an adequate pregnant leach solution (PLS) for solvent extraction experiments. Sulphuric acid was used as the lixiviant. Table 3.8 shows the conditions that were used during the acid leaching.

Table 3.8: Conditions for first stage leaching

Parameter	Fixed set point
Acid Concentration	2 M
Temperature	25 °C
Agitation Speed	600 rpm
S/L Ratio	10 % (w/v)
Time	6 hours

A total of 4 L of PLS was prepared for the experiments to investigate the effect of three key variables (pH, O/A ratio and extractant concentration) on solvent extraction. A full factorial experimental design was conducted. The conditions investigated are presented in Table 3.9

Table 3.9: Experimental conditions investigated in solvent extraction experiments

Parameter	Level
Extractant Concentration [M]	0.5
	1
O/A Ratio	0.25
	0.5
	1
	1.5
	2.5
	5
pH	-0.25
	0.5
	1

3.6.1.2 Equipment

The leaching set up described in section 3.3.2 was used to prepare the PLS for the subsequent solvent extraction tests. Most published work on rare earth metal solvent extraction was carried out in a batch fashion (Morais and Ciminelli, 2007; Song *et al.*, 2009; Wang *et al.*, 2010; Tunsu *et al.*, 2014). Two magnetic stirrer hot plates and 2*100 mL beakers were used during solvent extraction experiments. Pipettes were used to transfer the extractant and aqueous phase into the beakers. In order to adjust pH, NaOH was added to the organic/aqueous dispersion using an adjustable pipette. A pH meter was used to measure the pH of the aqueous solution. Mixing of the organic/aqueous dispersion was done using magnetic stirrer. After agitation, the dispersion was transferred into 2*100 mL separation funnels for phase separation to take place. Sufficient time was allowed for the organic and aqueous phases to separate. Once separation was complete, the aqueous phases were collected from the separation funnels. The volume of the remaining aqueous solution was measured in a measuring cylinder prior to dilution for analysis.

3.6.1.3 Materials

Sulphuric acid used as lixiviant for acid leaching and stripping experiments was supplied by Kimix at 98 wt%. Demineralised water was used to dilute the concentrated acid to the desired concentration. DEHPA used for solvent extraction experiments was supplied by a Chinese company called Hong Kong Guokang Bio-Technology Co. Ltd. Kerosene supplied by Kimmix was used to dilute the DEHPA to desired concentration. NaOH pellets used to make 2 M and 5 M NaOH solutions for pH adjustments were also supplied by Kimmix.

3.6.1.4 Experimental Procedure

Before commencement of solvent extraction experiments, two leaching experiments were conducted to prepare 4 litres of pregnant leach solution. After leaching, the PLS was filtered from the solids using a glass Büchner funnel, filter flask and filter paper. 5 M NaOH solution was used for pH adjustment. Appropriate amounts of 0.5 M and 1 M DEHPA solutions were prepared using kerosene as the diluent. Measured volumes of the aqueous phase were added to a beaker using a pipette. Thereafter, the addition of the organic phase followed depending on the O/A ratio. Solvent extraction experiments were conducted at O/A ratios of 0.25, 0.5, 1, 1.5, 2.5 and 5. Mixing of the organic/aqueous dispersion was done using a magnetic stirrer. After every 2 minutes, a pH measurement was taken prior to adjustment using 2 M NaOH. This procedure was repeated until the pH of the aqueous phase stabilised at the desired value. This indicated that the system had reached equilibrium. Aqueous phase pH was maintained at 0.25, 0.5 and 1. Preliminary tests indicated that precipitation of Y and Eu occurred at pH levels beyond 2, as a result solvent extraction experiments were carried out at lower pH levels. Once equilibrium was reached, the dispersion was transferred to a separation funnel and adequate time was allowed for phase separation to take place before collection of the organic and aqueous phases. The aqueous phase volume after separation was then measured before storage into 15 mL centrifuge tubes. Thirty-six solvent extraction experiments were performed.

Solvent extraction tests at a pH of -0.25 were conducted using PLS2 as the aqueous phase without any addition of NaOH for pH adjustment. Each experiment lasted for about 30 minutes before equilibrium could be achieved. For higher pH, NaOH was added for pH adjustment. Experiments at pH 0.5 were conducted using PLS2 as the aqueous phase. For solvent extraction tests performed at pH 1, PLS1 was used as the aqueous phase at O/A ratios of 0.5, 1, 1.5, 2.5 and 5, while PLS2 was used as the aqueous phase at O/A ratios of 0.25.

3.6.2 Cerium and Terbium Solvent Extraction

3.6.2.1 Experimental Strategy

Alkali fusion product from the second phase of experiments was leached with HCl to prepare a bulk leach solution for Ce and Tb solvent extraction experiments. A 1.5 L PLS was prepared using conditions shown in Table 3.10.

Table 3.10: Conditions for second stage leaching

Parameter	Fixed set point
Acid Concentration	5 M
Temperature	60 °C
Stirring Speed	600 rpm
S/L Ratio	5 % (w/v)
Time	45 minutes

The effect of three key variables (pH, O/A ratio and extractant concentration) was investigated using a full factorial experimental design. The conditions investigated are shown in Table 3.11.

Table 3.11: Experimental conditions for Ce and Tb solvent extraction tests

Parameter	Value
Extractant Concentration [M]	0.5
	1
O/A Ratio	1
	1.5
	2
	2.5
	5
pH	0.25
	0.5
	1
	1.5
	2

3.6.2.2 Equipment

The solvent extraction equipment for Ce and Tb was the same as that used for Y and Eu solvent extraction.

3.6.2.3 Materials

HCl used as lixiviant for acid leaching and stripping experiments was supplied by Kimix at 32 wt%. Demineralised water was used to dilute the concentrated acid to the desired concentration (5 M). DEHPA supplied by a Hong Kong Guokang Bio-Technology Co. Ltd was used in Ce and Tb solvent extraction tests. As discussed in section 3.6.1.3, kerosene supplied by Kimmix was used in the dilution of DEHPA to the desired concentration. NaOH pellets supplied by Kimmix were used to make NaOH solution for pH adjustment.

3.6.2.4 Experimental Procedure

Before commencement of solvent extraction experiments, a 1.5 L leach solution was prepared using conditions that gave the best Ce and Tb recoveries. After leaching, the leach solution was filtered from the solids using a vacuum filter. 5 M NaOH solution was used for pH adjustment. 700 mL of 0.5 M and 1 M DEHPA solutions were prepared using kerosene as the diluent. 10 mL of aqueous solution was measured and added to a beaker using a pipette. DEHPA was then added depending on the O/A ratio. Solvent extraction experiments were conducted at O/A ratios of 1, 1.5,2, 2.5 and 5. Adequate mixing of the organic/aqueous dispersion was achieved using a magnetic stirrer at 300 rpm. After every 2 minutes of mixing, a pH measurement was taken before pH adjustment using NaOH solution. This procedure was repeated until the pH of the aqueous phase stabilised at the desired value. Aqueous phase pH was maintained at 0.25, 0.5, 1, 1.5 and 2. After achieving the desired pH, the dispersion was transferred to a separation funnel and adequate time was allowed for phase separation to take place. The aqueous phase was then collected and filtered using, 0.22 µm syringe filters to get rid of any trace amounts of the organic phase. Solution samples were stored in 15 mL centrifuge tubes before dilution. The procedure for sample dilution and analysis was the same as that outlined in section 3.5.

3.7 Repeatability

The repeatability of the solvent extraction tests was interpreted using Equation 25 (Measey, 2003)

$$r = \frac{MS_{between} - MS_{within}}{MS_{between} + (n-1)MS_{within}} \qquad (25)$$

Where:　　　　$MS_{between}$ = Mean squares between groups

MS_{within} = Mean squares within groups

n = Number of repeated measurements

r = Repeatability

The repeatability given by equation 25 ranges from 0 to 1. It gives the extent of discrepancy which comes from differences between groups. Table 3.12 shows the terms that are used to describe repeatability.

Table 3.12: Terms used to describe repeatability

R	Term
0-0.2	Slight repeatability
0.2-0.4	Low repeatability
0.4-0.7	Moderate repeatability
0.7-0.9	High repeatability
0.9-1	Very high repeatability

The mean square values used in the calculation of the repeatability value were obtained from a single factor ANOVA analysis carried out on Microsoft Excel.

4. Results and Discussion

4.1 Phosphor Powder Characterisation

4.1.1 Metal Content Determination

As discussed in Section 3.2, aqua regia digestion followed by ICP analysis was used to determine the rare earth content of the waste phosphor powder used as feed material. Three characterisation tests were conducted and the average metal content of the phosphor powder is shown in Table 4.1, together with the associated standard deviations. The aqua regia test results on the feed were presumed to be representative of the entire sample.

Table 4.1: Metal content in as-received waste fluorescent powder

Metal	Average metal content (g/kg)	Metal	Average metal content (g/kg)
Al	12.19 ± 2.1	Fe	5.6 ± 0.2
B	0.55 ± 0.03	Gd	0.8 ± 0.03
Ba	1.2 ± 0.09	La	2.2 ± 1.3
Ca	231 ± 7.1	Mg	2.9 ± 0.04
Ce	2.1 ± 0.5	Tb	1.8 ± 0.2
Cu	0.6 ± 0.03	Y	42.3 ± 0.02
Eu	2.9 ± 0.02	Zn	7.1 ± 3.9

The targeted REEs Y, Eu, Ce, Tb, La and Gd were present in the waste powders. Other elements mainly Ca were also present together with a variety of metal ions (Al, Fe, Ba, Cu etc.). The most prevalent REE was Y with an average of 42.3 ± 0.02 g/kg followed by Eu averaging at 2.9 ± 0.02 g/kg. This is no surprise since Y and Eu constitute the red phosphor which accounts for more than 50 % of the waste phosphor powder (Wu *et al.*, 2013).

4.1.2 Particle Size Analysis

Particle size analysis of the received powder was conducted as discussed in Section 3.2. The results obtained are shown in Figure 4.1. The results indicate the presence of two distinct particle sizes in the waste phosphor powders. The phosphors particles are mainly concentrated in the <25 µm fraction. The coarser fraction (> 50 µm) consists mainly of broken glass fragments (De Michelis *et al.*, 2011; Binnemans and Jones, 2014; Eduafo, 2016). The glass particles vary significantly in size, ranging from over 300 µm to less than 25 µm. This was

verified using a wet sieve analysis using a 25 µm laboratory sieve. Glass and other impurity fractions are generated during lamp dismantling.
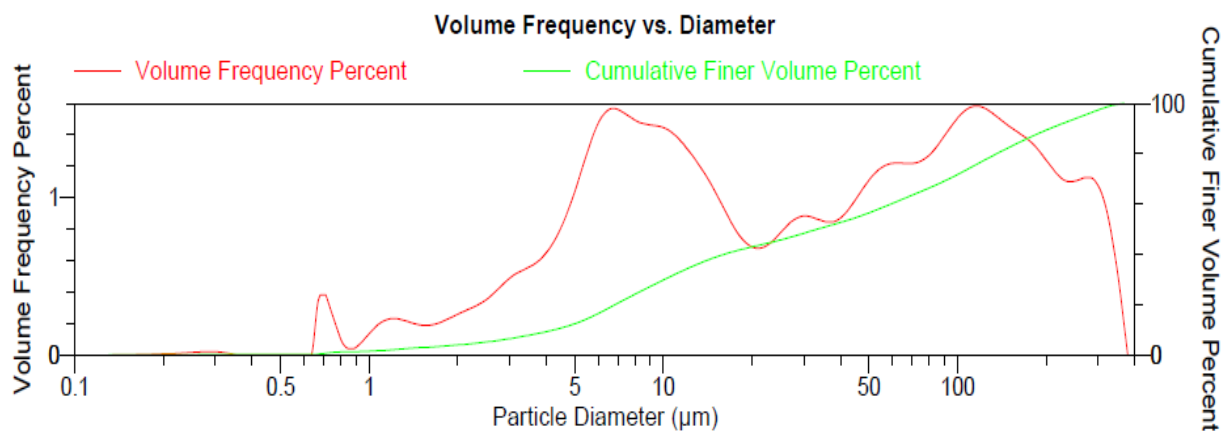
Figure 4.1: Particle size analysis

4.1.3 X-ray Diffraction Analysis (XRD)

X-ray diffraction was carried out to determine the phases of the minerals present in the received powder. The results obtained are shown in Figure 4.2 below.
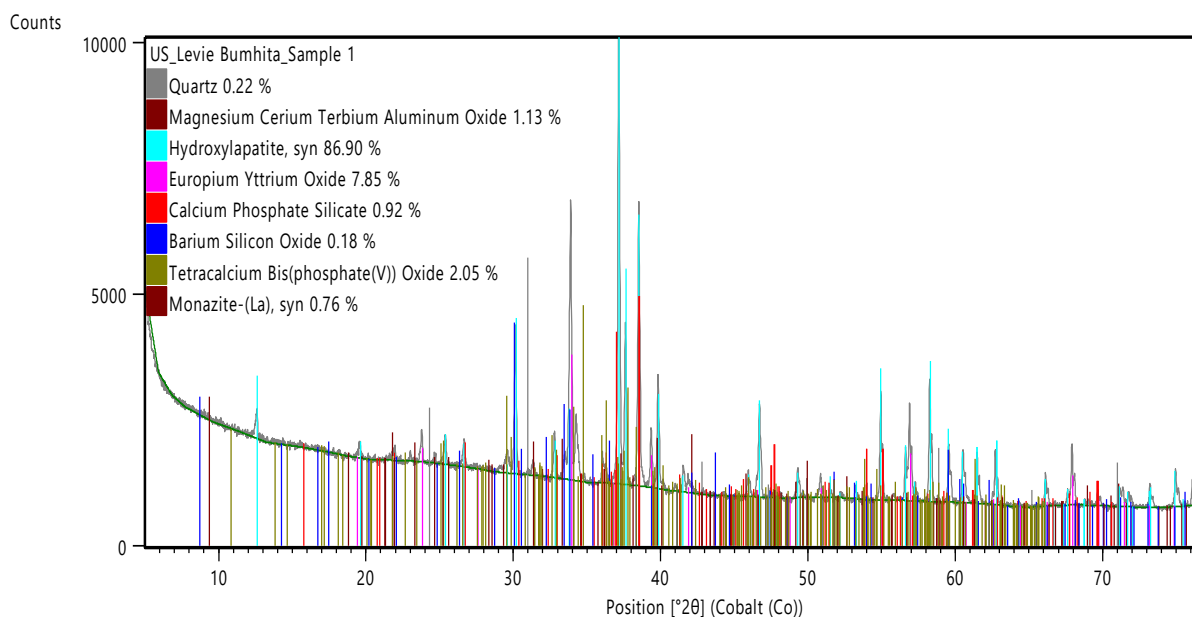
Figure 4.2: XRD plot of waste florescent powders for phase identification

The major phases identified were quartz (SiO_2), magnesium cerium terbium aluminium oxide (($Ce,Tb)MgAl_{11}O_{19}$), hydroxylapatite($Ca_5(PO_4)_3(OH)$), yttrium europium oxide ($Y_2O_3:Eu^{3+}$), monazite(($Ce,La,Nd,Th)(PO_4,SiO_4$)), barium silicon oxide ($BaSiO_3$), tetracalcium bis(phosphate(V)) oxide ($Ca_4(PO_4)_2O$), and calcium phosphate silicate (CSPH). The strong peaks of hydroxylapatite (86.90 %) are a result of the addition of white phosphors, which are

54

similar in nature to the apatite phase. SiO_2 (0.22 %) is barely present in the feed material despite the presence of glass as revealed by visual inspection of the powder. This is because the bulk of SiO_2 is present as glass which is amorphous and is undetectable by X-ray analysis. Yttrium oxide, magnesium cerium terbium aluminium oxide and monazite that contain most of REE concentrate are mainly present in the finest particles present in the powder (De Michelis *et al.*, 2011; Binnemans and Jones, 2014; Eduafo, 2016). The blue phosphors were undetected by XRD probably due to low concentration.

4.2 Y and Eu Leaching

In order to explain rare earth leaching with inorganic acids, three main factors that affect the rate and extent of leaching will be discussed in this section. These factors are:

- Enthalpy of reaction

- Solubility of impurity precipitates

- Solubility of rare earth products

The extent of leaching is dependent on whether the reaction is endothermic or exothermic. As shown in Appendix D, Table D.1 and D.2, the reactions between Y and Eu with sulphuric acid are exothermic. Although an increase in temperature results an increase in rate of reaction, this is not the case when it comes to the extent of reaction. With an increase in temperature, the reacting species possess more kinetic energy thereby increasing the frequency of collisions. However, with an increase in temperature, in keeping with Le Chatelier's principle, the reaction will shift in such a way as to favour the backward reaction until a new equilibrium has been achieved. The higher the temperature increase, the further the balance at equilibrium shifts back toward reactants resulting in a decrease in the extent of reaction (less products produced). Tables 2.4 and 2.5 show that the equilibrium constant decreases with increasing temperature.

Co-precipitation may also occur during acid leaching. Rare earth sulphates, lead sulphate, barium sulphate and calcium sulphates were reported to form during digestion with sulphuric acid (De Michelis *et al.*, 2011; Zhang *et al.*, 2013). Calcium orthophosphate present in phosphor powder is attacked by H_2SO_4 to produce orthophosphoric acid and calcium sulphate slurry (Rabah, 2008) according to Equation 26.

$$Ca_3(PO4)_2 + 3H_2SO_4 \longrightarrow 3CaSO_4 + 2H_3PO_4 \hspace{2cm} (26)$$
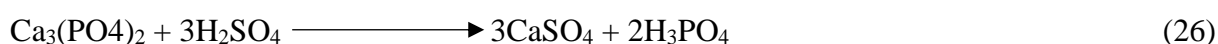
Calcium sulphate precipitation is due to its low solubility (De Michelis *et al.*, 2011; Innocenzi *et al.*, 2013). The solubility of calcium sulphate and its hydrates generally decreases with

increasing temperature (Zeng and Wang, 2011). When co-precipitation occurs, impurity precipitates can entrap normally soluble rare earths and carry them out of solution during filtration. The impurities can also entrap Y^{3+} and Eu^{3+} (Chen *et al.*, 2017). Normally soluble compounds may also precipitate as $Y_2(SO_4)_3.8H_2O$ and $Eu_2(SO_4)_3.8H_2O$ (Innocenzi *et al.*, 2013; Zhang *et al.*, 2013). This can happen through formation of mixed crystals by adsorption, occlusion or mechanical entrapment. In this case, the rare earths are lost in the residue.

$PbSO_4$, and $BaSO_4$ precipitates form according to Equation 27 where M is Pb or Ba.

$$M^{2+}_{(aq)} + SO_4^{2-}_{(aq)} \longrightarrow MSO_{4\,(s)} \hspace{3cm} (27)$$

Although solubilities of $PbSO_4$ and $BaSO_4$ increase with increasing temperature in sulphuric acid solutions (Crockford and Addleston, 1935), the solubilities are very low (De Michelis *et al.*, 2011). The effect of temperature on the solubility of the metal sulphates is shown in Table 4.2.

Table 4.2: Effect of temperature on the solubility of precipitates that form during acid leaching (Innocenzi et al., 2013; Zhang et al., 2013)

Substance	Solubility (g/100 g H_2O)
$CaSO_4.2H_2O$	0.264, 0.244 and 0.205 at 30, 60 and 90 ℃
$BaSO_4$	0.000248 and 0.000285 at 20 and 30 ℃
$PbSO_4$	0.003836 at 20 ℃
$Eu_2(SO_4)_3.8H_2O$	2.56 at 20 ℃
$Y_2(SO_4)_3.8H_2O$	6.78, 4.44 and 2.2 at 30, 60 and 90 ℃

Acid concentration also affects the rate and extent of leaching. An increase in concentration generally results in an increase in frequency of collisions between reacting species. This causes an increase in the rate of reaction. An increase in acid concentration however may also favour side reactions which cause the formation of precipitates. According to Equation 23 and 24 if acid concentration increases, the rate of precipitate formation also increases. Zeng and Wang (2011) reported that the solubility of gypsum first increases and then decreases with increasing sulphuric acid concentration. Faster kinetics in impurity formation negatively hinder rare earth metal leaching in two ways. Firstly, the formed precipitates may entrain the rare earth ions during filtration. Secondly, according to Equation 28, an increase in acid concentration results

in an increase in SO_4^{2-} ions within the system. When this occurs, the system will shift in order to get rid of the anions hence favouring the reverse reaction.

$$Y_2(SO_4)_3.8H_2O \longleftrightarrow 2Y^{3+} + 3SO_4^{2-} + 8H_2O \tag{28}$$

4.2.1 Effect of Temperature on Y and Eu Leaching

Figure 4.3 (a) to (e) show the effect of temperature on the rate and extent of Y and Eu leaching at constant acid concentration. Graphs (a) and (b) show the effect of temperature at an acid concentration of 2 M. It can be seen that an increase in temperature from 30 to 60 ºC results in an increase in the rate and extent of leaching for both Y and Eu. Percentage dissolution for both Y and Eu increase gradually with time at 30 ºC. Equilibrium could only be achieved after about 240 minutes of leaching. For both 60 and 90 °C, equilibrium was achieved faster after about 30 minutes of dissolution. Temperature does not have a significant impact on the kinetics and extent of Y recovery from 60 °C to 90 °C with the overall recovery varying within a range of roughly 5%. This suggests that the leaching reaction at the two temperatures had reached equilibrium. This is also in agreement with what Yang *et al.* (2013) found in their study where they reported that Y recovery reaches constant values beyond a temperature of 70 ºC. At 2 M, sulphate ions concentration is low hence it possible that co-precipitation is minimum.

There was a notable decrease in the extent of Eu leaching when temperature was increased from 60 to 90 ºC. This is probably due to preferential dissolution of Y compared to Eu. It is possible that most of the acid was used for Y dissolution with only a little left for Eu dissolution.
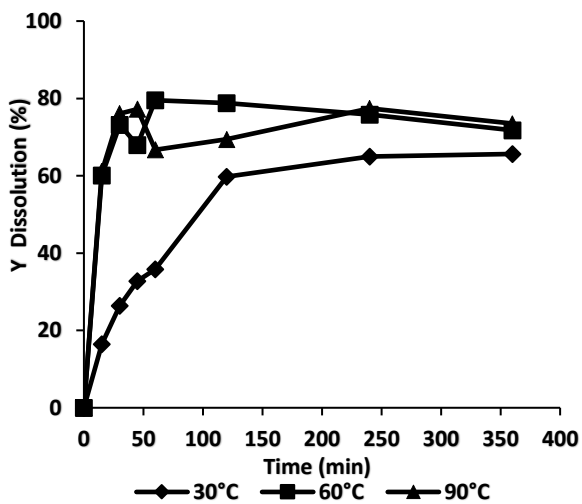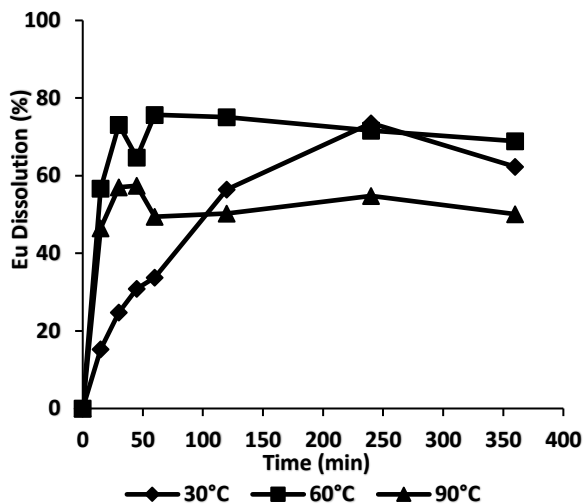
(a)   (b)
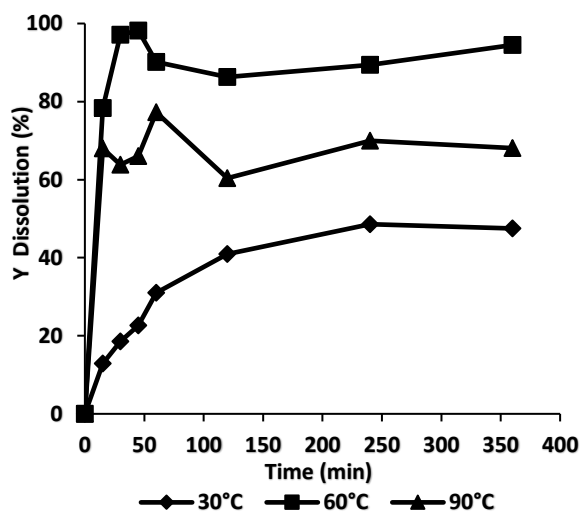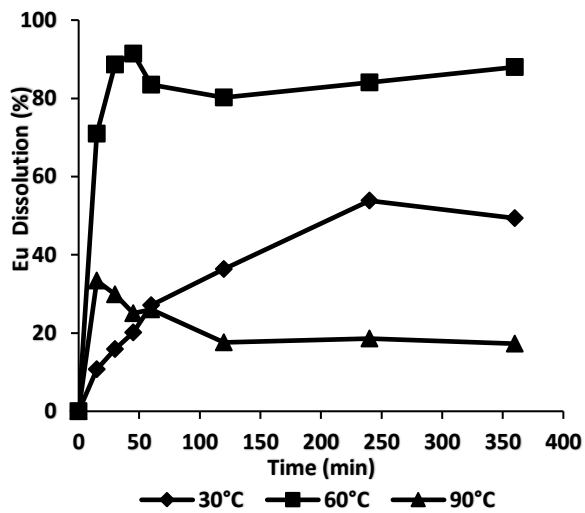
(c)   (d)
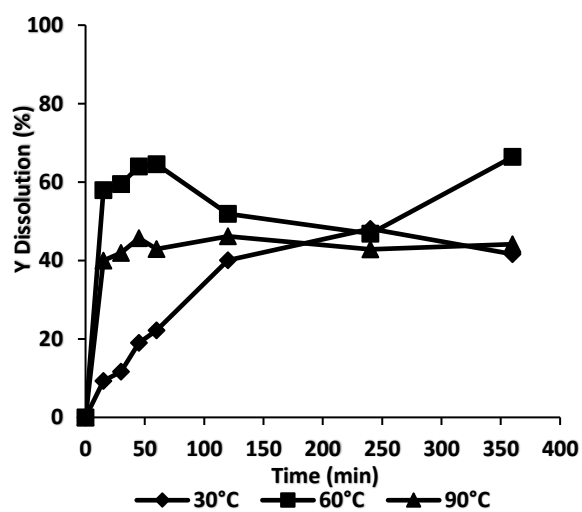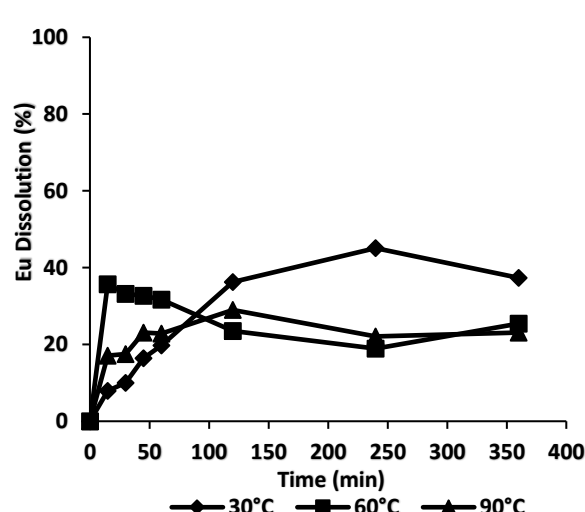
(e)   (f)

Figure 4.3: The effect of temperature on Y leaching at a) 2M, c) 3.5M, and e) 5M as well as Eu leaching at b) 2M, d) 3.5 M, and f) 5M

Figure 4.3 (c) and (d) show Y and Eu leaching at 3.5 M and variable temperature levels. For 30 ℃, the leaching reaction reached equilibrium after 240 minutes of leaching for both Y and Eu. Increasing the temperature to 60 ℃ resulted in an increase in the rate and extent of leaching with equilibrium achieved after 45 minutes of dissolution. As explained in section 4.2 faster leaching kinetics are expected with an increase in temperature. The highest Y and Eu recoveries were found to be 98.2 % and 91.4 % respectively. This increase in percentage dissolution can also be a result of increase in acid concentration from 2 M to 3.5 M. Increasing the temperature from 60 to 90 °C resulted in a significant decrease in the rate and and extent of leaching of both Y and Eu. A possible explanation for this phenomenon is rapid co-precipitation which may be occurring at 90 ℃ soon after the leaching commences. Co-precipitation affects the overall mass transfer of the system thereby inhibiting rare earth leaching. When temperature is increased from 30 to 60 °C the rate of precipitate formation is favoured less compared to the extent to which the rate of dissolution of the rare earths is favoured. However, as temperature is increased to 90 °C it is possible that the rate of precipitation of calcium sulphates, barium sulphate and lead sulphate increased more significantly. Calcium sulphate and its hydrates are the dominant precipitates that form during the leaching as evident in the XRD results shown in Figure 4.4.
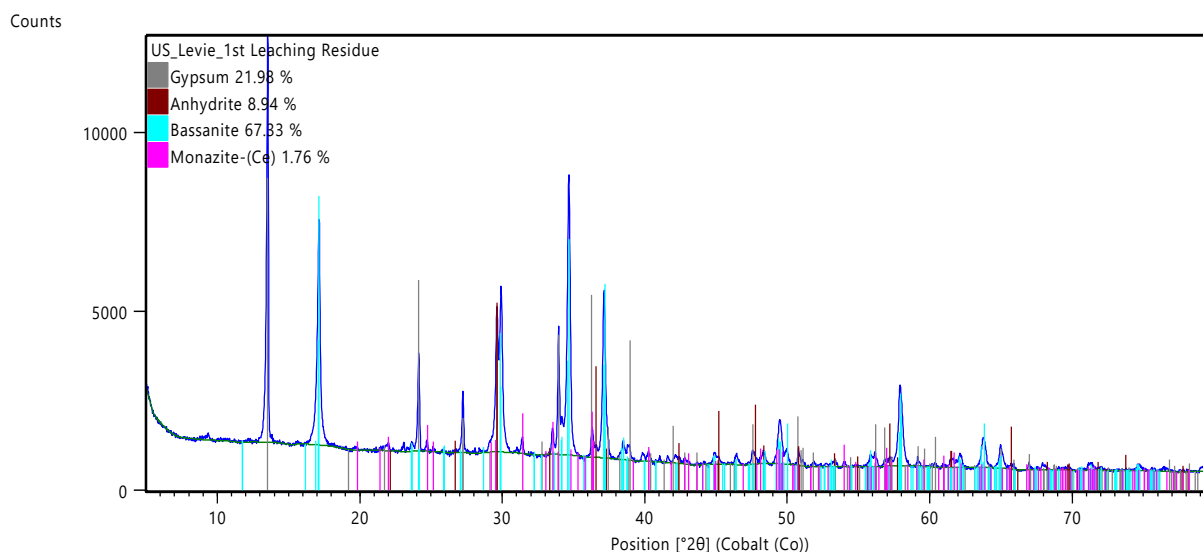
Figure 4.4: XRD plot of leach residue for phase identification

Calcium sulphate compounds such as gypsum ($CaSO_4 \cdot 2H_2O$), anhydrite ($CaSO_4$) and bassanite ($2CaSO_4.(H_2O)$) constitute 98.24 % of the identified phases. The remaining 1.76 % constituting monazite $(Ce,La,Nd,Th)(PO_4,SiO_4)$ which contains rare earths. Calcium sulphate precipitates have low solubility.The solubility of gypsum is known to increase up to 40 ℃ then decrease at higher temperatures (Zeng and Wang, 2011). As previously discussed, co-precipitation may result in entrainment of normally soluble rare earths and precipitation of rare earths. Another

possible reason for the decrease in leaching rate and percentage dissolution is $Y_2(SO_4)_3.8H_2O$ precipitation. As presented in Table 4.2, the solubility of $Y_2(SO_4)_3.8H_2O$ decreases with increase in temperature and is at its lowest at 90 ℃. It is therefore a possibility that this may have caused the decrease in leaching rate and percentage extraction. Maximum Y and Eu recovery was 77.2 % and 33.4 % respectively when the operating temperature was 90 ℃.

The effect of temperature on leaching kinetics and percentage dissolution at a constant H_2SO_4 molarity of 5 M was also investigated. When operating at 30 ℃, equilibrium was achieved after 240 minutes of leaching. This can be attributed to slow leaching kinetics at low temperatures. Maximum Y and Eu recoveries were 48.1 % and 45.1% respectively. An increase in temperature to 60 ℃ resulted in an increase in both leaching rate and percentage dissolution. This is expected since the overall kinetic energy of the system increases and more species now possess enough energy to react. For Y, equilibrium was achieved after 60 minutes corresponding to a percentage dissolution of 64.6 %. Equilibrium was achieved after only 15 minutes of leaching for Eu corresponding to a percentage dissolution of 35.7 %. Recoveries for both rare earths were lower compared to those obtained when operating at 3.5 M. This is probably due to rapid precipitation of calcium sulphates together with rare earth sulphates at 5 M. When operating at 90 ℃, a decrease in leaching rate and percentage rare earth dissolution was experienced. As was the case when operating at 90 ℃ and 3.5 M, it is possible that operating at such a high temperature favoured the rapid occurrence of side reaction. Increased precipitation rates may therefore be the reason for the decrease in rate and extent of leaching. Precipitation inhibits leaching. Another possible explanation for decrease in leaching rates and percentage is rare earth precipitation as discussed previously.Also, it is possible that since the reactions between both rare earths with sulphuric acid (Equations 7 and 8) are exothermic, increasing temperature will favour the backward reaction. Equilibrium was reached after about 120 minutes of leaching for both Y and Eu with recoveries of 45.7 % and 29 % respectively.

4.2.2 Effect of Concentration on Y and Eu Leaching

The effect of acid concentration on Y and Eu recovery at a constant temperature of 30 °C is shown in Figure 4.5 (a) and (b). The results show that the highest Y and Eu recovery could be achieved using 2 M sulphuric acid. This corresponds to recoveries of 65.5 % and 72.9 % for Y and Eu respectively. Leaching kinetics were generally slow and equilibrium for all the three concentrations was achieved after about 240 minutes of leaching.
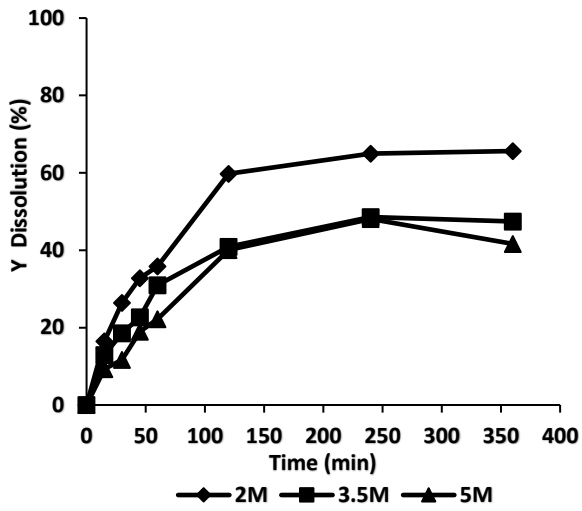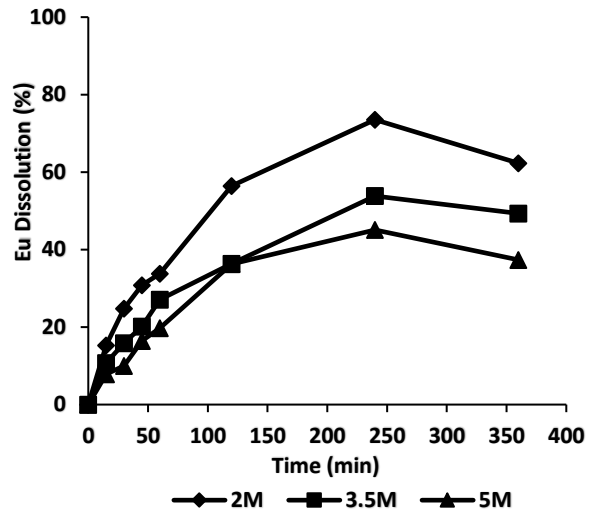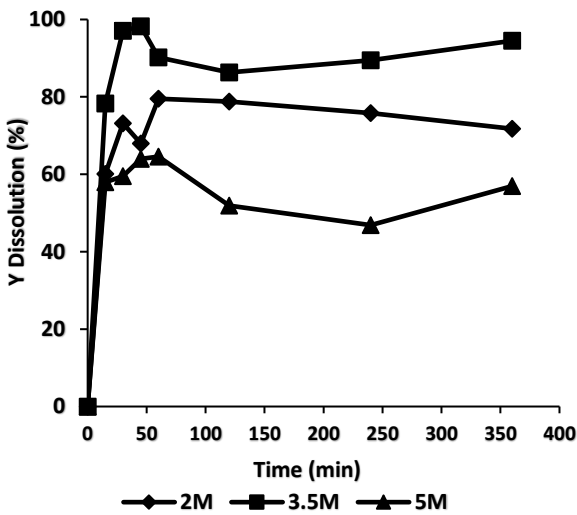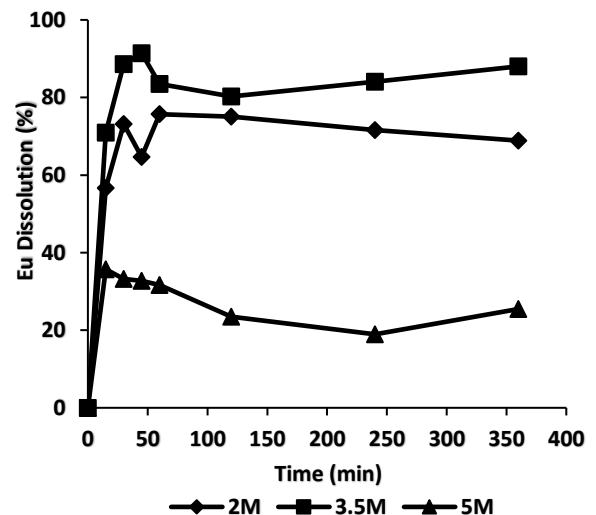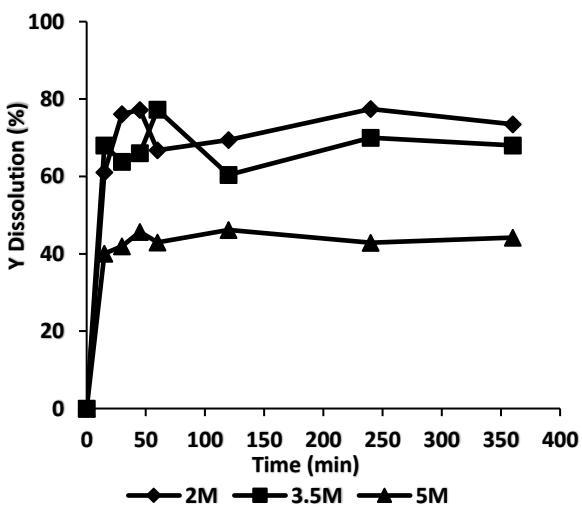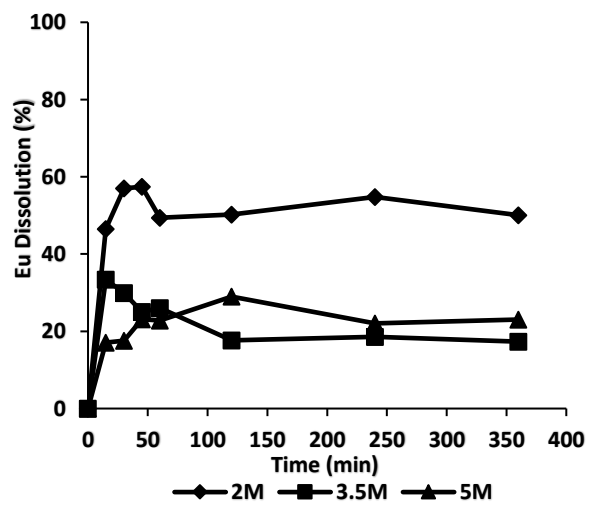
Figure 4.5: Y leaching at a) 30 ºC, c) 60 ºC, e) 90 ºC; Eu leaching at b) 30 ºC, d) 60 ºC, f) 90 ºC

Increasing acid concentration from 2 M to 3.5 M and 5 M caused a decrease in both the rate and percentage dissolution for both rare earths. A possible explanation for this behaviour is the fact that competing reactions are being favoured at higher acid concentrations in comparison to rare earth dissolution. According to Equations 26 to 28, increasing acid concentration favours the formation of insoluble precipitates that inhibit rare earth metal leaching as discussed in section 4.2. In order for a chemical reaction to take place, the reacting species must collide with enough energy for the reaction to take place. Since the leaching was performed at a low temperature of 30 ℃, it is a possibility that increasing acid concentration could not increase the rate and extent of reaction as expected since very few particles possessed enough energy for them to react.

Figure 4.5 (c) and (d) show the effect of concentration at 60 °C. The rate and extent of leaching increased with an increase in acid concentration from 2 M to 3.5 M. This is expected since the frequency of collisions between particle increases at higher concentrations. Beyond 3.5 M however, leaching kinetics and rare earth dissolution for both Y and Eu dropped significantly. This is contradictory to what Yang *et al.* (2013) found. They reported that constant recoveries are expected beyond 3 M. In this case there was a significant drop in recovery for both Y and Eu. A possible explanation is that at higher acid concentration, side reactions that favour precipitate formation become dominant. The rate of rare earth dissolution at 5 M probably becomes less to that of precipitate formation and as a result the extent of leaching decrease. It can therefore be concluded that in this study, 3.5 M is the optimum concentration. This behaviour is in contrast to findings obtained when using a temperature of 30 °C where the highest recovery was obtained at 2 M. It is therefore a possibility that an increase in kinetic energy of the reacting species at 60 °C resulted in better mass transfer hence better recoveries. In this case, the rate of rare earth dissolution is more rapid compared to that of precipitate formation.

Figure 4.5 (e) and (f) show the leaching behaviour of Y and Eu at 90 °C and variable acid concentrations. Generally, as temperature increases the solubility of rare earths sulphates and metal sulphate precipitates that form decreases. Increasing acid concentration from 2 M to 3.5 M resulted in a decrease in leaching extent. It is clear that in this case the effect of temperature is quite significant. Side reactions may have occurred at faster rates when using higher acid concentrations at this temperature hence leaching was inhibited. Zeng & Wang (2011) reported that calcium precipitates such as gypsum have solubilities that first increase

62

and then decrease with increasing acid concentration. It is therefore also a possibility that the decrease in impurity precipitate solubility at 5 M is contributing to the lower leaching rates and recoveries at all the temperatures investigated. It can therefore be concluded that a combination of high concentration and temperature results in low recoveries.

A statistical analysis was conducted to determine which one of the two investigated parameters (temperature and concentration) had the largest influence on yttrium recovery after 45 minutes of leaching. The p values given in Table F.1 (Appendix F) show that at a 95 % confidence level, both temperature and acid concentration have a significant quadratic effect on the rare earth metal recovery. The linear effect of temperature also has a significant effect on the extent of recovery. However, the linear effect of concentration and interaction effects were observed to have no significant effect on the extent of Y leaching. The findings of the statistical analysis were in agreement to what was observed from the graphs in Figure 4.3 and 4.5. The variation of recovery with temperature and concentration is given by surface profiles shown in Figure F.1 Appendix F.

4.2.3 Summary

The red phosphors in the waste powder could be readily leached in the first stage leaching using H_2SO_4. Y and Eu exist as rare earth oxides which are readily soluble in acidic solutions. Tb and Ce could barely be dissolved during the first step acid leaching. The rare earths exist in the green phosphor powder which comprises complex aluminates which are difficult to leach (De Michelis *et al.*, 2011). Based on the obtained leaching results, the use of conditions presented in Table 4.3 was suggested in order to prepare a bulk sample for subsequent experiments.

Table 4.3: Suggested conditions for first stage leaching

Parameter	Set point
Acid Concentration	3.5 M
Temperature	60 °C
Agitation Speed	600 rpm
S/L Ratio	10 % (w/v)
Time	45 minutes

4.3 Ce and Tb Leaching

4.3.1 First Leach Residue and Alkali Fusion Product Characterisation

4.3.1.1 First Leach Residue Particle Size Analysis

Particle size analysis results of the first leach residue are shown in Figure 4.6. The results indicate that one of the peaks shown in Figure 4.1 (< 25 µm) had disappeared due to the first stage leaching. This was expected since waste phosphor powders contain about 55 % of red phosphor component (Y_2O_3: Eu) which could easily be leached. The remaining peak represented mainly fragmented glass particles and other impurity fractions as discussed in section 4.1.2. This explanation is supported by XRD results on the leach residue shown in Figure 4.4. In this case peaks corresponding to yttrium europium oxide (7.85 %) are seen to have disappeared due to acid leaching.
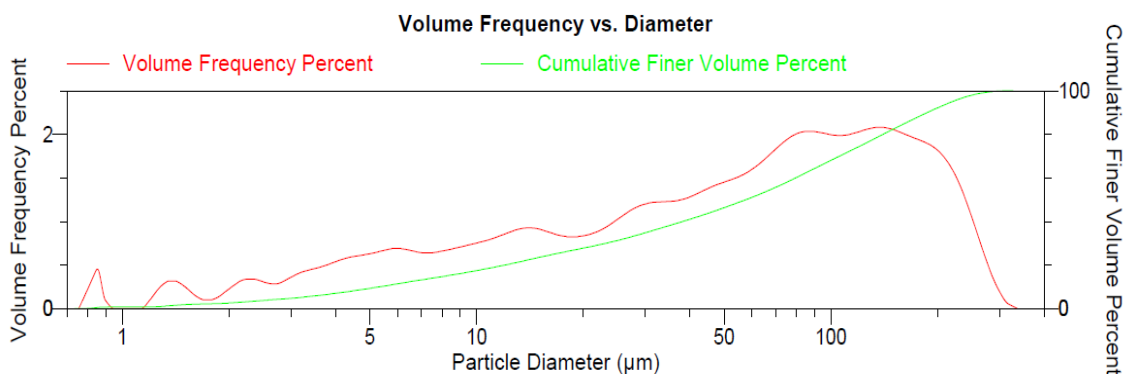
Figure 4.6: Particle size analysis

4.3.1.2 Alkali Fusion Product XRD

Alkali fusion was conducted as discussed in Section 3.4. The alkali fusion product was taken for XRD analysis in order to identify the phases present after the fusion process. Figure 4.7 shows the XRD pattern of the product. The main phases identified and their chemical formulae are shown in Table 4.4. As expected, the results indicate that the red phosphor component as observed in Figure 4.2 had disappeared due to the first stage leaching. The results also show that the only rare earth bearing phase identified was britholite. It was expected to identify the rare earth oxides of Ce and Tb. However, due to the relatively low amounts in comparison to the other phases, the rare earth oxides could not be identified. Nevertheless, it was observed that the alkali fusion process had occurred due to the sodium compounds in the product. These compounds were absent from the XRD results of the first leach residue shown in Figure 4.4.

64
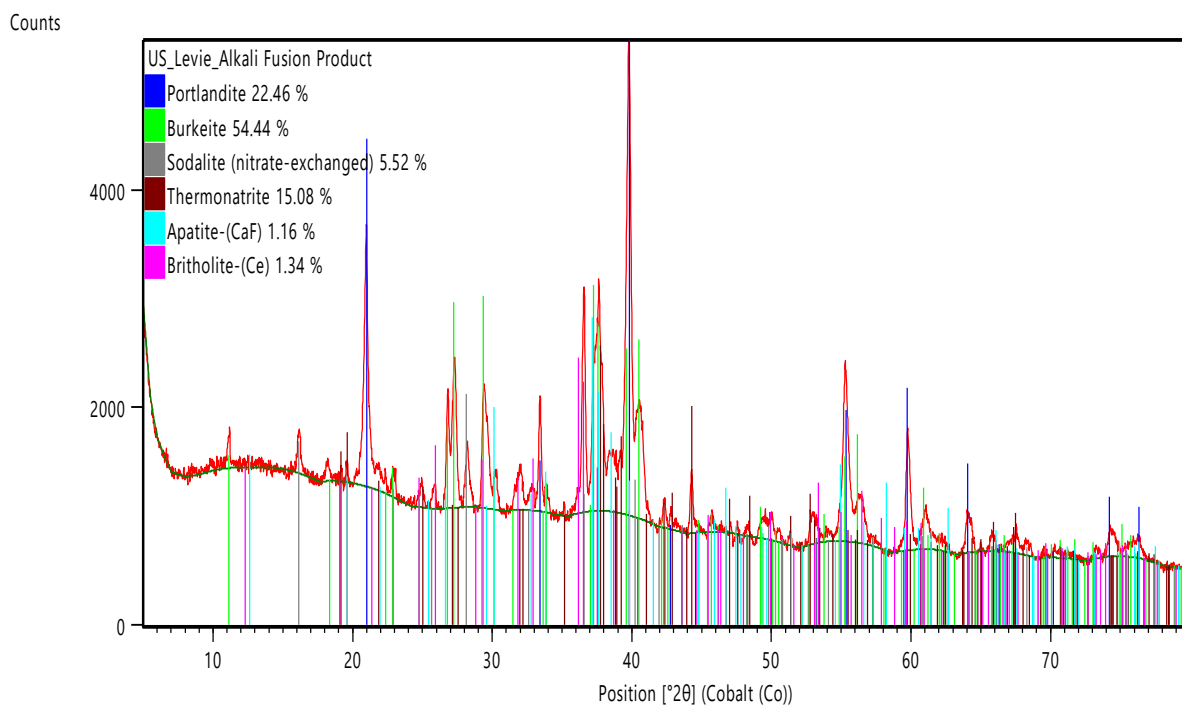
Figure 4.7: Alkali fusion product XRD results.

Table 4.4: Alkali fusion product phases

Phase	Formula
Portlandite	$Ca(OH)_2$
Burkeite	$Na_6(CO_3)(SO_4)_2$
Sodalite	$Na_8(Al_6Si_6O_{24})Cl_2$
Thermonatrite	$Na_2CO_3.(H_2O)$
Apatite	$Ca_5(PO_4)_3(OH,F,Cl)$
Britholite	$(Ce,Ca)_5(SiO_4)_3OH$

4.3.2 Ultrasound Assisted Digestion

Preliminary ultrasound assisted digestion experiments were conducted as explained in section 3.4.1.1. The obtained results are shown in Figure 4.8.

65
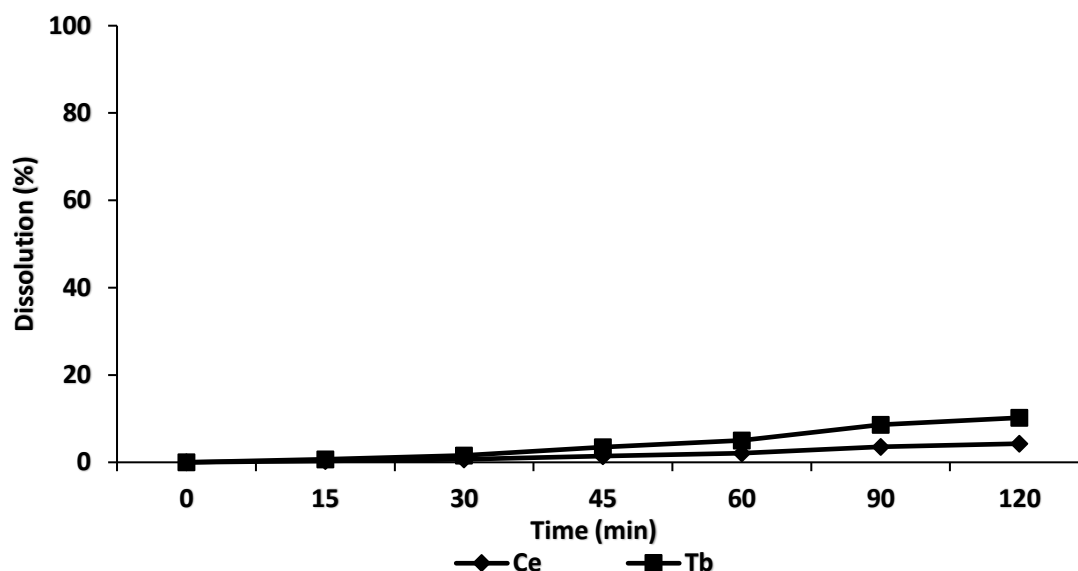
Figure 4.8: Ce and Tb ultrasound leaching results using an acid concentration of 5 M, S/L ratio of 10 % (w/v), frequency of 20 kHz, power of 200 W and 2 hours residence time

Preliminary ultrasound assisted digestion experiments were conducted as discussed in section 3.4.1.1. The results obtained show that Ce and Tb recoveries were poor (<10 % for both rare earths after 120 minutes of leaching) using ultrasound assisted digestion. This was probably due to the low nominal ultrasonic power that could be supplied by the ultrasound probe. Diehl *et al*. (2018) did a comparison on different ultrasound systems. They reported that the highest rare earth recovery (82 %) could be obtained using the ultrasound system possessing the highest power (750 W). In this study, the highest ultrasound power that could be supplied was 200 W. It is therefore recommended to further investigate the use of ultrasound assisted leaching at higher ultrasonic power.

4.3.3 Alkali Fusion Product Acid Leaching

4.3.3.1 Effect of temperature on Ce and Tb leaching

Figure 4.9 (a) to (f) show the effect of temperature on rate and extent of Ce and Tb leaching. The effect of temperature at 1 M HCl concentration is shown in (a) and (b). As expected, the rate and extent of leaching increased with temperature for both metals. The rate and extent of leaching is lower for Ce in comparison to Tb for all three temperatures. Maximum recovery was 17.2 % for Ce compared to 75 % for Tb at the same acid concentration. A possible explanation for this is that Tb is preferentially leached compared to Eu. Tb is possibly leached at a faster rate than Ce. Another reason could be that, although the dissolution reactions for both Ce and Tb are exothermic as shown in Table 2.6 section 2.7, the equilibrium constant values

for Ce are much smaller and gradually decrease with increase in temperature. This suggests that the solubility of cerium chloride in HCl is much lower compared to that of terbium. From the graphs, it can be deduced that the leaching reaction equilibrium was achieved at the three temperature levels for both metals.

Figure 4.9 (c) and (d) show the effect of temperature on Ce and Tb recovery using 3 M HCl. Equilibrium was achieved after 45 minutes of leaching but it can be seen from the graphs that leaching kinetics were very fast within the first 15 minutes. Increasing the temperature from 30 to 60 and 90 °C does not have a significant effect on the leaching recovery for both Ce and Tb. A possible explanation for this behavior is that for an exothermic reaction, and increase in temperature does not enhance the extent of leaching. This is evident in the results since both reactions are exothermic (Table 2.6 and 2.7).
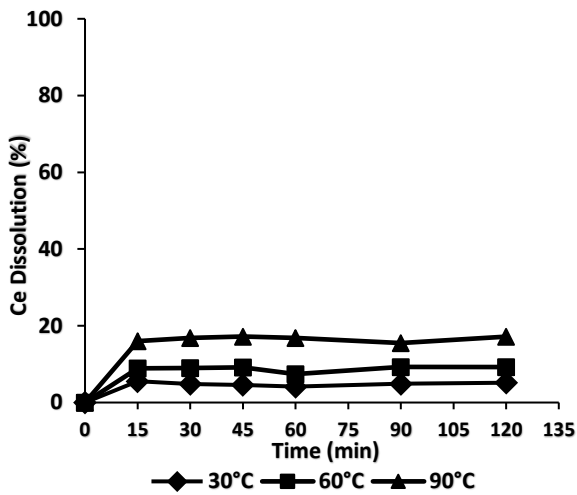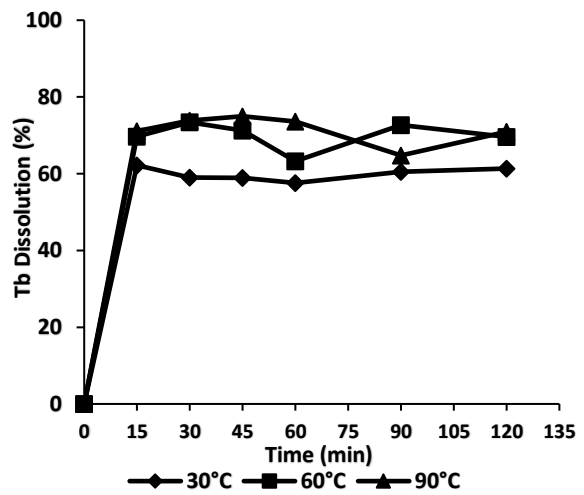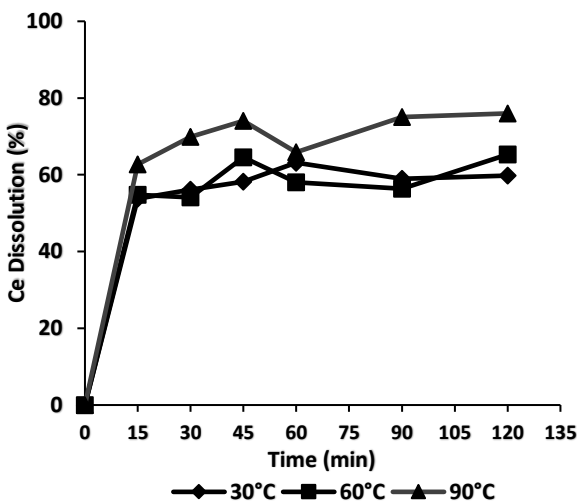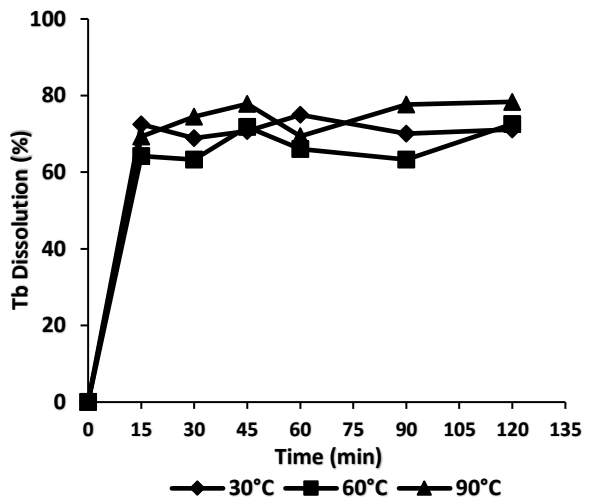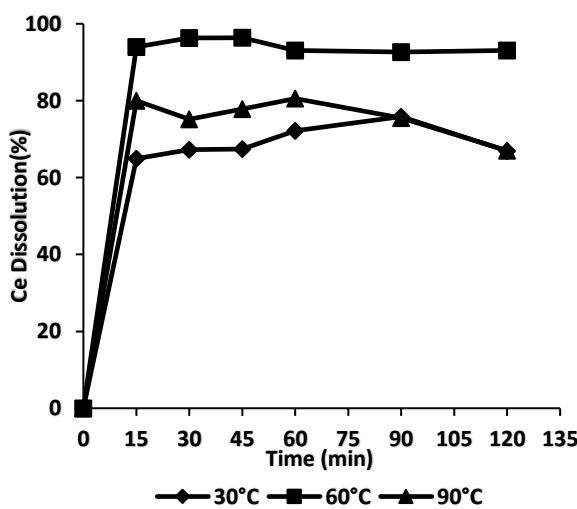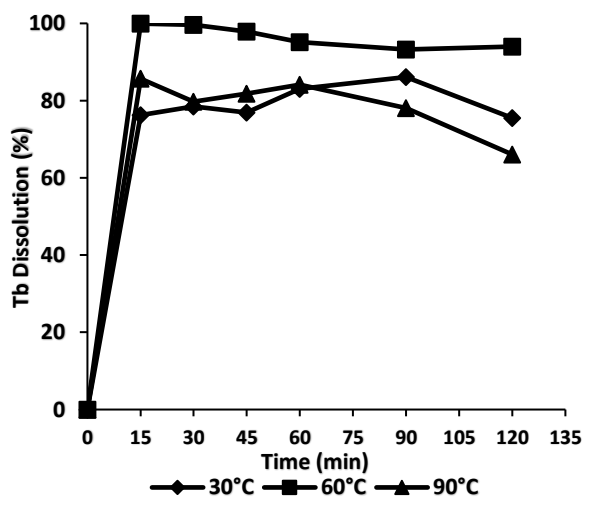
Figure 4.9: Ce leaching at a)1M ,c)3M, e) 5M ; Tb leaching at b) 1M, d) 3M, f) 5M

The effect of temperature when operating at an acid concentration of 5 M is shown by Figure 4.9 (e) and (f). The rate and extent of leaching increases with increasing temperature from 30 to 60 °C. Beyond 60 °C the rate and extent of leaching decreases. Since the reaction is exothermic, the extent of leaching decreases with temperature. This happens because the backward reaction (endothermic) is favoured when the leaching equilibrium shifts. It can therefore be concluded that 60 ℃ is the optimum temperature at the given concentration. Optimal recoveries were obtained using a temperature of 60 °C corresponding to 96.3 % and 99.6 % Ce and Tb dissolution after about 30 minutes of leaching respectively

4.3.3.2 Effect of Concentration

Figure 4.10 (a) to (f) show the effect of concentration on Ce and Tb leaching. Graphs (a) and (b) show that the rate and extent of leaching for Ce and Tb increases with increasing acid concentration when operating at a temperature of 30 °C. This behaviour is expected since leaching kinetics occur at a faster rate due to increased interactions between reacting species. Dissolution of Ce using 1 M HCl is much lower than that of Tb as shown by graphs (a) and (b).A possible explanation for this behaviour is preferential dissolution of Tb compared to Ce. It is therefore a possibility that most of the acid was used to dissolve Tb and very little was left for Ce dissolution. The best leaching results were obtained using 5 M HCl for the given temperature.

The effect of acid concentration at 60 ℃ is shown by Figure 4.10 (c) and (d).As expected, the rate and extent of leaching was found to increase with increasing concentration for both rare earths. The highest recoveries for both metals were obtained when operating at an acid concentration of 5 M corresponding to 96.3 % Ce and 99.7 % Tb after 30 minutes of leaching. Ce recovery remained much lower than Tb recovery at 1 M. Figure 4.5 (d) shows that increasing concentration from 1 M to 3 M has no significant effect on the leaching kinetics and recovery of Tb. This validates the explanation that Tb is preferentially leached compared to Ce leaching.
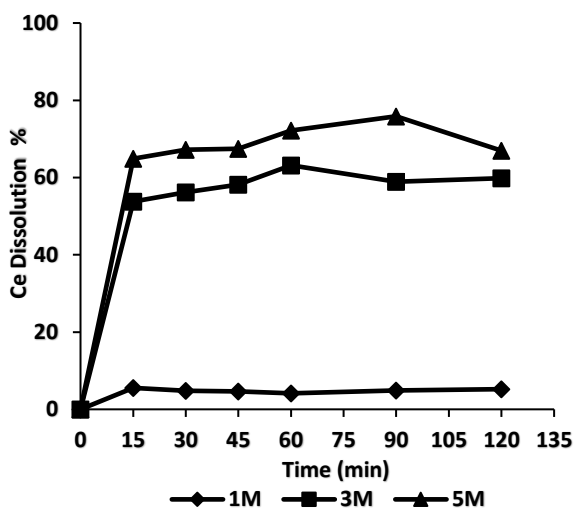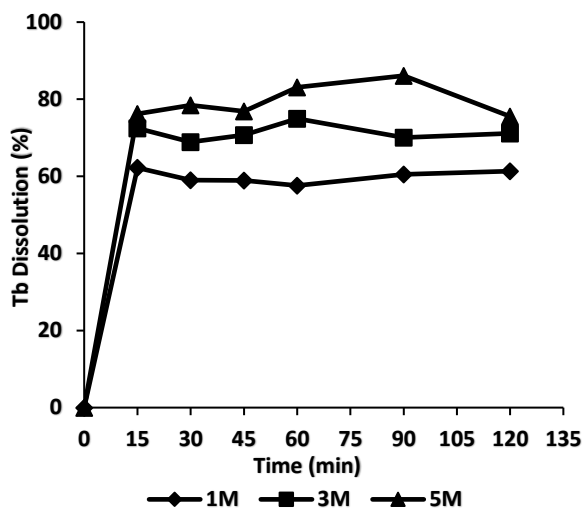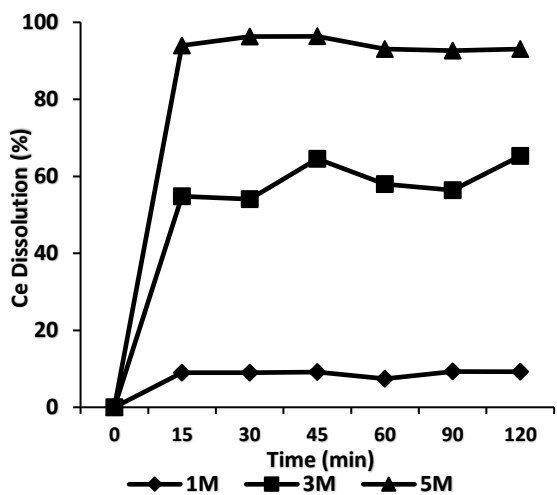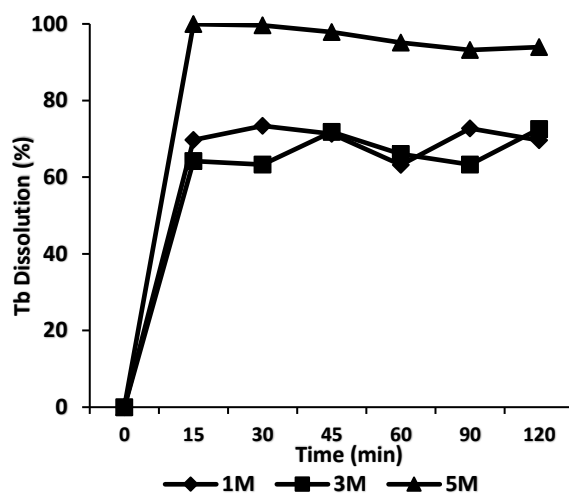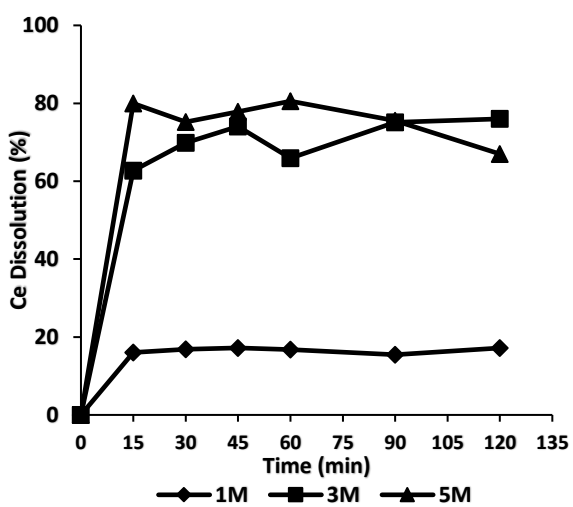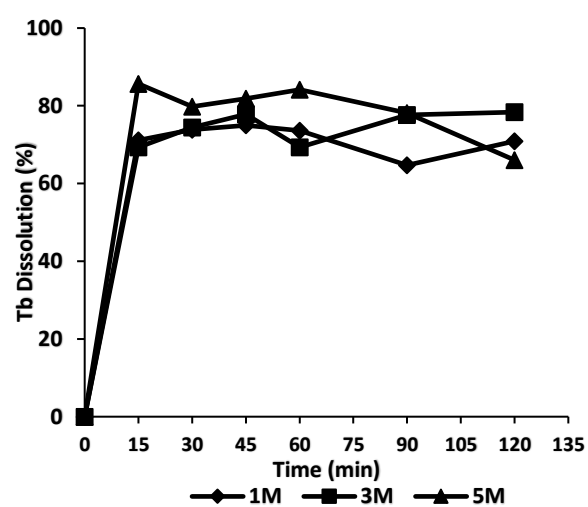
Figure 4.10*: Ce leaching at a) 30 ºC, c) 60 ºC, e) 90 ºC; Tb leaching at b) 30 ºC, d) 60 ºC, f) 90 ºC*

Figure 4.10 (e) and (f) show the effect of acid concentration on Ce and Tb leaching at 90 ℃. For Ce leaching, the leaching behaviour remains the same as reported when using 30 ℃ and 60 ℃. There was no significant increase in Tb percentage dissolution since the leaching reaction equilibrium was achieved at the three acid concentrations. Optimal leaching conditions were found to be a temperature of 60 ℃ and a concentration of 5 M for all the three temperature levels.

A statistical analysis was performed to determine if either temperature, concentration interaction effects had a significant influence on Tb recovery after 30 minutes of leaching. The p values given in Table F.2 show that at a 95 % confidence level, only the linear effect of acid concentration had a significant effect on the extent of rare earth metal recovery. The linear effect of temperature, the quadratic effect of temperature and the quadratic effect of acid concentration had an insignificant effect on the extent of recovery as reported by the high p values. Interaction effects of temperature and concentration also had no effect on the rare earth metal recovery. The findings of the statistical analysis were in partial agreement to what was observed from the graphs in Figure 4.5 since from the graphs the effect of temperature was found to be significant. The surface plots for the statistical analysis is presented in Figure F.2 (Appendix F).

4.3.3.3 Summary

The results obtained show that HCl leaching after alkali fusion can be used to recover Ce and Tb from the green phosphor powders. Results obtained from ultrasound-assisted digestion are inconclusive since the available equipment had a lower power output than ultrasound devices used in previous studies. The conditions given in Table 4.5 and Table 4.6 were recommended for alkali fusion and Ce and Tb leaching.

Table 4.5: Alkali fusion conditions

Parameter	Set point
Residue to NaOH ratio	1:1.5
Temperature	800 ℃
Time	2 hours

71

Table 4.6: Suggested conditions for second stage leaching

Parameter	Set point
Acid Concentration	5 M
Temperature	60 °C
Agitation Speed	600 rpm
S/L Ratio	5 % (w/v)
Time	30 minutes

4.4 Y and Eu Solvent Extraction

The experimental data discussed in this section was obtained from solvent extraction experiments conducted by A.E Anderson, a final year Process Engineering student in 2017. During the course of the experiments by the final year student, the author was investigating the optimal conditions for Y and Eu leaching. As such, the results reported in section 4.4.1 were different from the ones obtained by the author since the operating conditions used to prepare the bulk solution used in the solvent extraction tests were different. The data used in this discussion was obtained from leaching experiments conducted at a temperature of 25 °C, H_2SO_4 concentration of 2 M and a residence time of 6 hours.

4.4.1 Y and Eu Leaching Results

Two leaching experiments were conducted to produce adequate pregnant leach solution for solvent extraction experiments. The pregnant leach solutions are referred to as PLS1 and PLS2. PSL2 was prepared upon depletion of PSL1. This was done to avoid precipitation occurs in the leach solution with time (Innocenzi *et al.*, 2013). Table 4.7 shows the metal content of the analysed leach solutions.

Table 4.7: Leaching experiments results

	Metal Content (ppm)										
	Al	**B**	**Ba**	**Ca**	**Ce**	**Eu**	**Gd**	**La**	**Mg**	**Tb**	**Y**
PLS1	191.0	22.2	ND	529.9	1.3	137.1	3.6	ND	157.8	0.9	2095.2
PLS2	209.6	23.8	ND	533.0	2.7	226.2	6.5	ND	155.3	1.3	3360.9

The results presented in Table 4.7 show differences in metal content between PLS1 and PLS2. Y concentration was 60.4 % higher in PLS2 compared to PLS1. The same applies for Eu which was 65 % higher. The difference in metal concentration was probably due to differences in

composition between the two waste phosphor powder samples used to prepare the bulk solutions. The other rare earths Ce, Gd and Tb were found to be 103 %, 81 % and 43 % higher in concentration respectively. Table 4.6 also shows that the concentration of impurities such as Al, B, Ca and Mg increased slightly in PLS2 (<10 %) compared REEs.

4.4.2 Effect of Operating Variables on Y and Eu Solvent Extraction

The effect of three main variables on solvent extraction of Y and Eu were investigated. These variables are pH, extractant concentration, and O/A ratio. Percentage extraction and separation factors were used to understand and quantify the performance of the extractant of choice (DEHPA).

4.4.2.1 Effect of pH

Figure 4.11 and 4.12 show the percentage extraction of Y and Eu as calculated by Equation 12. Figure 4.11(a) shows that Y extraction increases with pH and O/A ratio at an extractant concentration of 0.5 M. An increase in extractant concentration to 1 M resulted in higher extraction percentages as shown in Figure 4.11(b).

(a)   (b)
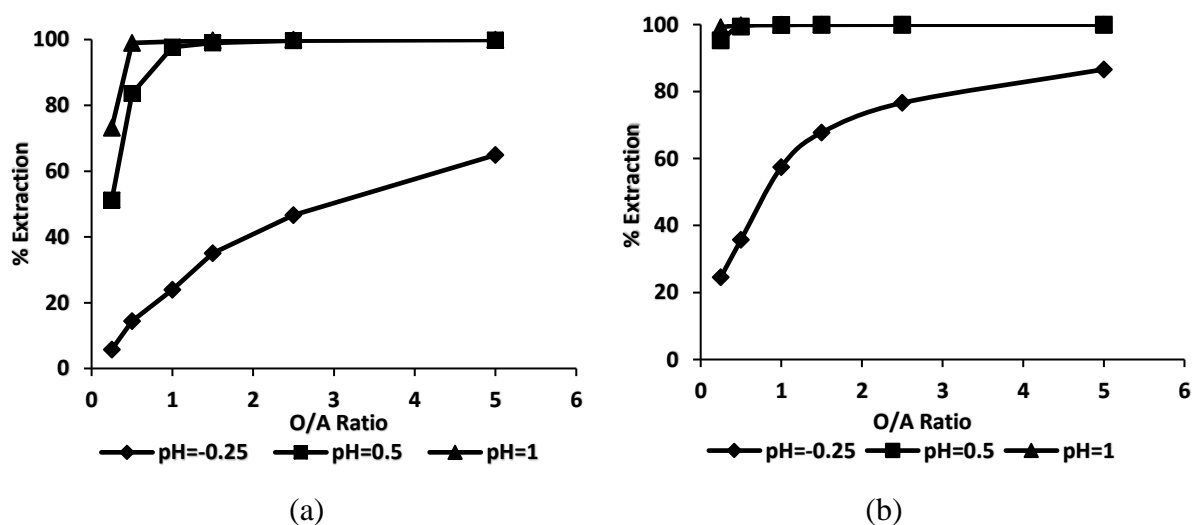
Figure 4.11: Yttrium percentage extraction at extractant concentrations of (a) 0.5 M and (b) 1 M

Figure 4.12 (a) and (b) show the percentage extraction of Eu at different O/A ratios and pH levels. It was found that no Eu extraction occurred at a pH of -0.25 for both extractant concentrations. Higher extraction percentages were found for Y compared to Eu. This could be due to the fact that DEHPA is known to have a higher affinity for heavier rare earths compared to lighter ones (Abreu and Morais, 2014; Xie *et al.*, 2014).

73
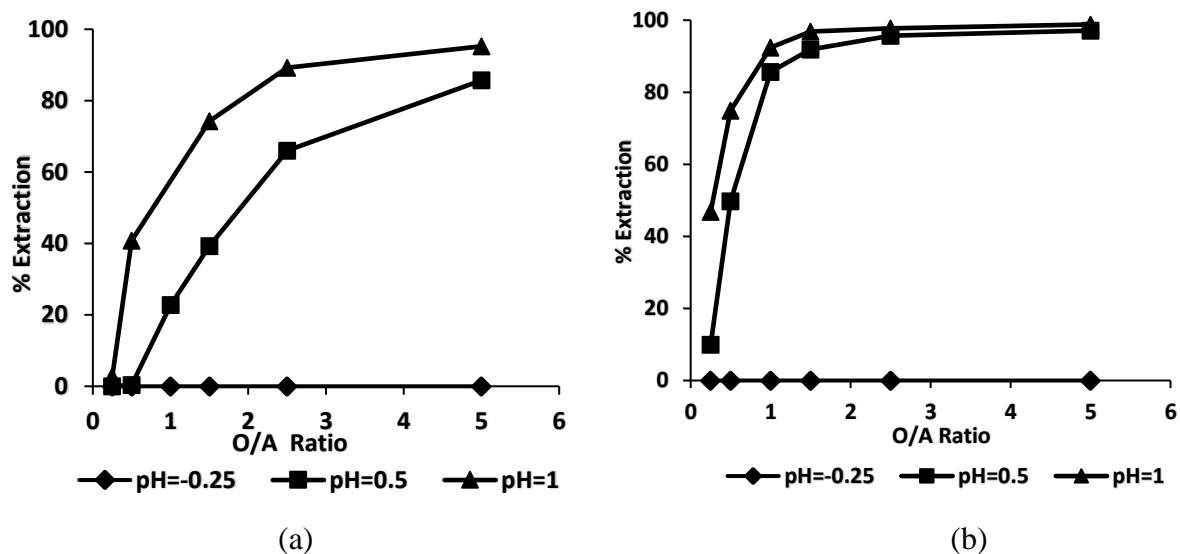
Figure 4.12: Europium percentage extraction at extractant concentrations of (a) 0.5 M and (b) 1 M

As explained in section 2.5 the solvent extraction of rare earths into the organic phase is based on the decrease in ionic radius across the lanthanide series. Yttrium creates stronger bounds with solvent molecules compared to Eu since it has a smaller ionic radius (0.88 Å) than Eu (0.95 Å) (Nash, 1993). Also, because of the difference in ionic radius, there exists a difference in the formation coefficient of both rare earth-extractant complexes thereby allowing preferential extraction of the Y complex into the organic phase (Rydberg *et al.*, 2004). The formation coefficient is an equilibrium constant for the formation of a complex in solution.

4.4.2.2 Effect of Extractant Concentration and O/A Ratio

Figure 4.13 shows the effect of extractant concentration on the extraction of Eu and Al at pH 0.5 and extractant concentration of 0.5 M and 1 M.
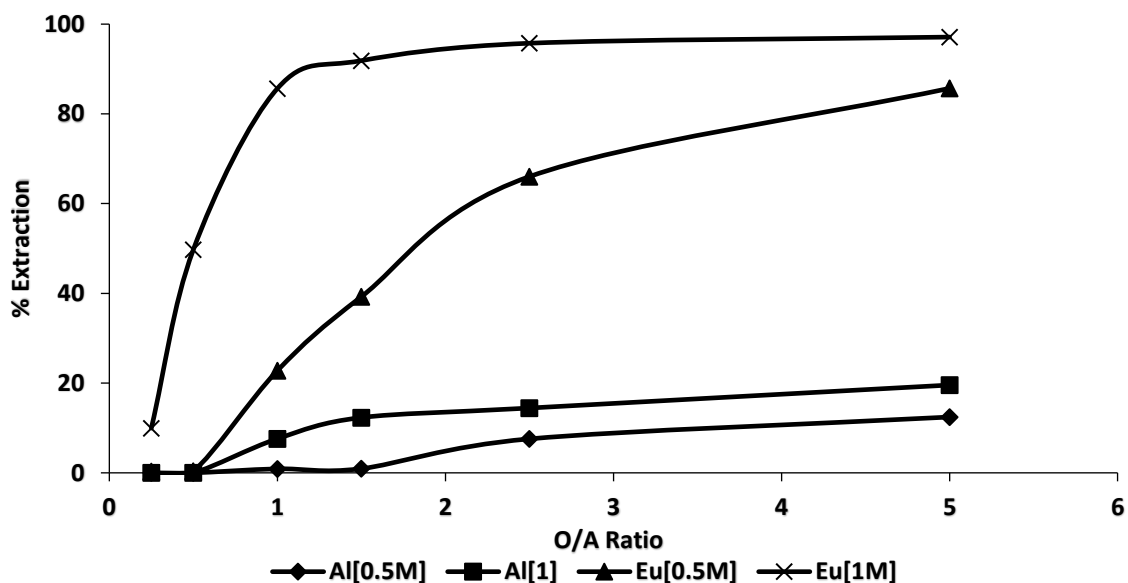
Figure 4.13: Effect of extractant concentration on percentage extraction at pH 0.5

Although Ca was the main impurity present in the PLS, the metal was not extracted into the organic phase at the conditions investigated. Al was therefore the main impurity extracted into the organic phase during the tests. Figure 4.13 shows an increase in percentage extraction of Eu and Al with increase in extractant concentration and O/A ratio. The same extraction behavior was also observed for the other rare earths and impurities present in the pregnant leach solution as shown in Appendix C.3.

4.4.3 Separation factor

In solvent extraction of metal ions, the separation factor is often more important than the percentage extraction (Abreu and Morais, 2014). Separation factors of Y relative to other metals were calculated using Equation 13. At pH -0.25, only Y and Tb were extracted as shown in Tables C.3.1 and C.3.2 Appendix C. Figure 4.14 shows the separation factors of Y relative to Tb.
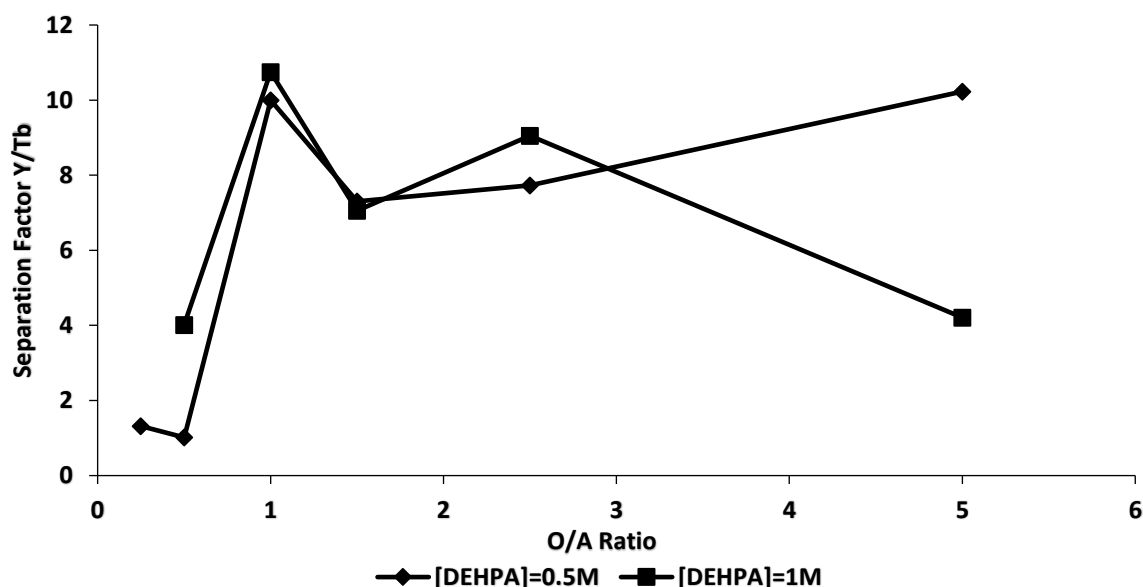
Figure 4.14: Separation factors of Y relative to Tb at pH of -0.25.

The graph shows that separation between Y and Tb is possible since all the separation factors obtained are greater than unity at both extractant concentrations. However, it was found that separation factors obtained at an extractant concentration of 1 M were in some instances larger than those obtained at a lower extractant concentration. This behavior was unusual since the separation factor normally decreases with increasing organic phase concentration. This anomaly may be due to analytical error. The greatest separation factor was found to be 11 at an O/A ratio of 1. Since Tb dissolution was found to be low (Table 4.7), solvent extraction at pH -0.25 can be used to get a relatively pure product of Y. According to the results obtained by the author, there was no Tb present in the leach solution after 45 minutes of acid leaching at the optimal conditions identified. This is therefore a promising route to obtain Y of high purity.

At pH 0.5 the rare earths Ce, Eu, Gd and Y were extracted together with Al and B as shown in Tables C. 3.3 and C. 3.4 Appendix C. Since Tb was undetected in the aqueous solution, it was assumed that complete extraction of the rare earth had occurred at both extractant concentrations and all six O/A ratios. Mg was not extracted at any of the six O/A ratios. Only Y and Tb were extracted at an O/A ratio of 0.25 and an extractant concentration of 0.5 M before extraction equilibrium was reached. Table 4.8.shows separation factors of yttrium relative to other identified metals at extractant concentrations of 0.5 and 1 M. Some elements were not extracted to the organic phase at a particular O/A ratio. In this case separation factors would tend to infinity. In other cases, some elements could not be detected in the remaining aqueous phase and therefore complete extraction was assumed. Separation factors of Y relative to other rare earths and impurities which could not be determined are denoted by '-' in Table 4.8.

76

Table 4.8: The separation factors of Y relative to other metals present in solution at pH 0.5 and 1

pH	O/A Ratio	DEHPA Concentration [M]	Y/Eu	Y/Al	Y/B	Y/Ce	Y/Gd	Y/Mg
0.5	0.25	0.5	-	-	-	-	-	-
		1	181.8	-	-	-	86.8	-
	0.5	0.5	1292.8	-	-	3.9	162.7	-
		1	171.8	-	-	-	94.9	-
	1	0.5	144.2	4730.1	1056.5	204.0	80.0	-
		1	149.2	10816.8	134976.3	-	117.3	-
	1.5	0.5	145.2	10013.5	2455.4	233.7	90.8	-
		1	145.5	11648.5	42086.5	15637.8	149.5	-
	2.5	0.5	142.1	3371.5	3735.2	360.6	87.0	-
		1	142.2	18981.6	-	11414.2	143.8	-
	5	0.5	135.1	5695.5	9050.6	4498.9	92.2	-
		1	126.5	17623.2	-	2283.1	42.1	-
1	0.25	0.5	96.8	-	51.9	-	-	184.9
		1	147.9	5435.0	1420.2	-	-	3292.7
	0.5	0.5	141.1	610.3	743.6	-	-	466.9
		1	166.2	6040.2	14296.8	-	-	5853.4
	1.5	0.5	152.9	3553.6	5682.0	-	-	3574.8
		1	143.9	8503.3	18628.5	-	-	12353.9
	2.5	0.5	150.8	6641.9	10711.3	-	-	8384.1
		1	160.8	10219.5	25763.2	-	-	25354.5
	5	0.5	145.0	9807.8	24494.5	-	-	36643.3
		1	143.0	14921.5	85957.5	-	-	-

77

The separation factor for Y relative to Eu generally decreases with increase in O/A ratio and extractant concentration. As extractant volume increases, more rare earth ions are extracted into the organic phase. The highest separation factor was found to be 1292 obtained at an O/A ratio of 0.5 and extractant concentration of 0.5 M. Y extraction is more efficient than that of Eu at this particular pH since DEHPA has a higher affinity of heavy rare earths compared to lighter ones. When operating at pH 0.5 and low extractant concentration equilibrium is reached when Y only has been extracted. Very little amounts of Eu would have been extracted at this stage hence the high separation factors. Nevertheless, with an increase in extractant volume, more Eu will be extracted resulting in a decrease in the separation factors. Beyond O/A ratio of 1 separation factors are fairly constant for both pH values and extractant concentrations. Separation factors of Y to Al, B, Gd and Ce at both extractant concentrations were high (+40) indicating that the elements could hardly be extracted. As a result, these impurities do not pose a challenge in obtaining Y of high purity. Impurities separation from Y would only require a few stages of solvent extraction.

The elements Al, B, Ce, Eu, Gd, Mg, Tb and Y were extracted at pH 1. The results obtained (Table C.3.5 and C.3.6 Appendix C) indicate that all the Tb, Ce and Gd were extracted into the organic phase. Separation factors at an O/A ratio of 1 and 0.5 M DEHPA concentration were omitted from Table 4.8 because the calculated values were very large and completely out of trend clearly showing an experimental error. The obtained results indicate that separation factors at both extractant concentrations were also high showing that impurities will not present a challenge during separation to obtain Y and Eu of high purity. A few stages will be required during the separation. At pH 1, it is only possible to produce a mixed rare earth product of Y and Eu, since complete Y and Eu extraction was found at an O/A ratio of 1.

4.4.4 Extraction Isotherms

Appendix C.3 shows ICP results of Y and Eu present in the aqueous and organic phases after equilibrium had been achieved during solvent extraction tests. These concentrations were used to draw extraction isotherms displayed in Figure 4.15

(a)   (b)
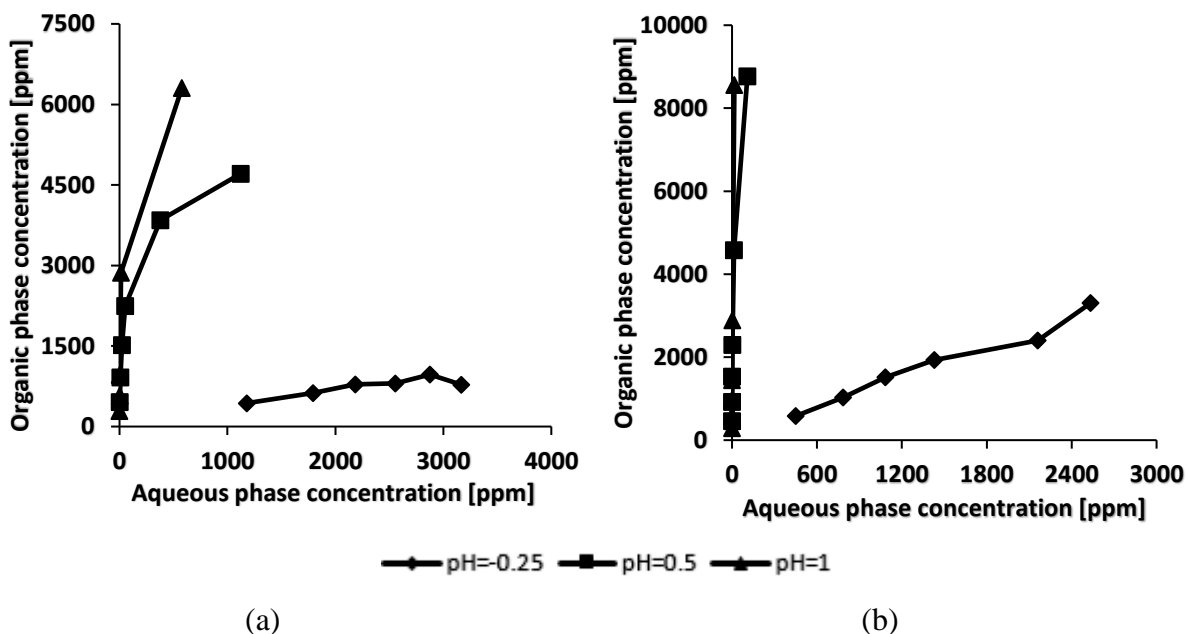
Figure 4.15: Y extraction isotherms at extractant concentration of (a) 0.5 M and (b) 1 M

Figure 4.15 shows that the higher the pH, the steeper the isotherm at both extractant concentrations. More Y extraction was achieved at 1 M extractant concentration as shown by the steeper isotherms. Figure 4.16 shows Eu isotherms at pH 0.5 and 1.The extraction isotherm at pH -0.25 is not shown since there was no Eu extraction.

(a)   (b)
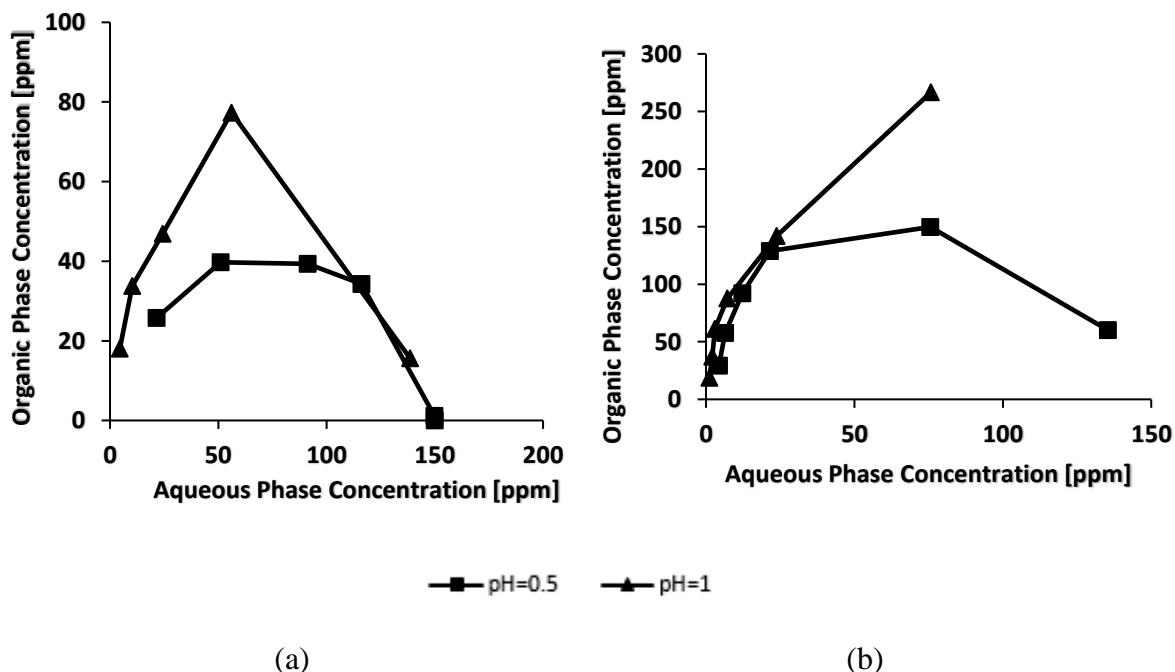
Figure 4.16: Eu extraction isotherms at extractant concentration of (a) 0.5 M and (b) 1 M

79

Europium isotherms are different from those obtained for yttrium. Only at pH 1 and extractant concentration of 1 M do we observe a net positive gradient. There was little or no Eu extraction at pH 0.5 and O/A ratio of 0.25. Since the extractant has a higher affinity for Y compared to Eu it is possible that equilibrium was reached when only Y had been extracted into the organic phase. Based on stoichiometric calculations using Equation 14 it was found that the mole ratio of the rare earth Y relative to the extractant is almost in the ratio 1:1, hence it was assumed that all the extractant was used to extract Y until equilibrium was achieved. Comparing Y isotherms to Eu isotherms suggest that Eu extraction occurs after most of the Y has been extracted. It is also shown that it is possible to reach equilibrium without any Eu extraction.

4.4.5 McCabe-Thiele Analysis

The McCabe-Thiele method was used to determine the number of stages required to produce Y and Eu of high purity either as separate elements or as a mixed product. The experimental conditions shown in Table 4.9 were employed

Table 4.9: Conditions used in the McCabe -Thiele analysis

Set	pH
1	-0.25
2	0.5
3	1

Organic phase concentration of 1 M and O/A ratio of 1 was used in this analysis for all process conditions. This was important in determine the effect of pH on industrial application. Figure 4.17 shows the McCabe-Thiele analysis for Y performed at pH -0.25.
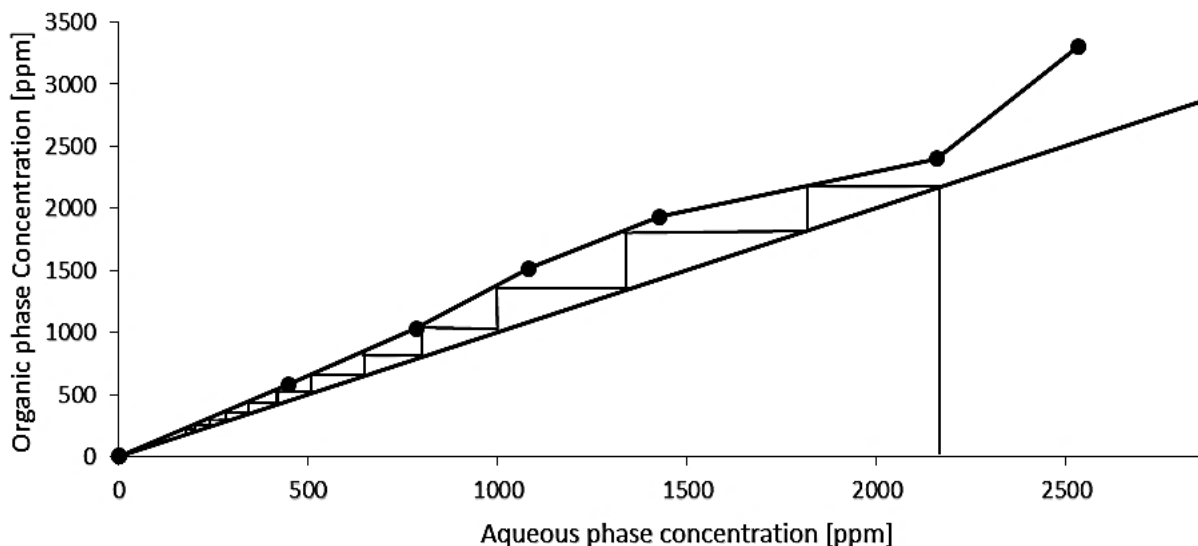
Figure 4.17: McCabe-Thiele diagram for Y at pH -0.25 and extractant concentration of 1 M

According to Figure 4.17, 11 countercurrent equilibrium stages are required to extract more than 95 % Y. A major advantage for operating at this pH is that NaOH is not required for neutralisation. Another advantage is that Y of high purity can also be extracted since no other element is extracted. On the contrary, too many equilibrium stages are required for the extraction.

(a)

(b)
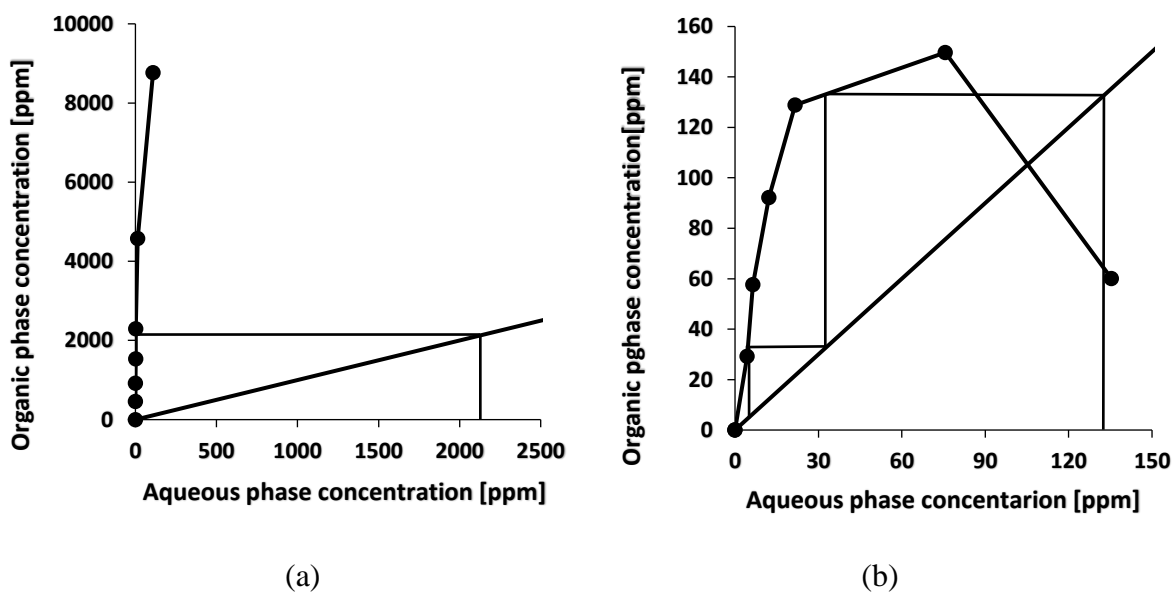
Figure 4.18: McCabe-Thiele diagram of (a) Y and (b) Eu at a pH of 0.5

Figure 4.18 (a) shows that only one equilibrium stage is required to extract more than 97 % Y at a pH of 0.5. For Eu, (Figure 4.18b) only two countercurrent equilibrium stages are required to extract more than 96 % of Eu. Contrary to operating at a pH of -0.25, very few equilibrium stages are required to achieve high Y and Eu extraction. However, NaOH will be required in this case for pH adjustment. Trace amounts of impurities (Ce, Gd and Tb) are also available in

81

the product stream. Operating at a higher O/A ratio is possible and this typically results in less equilibrium stages for the same amount of extraction.

(a)   (b)
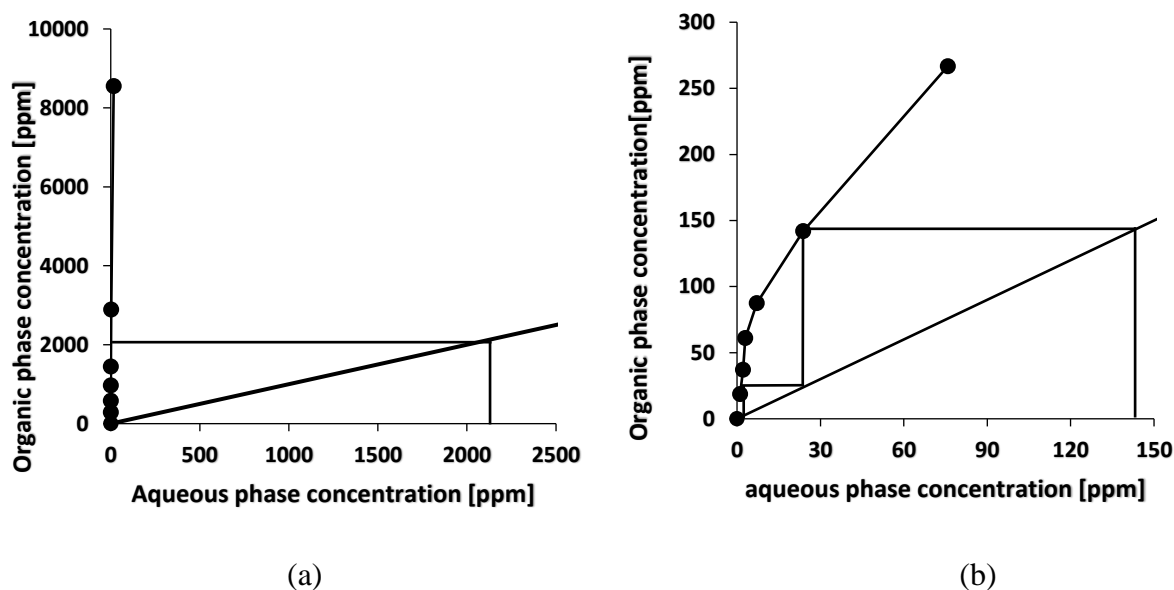
Figure 4.19: McCabe-Thiele diagram of (a) Y and (b) Eu at a pH of 1

Figure 4.19 shows the McCabe-Thiele diagrams of Y and Eu when operating at a pH of 1. A single equilibrium stage is sufficient to obtain Y of high purity (about 100 %) as shown in Figure 4.19(a). However, two equilibrium stages are required to produce about 97 % Eu. In this regard, two equilibrium stages will be required to produce a mixed rare earth product containing Y and Eu. A major advantage of operating at these conditions is that only 2 equilibrium stages are required for the rare earth extraction. However, the major drawback is that a large volume of NaOH is required for pH adjustment hence more reagent expenses incurred. The product purity is also compromised since non-rare earths such as Al, B and Mg are co-extracted. In this study, it is recommended to recover Y first at an aqueous phase pH of -0.25 before adjusting it to 0.5 for Eu recovery. This recommendation is due to a higher market value of Y and a wider variety of uses compared to the other rare earths.

4.5 Ce and Tb Solvent Extraction

4.5.1 Ce and Tb Leaching Results

The metal content results for the digestion of the alkali fusion product are presented in Table 4.13. The results indicate the presence of the rare earths Ce, Tb, Y and Eu in the leach solutions. The results also show the presence of the main impurities Ca and Al. Unlike sulphuric acid, hydrochloric acid does not suppress the dissolution of Ca. It was therefore expected to have a

high calcium content in the leach solution as found. Y and Eu concentrations were relatively low since they were recovered during the first stage leaching.

Table 4.10: Pregnant leach solution concentration

	Metal content (ppm)								
	Al	**Ba**	**Ca**	**Ce**	**Eu**	**Gd**	**La**	**Tb**	**Y**
PLS	1245.9	ND	9505.7	195.6	42.3	ND	ND	203.5	129.3

4.5.2 The Effect of Operating Variables on Ce and Tb Solvent Extraction

The effect of pH, extractant concentration and O/A ratio on the extraction of Ce and Tb was investigated. The percentage extraction and separation factors were used to understand and quantify the performance of the extractant (DEHPA) on Ce and Tb extraction.

4.5.2.1 Effect of pH

Figure 4.20 shows the effect of pH on percentage extraction of Ce. It was found that pH and O/A ratio have a significant influence on Ce extraction. Ce extraction was observed to increase with increasing pH and O/A ratio for both extractant concentrations. Over 99 % Ce extraction was only possible at pH I.5 and beyond. This was expected since according to Equation 14, for cationic exchangers, percentage extraction increases with increase in pH. An increase in extractant concentration also caused an increase in percentage extraction as expected.

(a)   (b)
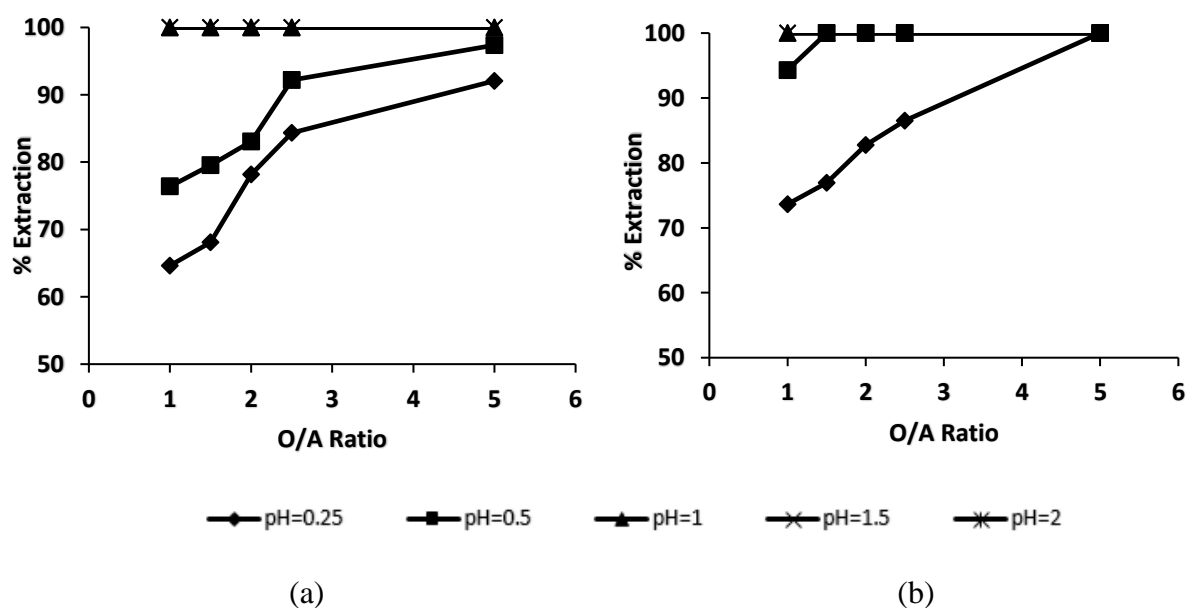
Figure 4.20: Cerium percentage extraction at extractant concentrations of (a) 0.5 M and (b) 1 M

As was the case with Y and Eu extraction, DEHPA showed a higher affinity for Tb than for Ce. More than 99 % Tb was extracted even when operating at the lowest O/A ratio and pH. This shows that DEHPA is a powerful extractant capable of extracting heavy rare earths even at low pH (Rydberg *et al.*, 2004; Xie *et al.*, 2014). Heavy elements of the lanthanide series form stronger bounds with extractant molecules than lighter members (Nash, 1993). It was found that there was no significant increase in percentage extraction for Tb with increase in extractant concentration from 0.5 M to 1 M.

 Y and Eu were co-extracted during the solvent extraction tests. Both rare earths were now present in relatively low concentrations since more than 90 % recoveries were achieved during the first stage leaching. After extraction, Y could not be detected in all the remaining aqueous solutions using ICP OES analysis. It was therefore assumed that complete extraction of the rare earth had occurred at all the investigated conditions. More than 90 % Eu extraction was found at pH 0.25 and O/A ratio of 1. The percentage extraction increased with increasing O/A ratio and more than 99 % extraction was achieved at O/A ratio 2.5 and beyond. Extraction percentage was more than 99 % for all the other conditions.

The effect of pH and O/A ratio on the percentage extraction of impurities such as Ca and Al was also investigated. Figure 4.21 shows the extraction behavior of the main impurity (Ca) with respect to pH and O/A ratio at a fixed extractant concentration. It is clear from the graph that an increase in aqueous phase pH resulted in an increase in Ca extraction to the organic phase. Percentage extraction was also found to increase with increase in O/A ratio. More than 99 % Ca extraction was achieved at pH 1.5 and 2 when operating at an O/A ratio of 5.
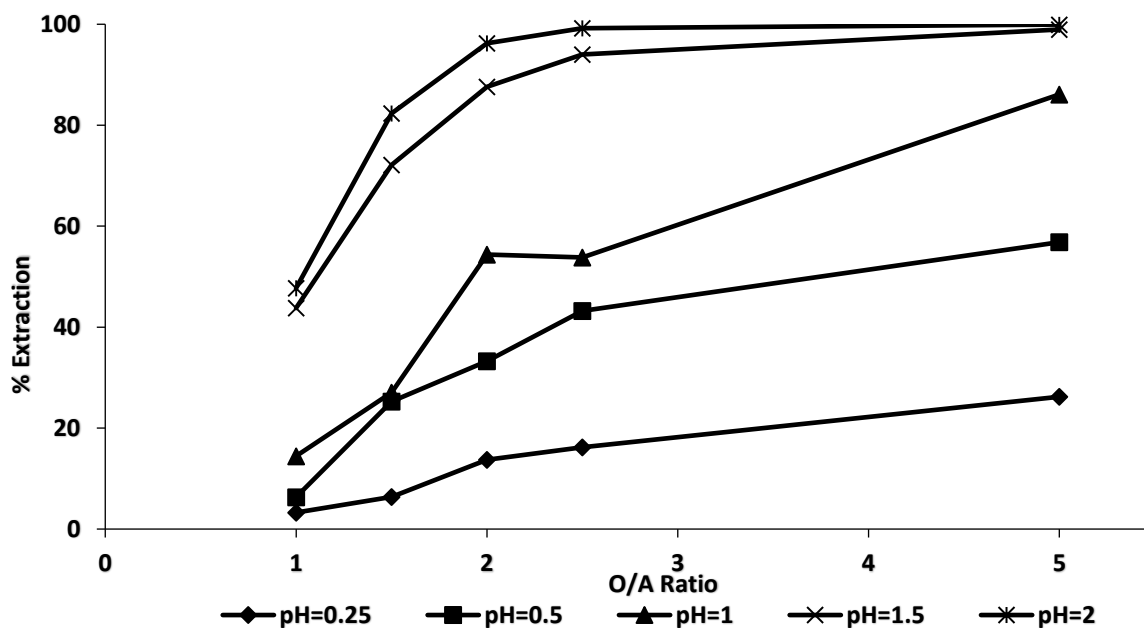
Figure 4.21: Percentage extraction of Ca at an extractant concentration of 1 M

The extraction behavior of the other main impurity (aluminium) is shown in Figure C.4.1 Appendix C.4. The extraction behavior was the same as that for Ca. More than 99 % Al extraction was achieved at pH 2.

4.5.2.2 Effect of Extractant Concentration

Figure 4.22 shows the effect of extractant concentration on the extraction of Ce and the main impurity Ca at a constant pH 0.5 and extractant concentration of 0.5 M and 1 M.
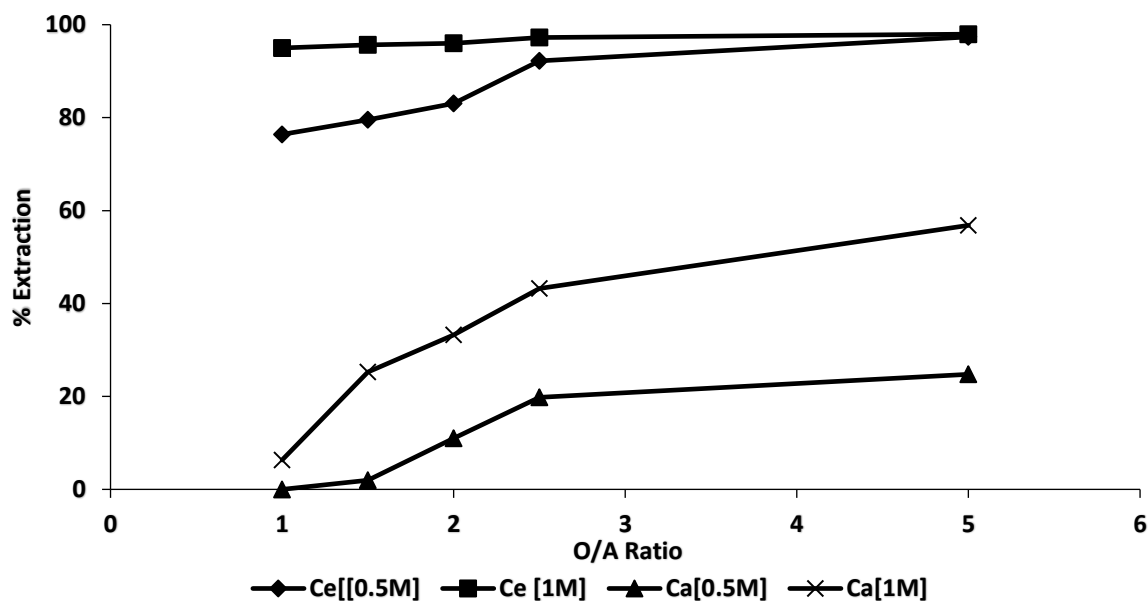
Figure 4.22: Effect of extractant concentration on percentage extraction at pH 0.5

85

The graph shows a general increase in percentage extraction for Ce and Ca with increase in extractant concentration. More than 95 % Ce extraction could be achieved at an O/A ratio of 1 and 1 M extractant concentration against 76.4 % achieved at the same O/A ratio and 0.5 M extractant concentration. The results also show that there was no Ca extraction when operating at an extractant concentration of 0.5 M and O/A ratio of 1. Ca extraction was only possible when using 1 M extractant concentration. The same extraction behavior was also observed for the other impurities and rare earths except Y.

4.5.3 Separation Factors

The separation factors of Tb and Ce relative to other present elements was determined using Equation 13. The separation factors obtained at an extractant concentration of 0.5 M and a pH of 0.5 are shown in Table 4.11. Separation factors that could not be determined due to complete extraction of one or both metals of interest into the organic phase are denoted by '-'.Separation factors for the two rare earths relative to Y could not be determined since the distribution ratio could not be calculated due to complete extraction of Y. Previous literature on rare earth recovery mostly focused on separation factors between adjacent rare earths (Michelsen and Smutz, 1971; Gschneidner Jr, 1980; Sato, 1989; Mishra, Singh and Gupta, 2000; Thakur, 2000; Abreu and Morais, 2014). There was therefore no basis of comparison for separation factors of the rare earths with other impurities present.

Table 4.11: Separation factors of Tb and Ce relative to other elements at an extractant concentration of 0.5 M.

pH	O/A	Tb/Ce	Tb/Al	Ce/Al	Tb/Ca	Ce/Ca	Tb/Y, Ce/Y	Tb/Eu	Ce/Eu
0.25	1	217.9	-	-	20488.8	94.0	-	12.2	0.06
	1.5	94.4	14492.8	153.5	6609.8	70.0	-	6.6	0.07
	2	88.2	38147.6	432.3	2534.8	28.7	-	4.1	0.05
	2.5	116.7	4127.5	35.4	3600.6	30.9	-	3.5	0.03
	5	101,4	6662.7	65.7	2373.7	23.4	-	2.3	0.02
0.5	1	181.8	-	-	-	-	-	-	-
	1.5	69.3	-	-	13216.8	190.6	-	-	-
	2	45.0	5355.1	119.0	1789.1	39.8	-	-	-
	2.5	9.4	1088.7	116.0	448.8	47.8	-	-	-
	5	3.0	2071.2	701.1	332.3	112.5	-	-	-
1	1	10.3	1137.6	110.5	3997.2	388.2	-	-	-
	1.5	10.8	749.7	69.6	481.0	44.7	-	-	-
	2	9.2	880.3	95.4	569.2	61.7	-	-	-
	2.5	9.2	320.9	35.0	373.5	40.8	-	-	-
	5	5.9	151.7	25.7	141.4	24.0	-	-	-
1.5	1	-	112.8	-	1278.9	-	-	3.3	-
	1.5	-	92.9	-	768.1	-	-	1.0	-
	2	-	54.5	-	131.0	-	-	0.2	-
	2.5	-	-	-	-	-	-	-	-
	5	-	-	-	-	-	-	-	-
2	1	-	-	-	-	-	-	-	-
	1.5	-	60.4	-	210.7	-	-	-	-
	2	-	7.9	-	113.4	-	-	-	-
	2.5	-	8.4	-	99.2	-	-	-	-
	5	-	0.3	-	2.1	-	-	-	-

Referring to Table 4.11, it is evident that the separation factors of Tb to Ce decrease with increase in pH and O/A ratio. The greatest separation was observed to occur at the lowest pH investigated where almost all the Tb (>99 %) was extracted and Ce extraction was relatively low. This behavior was expected since DEHPA has a higher affinity for heavier rare earths (Tb) compared to lighter ones (Ce). The separation factors at an operating pH of 1.5 and 2 could not be determined since both rare earths were below the detection limit of ICP OES. It was therefore assumed that complete extraction had occurred for both rare earths therefore separation was not feasible. Although an increase in pH was observed to favour the extraction of lighter rare earths (Ce and Eu), impurities co-extraction was found to increase. This is in support of the fact that selective separation of metals decreases with increasing pH when using DEHPA as reported by Abreu & Morais (2014).

The separation factors of Tb and Ce relative to Al and Ca were found to decrease with increasing pH. The separation factors of Tb to Al and Ca were greatest (+2000) when operating at pH 0.25 meaning these impurities will not be problematic in achieving Tb of high purity at such conditions. However, operating at higher pH (above pH 1.5) would result in co-extraction of the undesired impurities.

Separation of individual rare earths was found to be impossible since Y was completely extracted even at the lowest pH investigated. Separation factors of Tb relative to Eu were also low hence it was found that it is only possible to obtain a mixed product at all the investigated conditions. When operating at a pH of 2 more than 99 % Y, Eu, Ce and Tb was found. This is in agreement with what Rydberg *et al*. (2004) reported when they stated that all rare earths above Eu are extracted at pH 2 but stripping of the heavy earths is problematic. Separation factors were the lowest at this pH hence the mixed rare earth product obtained was highly contaminated with impurities. A large number of equilibrium stages are therefore required in order to obtain high purity rare earths. The lower the separation factors, the higher the number of equilibrium stages required to separate the products.

Separation factors obtained when operating at an extractant concentration of 1 M are shown in Table C. 4.11 Appendix C. As expected, it was found that separation factors at this extractant concentration were relatively lower than the ones obtained when operating at an extractant concentration of 0.5 M. However, despite the decrease in separation factors, the same extraction behavior as that found at extractant concentration of 0.5 M was observed.

In order to produce a mixed product of high purity, it is recommended to use a pH of 0.5, an O/A ratio of 1 and an extractant concentration of 1 M where impurities extraction is minimum and Ce and Tb extraction are more than 95 % and 99 % respectively. Complete Y and Eu extraction was found at these conditions.

4.5.4 Extraction Isotherms

Extraction isotherms for Ce were constructed using equilibrium data shown in Appendix C.4. The isotherms displayed in Figure 4.23 show a net positive increase with increase in pH for both extractant concentrations.

(a)   (b)
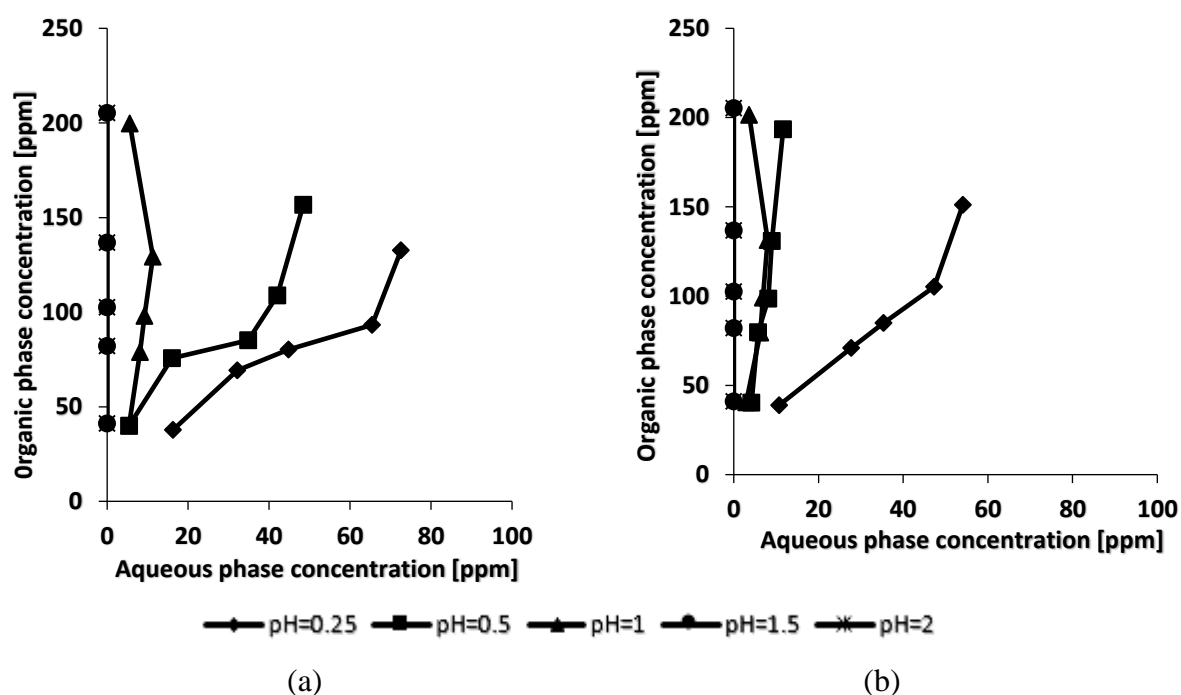
Figure 4.23: Ce extraction isotherms at extractant concentration of (a) 0.5 M and (b) 1 M

As displayed in Figure 4.23, Ce extraction is observed to be dependent on pH with complete extraction only possible at pH 1.5 and 2. The obtained results are in support of Equation 14 where an increase in pH favours the extraction of rare earths into the organic phase. It is clear from the graphs that a single stage is adequate to extract more than 95 % Ce at a pH of 0.5 and above. The extraction isotherms of Tb were omitted since more than 99 % extraction was observed at all pH levels. Only one equilibrium stage is required to extract more than 99 % Tb at the investigated pH levels.

4.5.5 Summary

The solvent extraction results show that it is only possible to obtain a mixed rare earth product at the investigated pH levels. Even at pH 0.25 (lowest pH investigated), Ce recovery was in excess of 64 % at the lowest O/A ratio. The other rare earths that were present in the initial

89

aqueous phase are Y and Eu. The results indicated that Y was extracted to completion before Tb since it is a heavier rare earth. This was in support of the fact that DEHPA has a higher affinity for heavier rare earths. From the results, it is clear that operating at a low pH and low extractant concentration suppresses the extraction of the impurities Al and Ca. It is therefore suggested to perform the extraction tests at a pH of 0.5 and extractant concentration of 1 M where more than 95 % Ce and more than 99 % Tb were extracted. Ca and Al extraction was below 7 %.

4.6 Repeatability Tests

4.6.1 Leaching Experiments

Repeat experiments for Y and Eu leaching tests were conducted at conditions given in Table 4.3. The results are shown in Figure 4.24 and 4.25 for Y and Eu leaching respectively. Repeat experiment results are presented in Table E.1 and E.2 Appendix E.
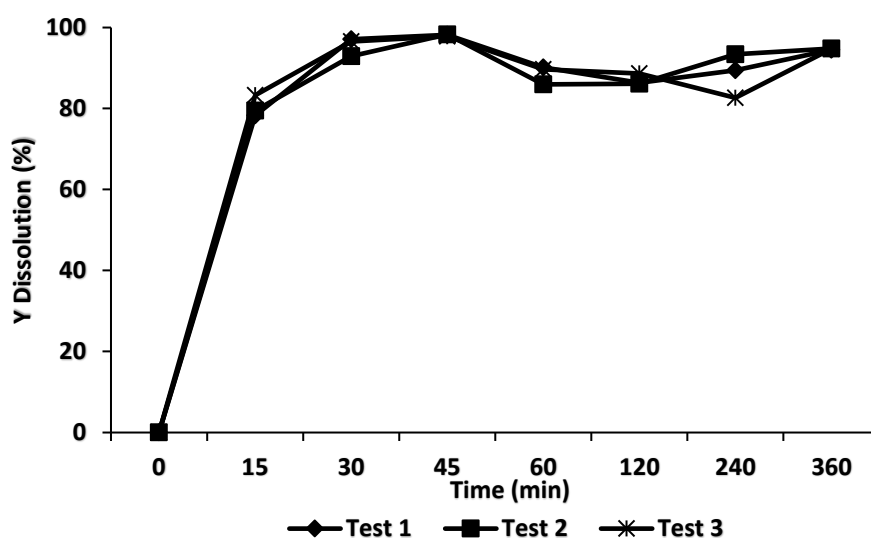
Figure 4.24: Y leaching repeatability test at a temperature of 60 ºC, acid concentration of 3.5 M, agitation speed of 600 rpm, S/L ratio of 10 % (w/v) and a residence time of 45 minutes

90
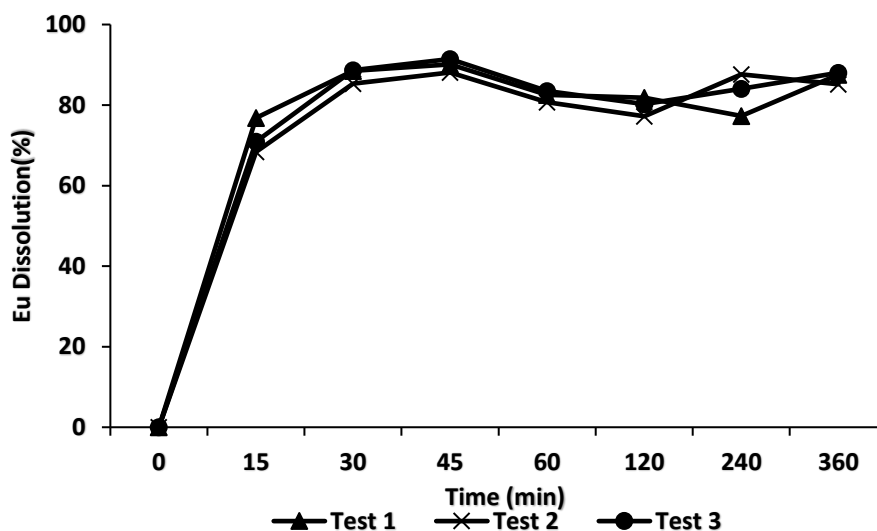
Figure 4.25: Eu leaching repeatability test at a temperature of 60 ºC, acid concentration of 3.5 M, agitation speed of 600 rpm, S/L ratio of 10 % (w/v) and a residence time of 45 minutes

Test 1 shows the initial results obtained during the acid leaching tests. Test 2 and 3 show the repeat experiment results. The results indicate that the findings are repeatable. A recovery of 98.1 ± 0.2 % was found for Y and 89.1 ± 1.4 % for Eu after 45 minutes of leaching.

Repeat experiments for Ce and Tb leaching tests were also conducted at conditions given in Table 4.6. The results are shown in Figure 4.26 and 4.27 for Ce and Tb leaching respectively. Repeat experiment results are presented in Table E.3 and E.4 Appendix E.
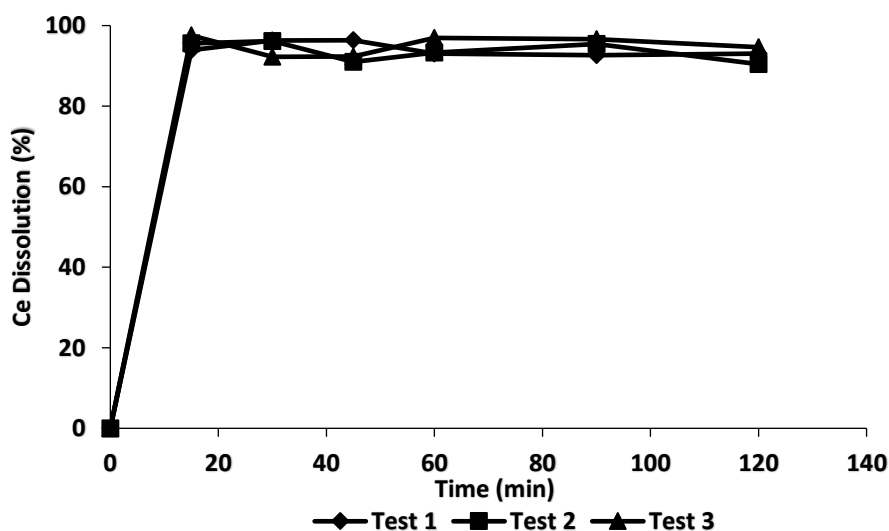
Figure 4.26: Ce leaching repeatability test after alkali fusion at a temperature of 60 ºC, acid concentration of 5 M, agitation speed of 600 rpm, S/L ratio of 5 % (w/v) and a residence time of 30 minutes

91
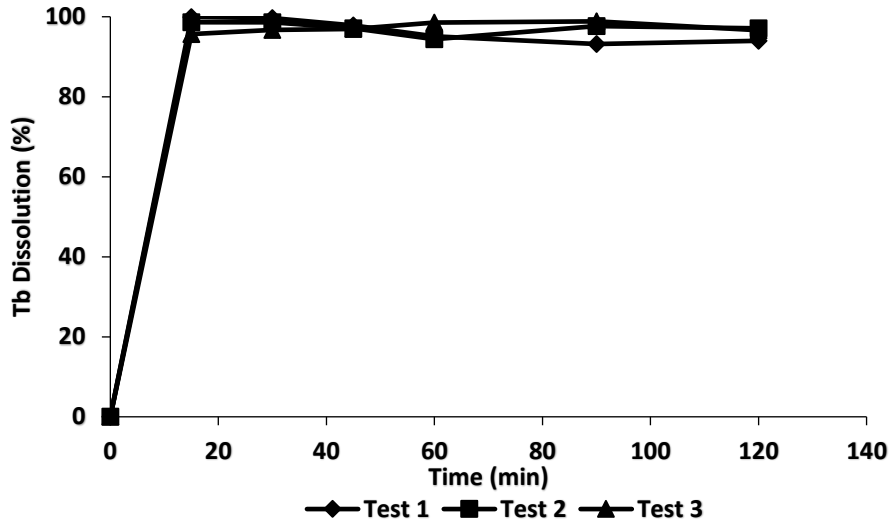
Figure 4.27: Tb leaching repeatability test after alkali fusion at a temperature of 60 ºC, acid concentration of 5 M, agitation speed of 600 rpm, S/L ratio of 5 % (w/v) and a residence time of 30 minutes

Test 2 and 3 show cerium and terbium percentage dissolution for repeat experiments 2 and 3. Both graphs show that the results obtained after acid digestion of both rare earths are repeatable. Optimal Ce recovery was found to be 96.9 ± 1.1 % and Tb recovery was 98.3 ±1.5 % after 30 minutes of leaching.

4.6.2 Solvent Extraction Repeatability Tests

Two Ce and Tb solvent extraction repeat experiments were performed at a pH of 0.5 and extractant concentration of 0.5 M. The results obtained are shown in Figure 4.28. The results generally show good repeatability for both Tb and Ce.
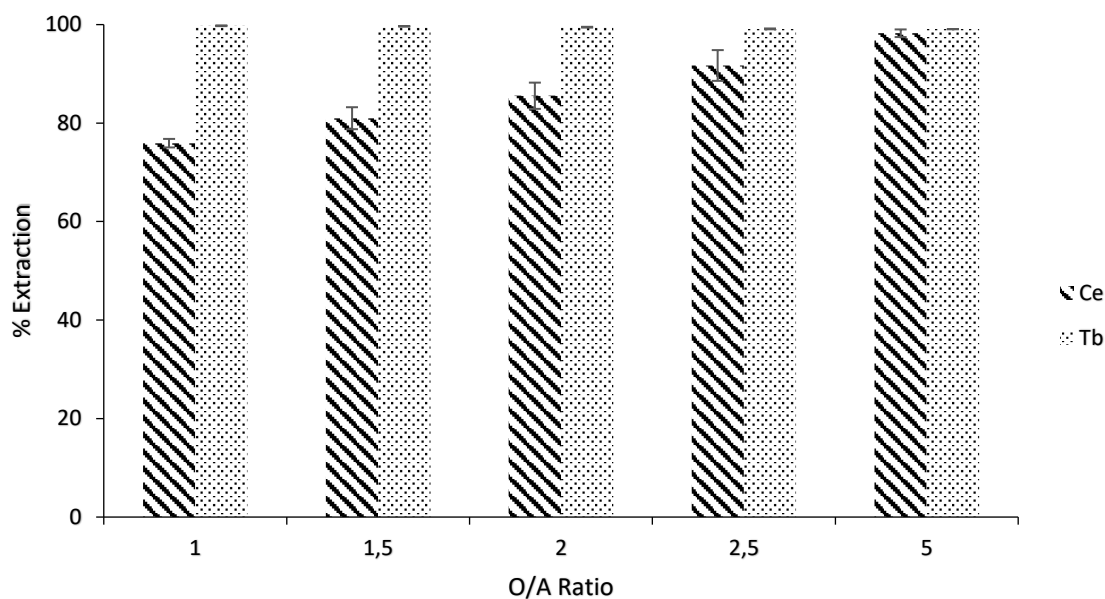
Figure 4.28: Ce and Tb solvent extraction repeatability tests at pH 0.5 and 0.5 M extractant concentration

The repeatability of the solvent extraction tests was also analysed using a single-factor ANOVA analysis to determine the mean squares between and within groups of the repeated runs. The results of the ANOVA analysis are given in Tables E.5 and E.6 Appendix E. Equation 25 was used to calculate the repeatability values for Ce and Tb solvent extraction. A repeatability of 0.94 and 0.96 was found for Ce and Tb respectively showing a very high degree of repeatability. Repeatability values for Y and Eu solvent extraction were found to be 0.998 and 0.997 respectively showing a very high degree of repeatability (Anderson, 2017). It was therefore assumed that results for all the other experiments were repeatable.

4.7 Proposed Flowsheet

Figure 4.29 shows the proposed flowsheet for the recovery of yttrium, europium, cerium and terbium. The suggested flowsheet involves Y and Eu leaching as the first step of metal recovery from the waste phosphor powder. In this step, sulphuric acid was the lixiviant of choice since it suppresses the dissolution of the main impurity calcium. Optimal conditions were found to be a temperature of 60 ℃, acid concentration of 3.5 M, residence time of 45 minutes, agitation speed of 600 rpm and a S/L ratio of 10 % (w/v). Recoveries of 98.1 ± 0.2 % Y and 89.1 ± 1.4 % were obtained.
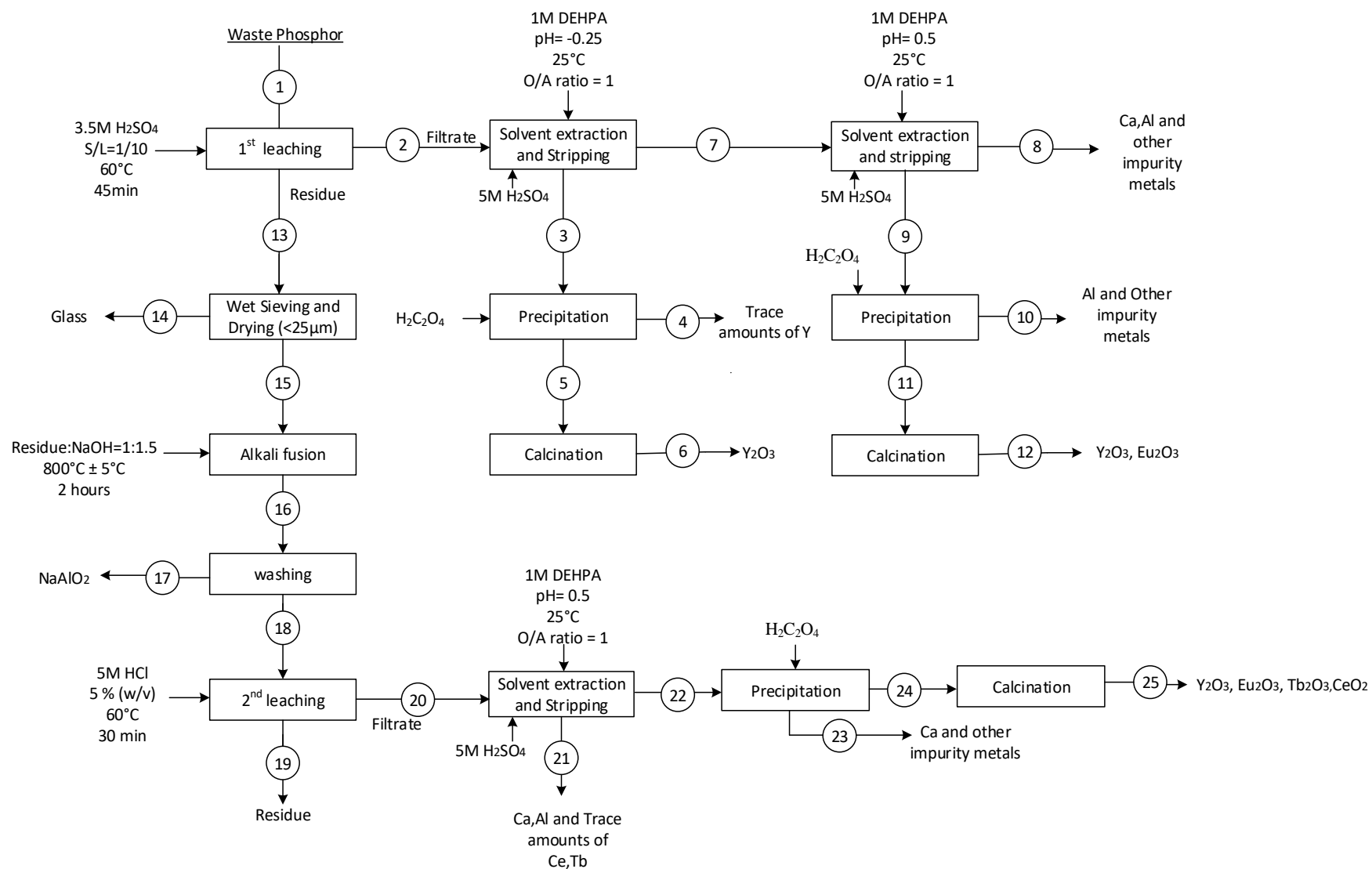
Figure 4.29: Proposed flowsheet for rare earth metals recovery from end-of-life fluorescent lamp powders

After the first staged leaching, the next step involves solvent extraction to recover the targeted rare earths from solution (Y and Eu). Only Yttrium is extracted when operating at a pH of-0.25, O/A ratio of 1, DEHPA concentration of 1 M and a temperature of 25 ℃. Eleven counter-current stages are required to recover more than 95 % Y from the aqueous solution. After solvent, Y is then stripped from the organic phase using 5 M sulphuric acid (as recommended by (Alberts, 2011)) in a 4-step stripping process to recover more than 95 % of the metal. The regenerated organic phase can be re-used for subsequent solvent extraction operations. pH adjustment of the strip liquor then follows prior to chemical precipitation using oxalic acid. More than 99 % Y recovery is achievable as discussed in section 2.7. Y is then recovered as Y_2O_3 after calcination of the rare earth oxalate.

Solvent extraction is also performed on the raffinate solution after Y extraction (stream 9). This process is conducted after adjusting pH to 0.5 using 5 M sodium hydroxide. More than 92 % Eu and 99 % of the residual Y can be recovered at this stage. Since 5 M sulphuric acid was found to strip more than 90 % Y from the organic phase (Alberts, 2011) it is assumed that all the other targeted rare earths will be much easier to strip under the same conditions. 5 M sulphuric acid can therefore be used to recover both Y and Eu from the organic phase using a series of 4 counter-current stages achieving more than 95 % rare earth recovery. Precipitation with oxalic acid then follows prior to calcination to produce a mixed rare earth product of Y and Eu oxides.

The first leach residue (stream 17) undergoes wet sieving to remove the glass fraction component which may be problematic during the alkali fusion process and other downstream processes. Wet sieving is performed using a 25 µm sieve prior to drying. The residue is then mixed with NaOH in the ratio 1:1.5 by mass before sintering at 800 ℃ for 2 hours. The alkali fusion product is cooled and then washed with water to remove sodium aluminate and other soluble components. Ce and Tb leaching then follows using HCl as the leaching agent. The leaching is performed at a temperature of 60 ℃, an acid concentration of 5 M, residence time of 30 minutes, S/L ratio of 5 % (w/v) and agitation speed of 600 rpm. More than 96 % Ce and 99 % Tb can be recovered into solution at this stage.

Cerium and terbium are then extracted from the aqueous solution after pH adjustment to 0.5 using 5 M NaOH. This can be achieved using 1 M DEHPA solution. Operating at an O/A ratio of 1 and a temperature of 25 ℃ will yield a mixed rare earth product containing Y, Eu, Ce and

Tb. 5 M sulphuric acid can be used at this stage to recover Ce, Tb and Eu from the aqueous phase prior to precipitation with oxalic acid. A mixed rare earth oxide product is produced. Using the proposed flowsheet, more than 96.9 ± 1.1 % Ce and 98.3 ± 1.5 % Tb can be recovered.

Using data obtained from experimental work, a mass balance was performed to evaluate metal recovery efficiency and effluent production. The stream balances for the proposed flowsheet are shown in Table 4.12. The individual stream balances were calculated based on a throughput of 100 kg/hr. Only Y, Eu, Ce, Tb and the main impurities Ca and Al were considered in the mass balances. Overall rare earth recovery is more than 90 %.

It is proposed to have an effluent treatment plant ETP where all liquid waste from different sections of the proposed plant is treated. The main effluent streams from the proposed flowsheet are stream 4, 8, 10, 14 17, 19, 21 and 23. Stream 4 containing trace amounts of Y in sulphuric acid can be reused in the first stage leaching. Stream 10 and 23 can undergo treatment in the ETP plant prior to neutalisation and disposal. Both streams can also be reused in the first stage leaching after further processing to remove impurities. Stream 8 and 21 can be further processed to recover Ca, Al and other metal impurities that remain in the aqueous phase after solvent extraction. The remaining solution is then treated and disposed. Fragmented glass from stream 14 can be taken for glass recycling while stream 19 can be taken for landfilling. Stream 17 can be treated prior to disposal.

Table 4.12: Proposed flowsheet mass balance

	Mass (kg/hr)												
	Input			Output		Output		Output		Output		Output	
Steam Number	**1**	**2**	**3**	**4**	**5**	**6**	**7**	**8**	**9**	**10**	**11**	**12**	**13**
Y	4.23	4.15	3.94	0.04	3.90	3.90	0.21	0.00	0.21	0	0.21	0.21	0.08
Eu	0.59	0.52	0	0	0	0	0.52	0.04	0.48	0.00	0.48	0.48	0.06
Ce	0.41	0	0	0	0	0	0	0	0	0	0	0	0.41
Tb	0.18	0	0	0	0	0	0	0	0	0	0	0	0.18
Ca	23.10	1.59	0	0	0	0	1.59	1.59	0.00	0.00	0	0	21.51
Al	24.38	4.00	0	0	0	0	4.00	3.52	0.48	0.48	0	0	20.38
Total	52.9			0.04		3.90		5.15		0.48		0.69	
Steam Number	Output			Output		Output		Output		Output		Output	
	14	**15**	**16**	**17**	**18**	**19**	**20**	**21**	**22**	**23**	**24**	**25**	
Y	0	0.08	0.08	0	0.08	0	0.08	0.00	0.08	0	0	0.08	
Eu	0	0.06	0.06	0	0.06	0	0.06	0.00	0.06	0	0	0.06	
Ce	0	0.41	0.41	0	0.41	0	0.40	0.02	0.38	0	0	0.38	
Tb	0	0.18	0.18	0	0.18	0	0.18	0.00	0.18	0	0	0.18	
Ca	0	21.51	21.51	4.52	16.99	8.90	8.09	7.58	0.51	0.51	0	0	
Al	0	20.38	20.38	7.54	12.84	8.10	4.74	4.74	0	0.00	0	0	
Total	0			12.06		17.02		12.34		0.51		0.70	
Overall input	52.883												
overall output	52.883												

97

5. Conclusions and Recommendations

5.1 Conclusions

A comprehensive literature review was conducted on the current best practices used in the recovery of rare earths from spent fluorescent lamps. The hydrometallurgical processing route was preferred over the pyrometallurgical route due to several advantages it offers as discussed in the literature review section. Hydrometallurgical operations such as leaching, solvent extraction, stripping and chemical precipitation were discussed and this provided a basis from which the methodology was designed.

Experimental work was performed and it was concluded that Y and Eu could be easily leached into solution since they exist in the waste phosphor powder as oxides (Y_2O_3). XRD analysis on the waste powder confirmed the presence of this oxide. The effect of temperature and acid concentration was investigated whilst holding other parameters constant. Optimal recoveries were obtained when operating at a temperature of 60 ºC, acid concentration of 3.5 M, residence time of 45 minutes, S/L ratio of 10% (w/v) and agitation speed of 600 rpm. Over 98 % Y and 89 % Eu recoveries were attained. Ce and Tb were not leached at this stage.

The use of ultrasound assisted digestion in Ce and Tb leaching was investigated as suggested in literature. Poor recoveries (<10 %) were obtained during preliminary experiments conducted hence this route was not further investigated. Alkali fusion proved to be an effective method in breaking the spinel structure of the blue (BAM) and green (CAT) phosphor components as suggested in literature. Ce and Tb were recovered after alkali fusion of the first stage leach residue with sodium hydroxide in the ratio 1:1.5. Optimal leaching conditions were found to be a temperature of 60 ºC, acid concentration of 5 M, 30 minutes residence time, S/L ratio of 5 % (w/v) and agitation speed of 600 rpm. Over 96 % Ce and 98 % Tb recoveries were achieved.

It was also concluded that DEHPA was effective in the extraction of all the targeted rare earths as found in literature. Y can be recovered separately at a pH of -0.25, O/A ratio of 1 using 1 M extractant concentration. Eu can be recovered after adjusting the pH to 0.5 but using the same O/A ratio and extractant concentration. Ce and Tb extraction occurs in a single stage extraction process where a mixed rare earth product is obtained. Y and Eu are also extracted. Optimum conditions for Ce and Tb extraction were an extractant concentration of 1 M, O/A ratio of 1, temperature of 25 ºC and a pH of 0.5.More than 95 % Ce and 99 % Tb recoveries were obtained.

Y and Eu were completely extracted. Stripping, chemical precipitation and calcination processes can then be used to obtain the targeted rare earths in the form of oxides.

5.2 Recommendations

There still exists a need for more research before finalising a full-scale recycling technology for rare earth recovery from spent fluorescent lamp phosphor powders in South Africa. The following recommendations are suggested to assess process viability.

1. Validate the viability of the proposed recovery technology to industry by evaluating the process on a pilot scale.

2. Further study is required to optimise other process variables such as S/L ratio and agitation speed which were not included in the leaching experiments.

3. Find an efficient process for Ca and Al recovery and recycling or disposal.

4. Perform solvent extraction at a lower pH to investigate if it is possible to recover Ce and Tb as separate rare earths.

5. Investigate the optimal stripping conditions for rare earth recovery from the organic phase after solvent extraction.

6. Perform further investigations on the use of ultrasound assisted digestion to recover Ce and Tb from green phosphor powders. This must be done using a device that provides a higher ultrasonic power output than the one used in this study.

References

Abreu, R. D. and Morais, C. A. (2014) 'Study on separation of heavy rare earth elements by solvent extraction with organophosphorus acids and amine reagents', *Minerals Engineering*. Elsevier Ltd, 61, pp. 82–87. doi: 10.1016/j.mineng.2014.03.015.

Alberts, E. (2011) *Stripping rare earth elements and iron from D2EHPA during zinc solvent extraction*. Stellenbosch : Stellenbosch University.

Anderson, A. E. (2017) *Evaluating solvent extraction for Y and Eu recovery from sulphuric acid leach solutions*. Stellenbosch University.

Baba, Y. *et al.* (2011) 'Recent advances in extraction and separation of rare-earth metals using ionic liquids', *Journal of Chemical Engineering of Japan*, 44(10), pp. 679–685.

Binnemans, K. *et al.* (2013) 'Recycling of rare earths: A critical review', *Journal of Cleaner Production*. Elsevier Ltd, 51, pp. 1–22. doi: 10.1016/j.jclepro.2012.12.037.

Binnemans, K. and Jones, P. T. (2014) 'Perspectives for the recovery of rare earths from end-of-life fluorescent lamps', *Journal of Rare Earths*. The Chinese Society of Rare Earths, 32(3), pp. 195–200. doi: 10.1016/S1002-0721(14)60051-X.

Cantrell, K. J. and Byrne, R. H. (1987) 'Rare earth element complexation by carbonate and oxalate ions', *Geochimica et Cosmochimica Acta*, 51(3), pp. 597–605.

Chang, T. C. and Yen, J. H. (2006) 'On-site mercury-contaminated soils remediation by using thermal desorption technology.', *Journal of hazardous materials*, 128(2–3), pp. 208–17. doi: 10.1016/j.jhazmat.2005.07.053.

Chen, X. *et al.* (2017) 'Recycling Y and Eu from Waste Fluorescent Powder and High Temperature Solid-State Synthesis of Y2O3:Eu Phosphors', *Minerals*, 7(3), p. 44. doi: 10.3390/min7030044.

Cox, M. and Flett, B. (1987) 'Modern extractants for copper, cobalt and nickel', *Chemistry and Industry*, pp. 188–93.

Crockford, H. D. and Addleston, J. A. (1935) 'The Solubility of Lead Sulfate in Aqueous Solutions of Sulfuric Acid at High Concentrations', *The Journal of Physical Chemistry*, 40(3), pp. 303–305. doi: 10.1021/j150372a002.

Cuif, J. P. *et al.* (2005) *Applications, in: Adachi, G., Imanaka, N., Kang, Z.C. (Eds.), Binary Rare Earth Oxides*. Springer.

CYTEC (2013) 'CYANEX 572 Extractant. Technical Brochure', p. 2. doi: https://www.cytec.com/sites/default/files/files/CYTEC_CYANEX_572_FINAL.

Desouky, O. A. *et al.* (2009) 'Liquid-liquid extraction of yttrium using primene-JMT from

acidic sulfate solutions', *Hydrometallurgy*. Elsevier B.V., 96(4), pp. 313–317. doi: 10.1016/j.hydromet.2008.11.009.

Diana, B. *et al.* (2011) *Critical material strategy*.

Diehl, L. O. *et al.* (2018) 'Ultrasound-assisted extraction of rare-earth elements from carbonatite rocks', *Ultrasonics Sonochemistry*. Elsevier, 40(December 2016), pp. 24–29. doi: 10.1016/j.ultsonch.2017.04.012.

Doyle, F. . *et al.* (2000) 'Direct production of mixed, rare earth oxide feed for high energy-product magnets', in *Rare Earths and Actinides: Science, Technology and Applications IV as held at the 2000 TMS Annual Meeting*, pp. 31–44.

Eduafo, P. M. (2016) 'Investigation of Recovery and Recycling of Rare Eerth Elements from Waste Fluorescent Lamp Phosphors'.

Ekberg, C. *et al.* (2016) 'Hydrochemical Routes to Recycle NiMH Batteries and Fluorescent Lamps', *Critical Metal Symphosium*, pp. 1–6.

EL-Yamani, I. S. and Shabana, E. I. (1985) 'Solvent extraction of lanthanum (III) from sulphuric acid solutions by Primene JMT', *Journal of the Less-Common Metals,* 105(2), pp. 255–261.

European Commission (2010) *Critical raw materials for the EU, Report of the Ad-hoc Working Group on defining critical raw materials*, *European Commission*. doi: 10.1002/eji.200839120.IL-17-Producing.

European Commission (2014) *Report on Critical Raw Materials for the EU,Report of the Ad hoc Working Group on defining critical raw materials*, *European Commision*. doi: Ref. Ares(2015)1819595 - 29/04/2015.

Feng, R. *et al.* (2002) 'Enhancement of ultrasonic cavitation yield by multi-frequency sonication', *Ultrasonics sonochemistry*, 9(5), pp. 231–236.

Gschneidner Jr, K. (1980) 'Rare earth speciality inorganic chemicals', in *Symposium on Speciality Inorganic Chemicals*. London, pp. 403–443.

Gupta, C. K. and Krishnamurthy, N. (2005) *Extractive metallurgy of rare earths*, *International Materials Reviews*. doi: 10.1179/imr.1992.37.1.197.

Habashi, F. (1999) *a Textbook of Hydrometallurgy*. 2nd edn, *Sainte-Foy, Quebec : Metallurgie extractive Quebec, Enr., 1993.* 2nd edn. Quabec City, Canada: Métallurgie Extractive Québec. doi: 10.1017/CBO9781107415324.004.

Hampel, C. A. (1968) 'No Title', *Encyclopedia of the chemical elements*. Reinhold Book Corp.

Haxel, G. B., Hedrick, J. B. and Orris, G. J. (2002) 'Rare Earth Elements — Critical Resources for High Technology', *United States Geological Survey Fact Sheet*, 087, pp. 1–4. doi:

10.1017/CBO9781107415324.004.

Huang, X. *et al.* (2008) 'Synergistic extraction of rare earth by mixtures of 2-ethylhexyl phosphoric acid mono-2-ethylhexyl ester and di-(2-ethylhexyl) phosphoric acid from sulfuric acid medium', *Journal of Rare Earths*, 26(3), pp. 410–413. doi: 10.1016/S1002-0721(08)60107-6.

Hudson, M. J. (1982) 'An introduction to some aspects of solvent-extraction chemistry in hydrometallurgy', *Hydrometallurgy*, 9(2), pp. 149–168. doi: 10.1016/0304-386X(82)90014-7.

Innocenzi, V. *et al.* (2013) 'Recovery of yttrium from cathode ray tubes and lamps' fluorescent powders: Experimental results and economic simulation', *Waste Management*. Elsevier Ltd, 33(11), pp. 2390–2396. doi: 10.1016/j.wasman.2013.06.002.

Iwata, Y., Imura, H. and Suzuki, N. (1990) 'Selective preconcentration of rare earth elements by substoichiometric precipitation of calcium oxalate and its application to the neutron activation analysis of biological materialSelective preconcentration of rare earth elements by substoichiometric pre', *Analytica chimica acta*, 239, pp. 115–120.

Jamrack, W. D. (1963) *Rare Metal Extraction by Chemical Engineering Techniques*.

Jang, M., Hong, S. M. and Park, J. K. (2005) 'Characterization and recovery of mercury from spent fluorescent lamps', *Waste Management*, 25(1), pp. 5–14. doi: 10.1016/j.wasman.2004.09.008.

Jun, L. *et al.* (1998) 'Recovery of Ce (IV) and Th (IV) from rare earths (III) with Cyanex 923', *Hydrometallurgy*, 50(1), pp. 77–87.

Jüstel, T., Nikol, H. and Ronda, C. (1998) 'New Developments in the Field of Luminescent Materials for Lighting and Displays', *Angewandte Chemie International Edition*. Wiley-Blackwell, 37(22), pp. 3084–3103.

Kilbourn, B. T. (1994) 'A Lanthanide Lanthology part 2 M-Z', *Molycorp*, (reprinted), pp. 1–63.

Konishi, Y., Satoh, D. and Takano, K. (2002) 'Precipitation of nickel hydroxide by hydrolytic stripping of nickel phosphinate', *Industrial \& engineering chemistry research*, 41(16), pp. 3999–4003.

Kraikaew, J., Srinuttrakul, W. and Chayavadhanakur, C. (2005) 'Solvent Extraction Study of Rare Earths from Nitrate Medium by the Mixtures of TBP and D2EHPA in Kerosene', *Journal of Metals, Materials and Minerals*, 15(2), pp. 89–95.

Kumar, M. (1994) 'Recent trends in chromatographic procedures for separation and determination of rare earth elements. A review', *The Analyst*. The Royal Society of

Chemistry, 119(9), p. 2013. doi: 10.1039/an9941902013.

Li, H. M. (2010) 'Recovery of rare earths from phosphor sludge by acid leaching', *Chinese Journal of Rare Metals*, 34(6), pp. 898–904.

Liu, H. *et al.* (2014) 'Rare earth elements recycling from waste phosphor by dual hydrochloric acid dissolution', *Journal of Hazardous Materials*. Elsevier B.V., 272, pp. 96–101. doi: 10.1016/j.jhazmat.2014.02.043.

Measey, G. J. (2003) 'Testing of repeatability in measurements of Length and Mass in Chthonerpeton indistinctum (Amphibia : Gymnophiona); Including a Novel Method of Calculating Total Length of Live Caec ...', (May 2014).

De Michelis, I. *et al.* (2011) 'Treatment of exhaust fluorescent lamps to recover yttrium: Experimental and process analyses', *Waste Management*. Elsevier Ltd, 31(12), pp. 2559–2568. doi: 10.1016/j.wasman.2011.07.004.

Michelsen, O. B. and Smutz, M. (1971) 'No Title', *Journal of Inorganic and Nuclear Chemistry*, 33(1), pp. 265–278.

Mishra, S. ., Singh, H. and Gupta, C. K. (2000) 'Simultaneous purification of dysprosium and terbium from dysprosium concentrate using 2-ethyl hexyl phosphonic acid mono-2-ethyl hexyl ester as an extractant', *Hydrometallurgy*, 56(1), pp. 33–40.

Mohapatra, D. *et al.* (2007) 'Liquid--liquid extraction of aluminium (III) from mixed sulphate solutions using sodium salts of Cyanex 272 and D2EHPA', *Separation and purification technology*, 56(3), pp. 311–318.

Morais, C. A. and Ciminelli, V. S. . (2007) 'Selection of solvent extraction reagent for the separation of europium (III) and gadolinium (III)', 20, pp. 747–752. doi: 10.1016/j.mineng.2007.02.010.

Morais, C. A. and Ciminelli, V. S. T. (2004) 'Process development for the recovery of high-grade lanthanum by solvent extraction', 73, pp. 237–244. doi: 10.1016/j.hydromet.2003.10.008.

Nakamura, T., Nishihama, S. and Yoshizuka, K. (2007) 'Separation and recovery process for rare earth metals from fluorescence material wastes using solvent extraction', *Solvent Extraction Research and Development-Japan*, 14, pp. 105–113.

Nash, K. L. (1993) 'A review of the basic chemistry and recent developments in trivalent f-elements separations', *Solvent Extraction and Ion Exchange*. Taylor & Francis Group, 11(4), pp. 729–768. doi: 10.1080/07366299308918184.

Olivier, M. C. (2011) *Developing a solvent extraction process for the separation of cobalt and iron from nickel sulphate solutions*. Stellenbosch University.

Peppard, D. F. and Wason, G. W. (1961) 'Liquid-liquid extraction of trivalent rare earths using acidic phosphonates as extractants', in *Rare Earth Research*. The Macmillan Company New York, pp. 37–50.

Porob, D. G. *et al.* (2012) 'Rare earth recovery from fluorescent material and associated method'. U.S. Patent 8,137,645.

Preston, J. S. *et al.* (1996) 'The recovery of rare earth oxides from a phosphoric acid by-product . Part 2 : The preparation of high-purity cerium dioxide and recovery of a heavy rare earth oxide concentrate', *Hydrometallurgy*, 41, pp. 21–44.

Rabah, M. A. (2004) 'Recovery of aluminium, nickel–copper alloys and salts from spent fluorescent lamps', *Waste Management*, 24(2), pp. 119–126. doi: 10.1016/j.wasman.2003.07.001.

Rabah, M. A. (2008) 'Recyclables recovery of europium and yttrium metals and some salts from spent fluorescent lamps', *Waste Management*, 28(2), pp. 318–325. doi: 10.1016/j.wasman.2007.02.006.

Rao, S. R. (2006) 'Chapter 4 Hydrometallurgical processes', *Resource recovery and recycling from metallurgical wastes*, pp. 71–108.

Raposo, C., Windmoller, C. C. and Junior, W. A. D. (2003) 'Mercury speciation in fluorescent lamps by thermal release analysis', 23, pp.879–886. doi:10.1016/S056-053X(03)00089-8.

Reddy, B. R., Kumar, B. N. and Radhika, S. (2009) 'Solid-Liquid Extraction of Terbium from Phosphoric Acid Medium using Bifunctional Phosphinic Acid Resin, Tulsion CH-96', *Solvent Extraction and Ion Exchange*. Taylor & Francis Group, LLC , 27(5–6), pp. 695–711. doi: 10.1080/07366290903270031.

Ritcey, G. M. and Ashbrook, A. W. (1984) *Solvent extraction : Principles and Applications to Process Metallurgy*. Amsterdam: Elsevier.

Ronda, C. R., Jüstel, T. and Nikol, H. (1998) 'Rare earth phosphors: fundamentals and applications', *Journal of Alloys and Compounds*, 275, pp. 669–676.

Rousseau, R. W. (1987) *Handbook of separation process technology*.

Rydberg, J. *et al.* (2004) *Solvent Extraction Principles and Practice*. 2nd edn. New York: Taylor & Francis Group.

Sato, T. (1989) 'Liquid-Liquid Extraction of Rare-Earth Elements from Aqueous Acid Solutions by Acid Organophosphorus Compounds', *Hydrometallurgy*, 22(1–2), pp. 121–140.

Shimizu, R. *et al.* (2005) 'Supercritical fluid extraction of rare earth elements from luminescent material in waste fluorescent lamps', *Journal of Supercritical Fluids*, 33(3), pp. 235–241.

doi: 10.1016/j.supflu.2004.08.004.

Song, N. *et al.* (2009) 'Extraction and separation of rare earths from chloride medium with mixtures of 2-ethylhexylphosphonic acid mono- (2-ethylhexyl) ester and sec - nonylphenoxy acetic acid', (August), pp. 1798–1802. doi: 10.1002/jctb.2248.

Song, X. I. N., Chang, M. and Pecht, M. (2013) 'Rare-Earth Elements in Lighting and Optical Applications and Their Recycling Rare-Earth Elements in Lighting and Optical Applications and Their Recycling', (October). doi: 10.1007/s11837-013-0737-6.

Takahashi, T. *et al.* (2001) 'Separation and recovery of rare earth elements from phosphor sludge in processing plant of waste fluorescent lamp by pneumatic classification and sulfuric acidic leaching', *Journal of the Mining and Materials Processing Institute of Japan(Japan)*, 117(7), pp. 37–43.

Takip, K. M., Markom, M. and Sulaiman, M. Y. M. (2015) 'Solvent Extraction of Light Rare Earths from Acidic Medium by Di- (2-ethylhexyl) Phosphoric Acid in Kerosene', *Jurnal Kejuruteraan*, 27, pp. 57–62.

Tan, Q., Li, J. and Zeng, X. (2015) 'Rare earth elements recovery from waste fluorescent lamps: a review', *Critical Reviews in Environmental Science and Technology*, 45(7), pp. 749–776.

Tanaka, Y., Zhang, Q. and Saito, F. (2002) 'Sonochemical recovery of metals from recording media', *Journal of Chemical Engineering of Japan*, 35(2), pp. 173–177. doi: 10.1252/jcej.35.173.

Tang, Y. B. *et al.* (2006) 'Progress in research on barium magnesium aluminate', *Mater. Rev*, 20, pp. 335–338.

Taniguchi, V. T., Doty, A. W. and Byers, C. H. (1988) '(CDC), Large scale chromatographic separations using continuous displacement chromatography', in *Rare earths*, pp. 147–161.

Thakur, N. V (2000) 'Separation of dysprosium and yttrium from yttrium concentrate using alkylphosphoric acid (DEHPA) and alkylphosphonic acid (EHEHPA-PC 88A) as extractants', *Solvent Extraction and Ion Exchange*, 18(5), pp. 853–875.

Tunsu, C. *et al.* (2014) 'Studies on the Solvent Extraction of Rare Earth Metals from Fluorescent Lamp Waste Using Cyanex 923', *Solvent Extraction and Ion Exchange*. Taylor & Francis, 32(6), pp. 650–668. doi: 10.1080/07366299.2014.925297.

Tunsu, C. (2016) *Hydrometallurgical Recovery of Rare Earth Elements From Fluorescent*. Chalmers University of Technology.

Tunsu, C., Ekberg, C. and Retegan, T. (2014) 'Characterization and leaching of real fluorescent lamp waste for the recovery of rare earth metals and mercury', *Hydrometallurgy*. Elsevier B.V., 144–145, pp. 91–98. doi: 10.1016/j.hydromet.2014.01.019.

US Department of Energy (2010) *Fluorescent Lighting | Department of Energy*.

USEPA (2012) *Rare Earth Elements: A Review of Production, Processing, Recycling, and Associated Environmental Issues*. Available at: http://nepis.epa.gov/PDF/P100EUBC

Wang, J. X. and Zheng, J. (2010) 'The status and analysis of mercury-containing waste fluorescent lamp', *Chin Environ Protect Ind*, 10, pp. 37–41.

Wang, L. *et al.* (2010) 'Recovery of rare earths from wet-process phosphoric acid', *Hydrometallurgy*, 101(1–2), pp. 41–47. doi: 10.1016/j.hydromet.2009.11.017.

Wang, X. *et al.* (2011) 'Notice of Retraction Recovery of Rare Earths from Spent Fluorescent Lamps', in *Bioinformatics and Biomedical Engineering,(iCBBE) 2011 5th International Conference on 2011 May 10*, pp. 1–4.

Wang, Y. G. *et al.* (2002) 'Solvent extraction of scandium(III), yttrium(III), lanthanides(III), and divalent metal ions with sec-nonylphenoxy acetic acid', *Solvent Extraction and Ion Exchange*, 20(6), pp. 701–716. doi: 10.1081/SEI-120016074.

Wu, D., Bao, B. and Zhang, Q. (2007) 'Synergistic effects in extraction and separation of praseodymium(III) and neodymium(III) with 8-hydroxyquinoline in the presence of 2-ethylhexyl phosphonic acid mono-2-ethylhexyl ester', *Industrial and Engineering Chemistry Research*, 46(19), pp. 6320–6325. doi: 10.1021/ie070098r.

Wu, D., Wang, X. and Li, D. (2007) 'Extraction kinetics of Sc(III), Y(III), La(III) and Gd(III) from chloride medium by Cyanex 302 in heptane using the constant interfacial cell with laminar flow', *Chemical Engineering and Processing: Process Intensification*, 46(1), pp. 17–24. doi: 10.1016/j.cep.2006.04.007.

Wu, Y. *et al.* (2013) 'Recovery of rare earth elements from waste fluorescent phosphors: Na2O2 molten salt decomposition', *Journal of Material Cycles and Waste Management*, 16(4), pp. 635–641. doi: 10.1007/s10163-014-0295-1.

Wu, Y. *et al.* (2014) 'The recycling of rare earths from waste tricolor phosphors in fluorescent lamps: A review of processes and technologies', *Resources, Conservation and Recycling*. Elsevier B.V., 88(100), pp. 21–31. doi: 10.1016/j.resconrec.2014.04.007.

Wu, Z. and Cormack, A. N. (2003) 'Defects in BaMgAl10O17: Eu^{2+} Blue Phosphor', *Journal of Electroceramics*, 10(3), pp. 179–191. doi: 10.1023/B:JECR.0000011216.01346.03.

Xie, F. *et al.* (2014) 'A critical review on solvent extraction of rare earths from aqueous solutions', *Minerals Engineering*. Elsevier Ltd, 56, pp. 10–28. doi: 10.1016/j.mineng.2013.10.021.

Yang, F. *et al.* (2013) 'Selective extraction and recovery of rare earth metals from phosphor powders in waste fluorescent lamps using an ionic liquid system', *Journal of Hazardous*

Materials. Elsevier B.V., 254–255(1), pp. 79–88. doi: 10.1016/j.jhazmat.2013.03.026.

Yoon, H.-S. *et al.* (2014) 'Leaching kinetics of neodymium in sulfuric acid of rare earth elements (REE) slag concentrated by pyrometallurgy from magnetite ore', *Korean Journal of Chemical Engineering*. Springer US, 31(10), pp. 1766–1772. doi: 10.1007/s11814-014-0078-3.

Zeng, D. and Wang, W. (2011) 'Solubility phenomena involving CaSO 4 in hydrometallurgical processes concerning heavy metals *', *Pure and Applied Chemistry ·*, 83(5), pp. 1045–1061. doi: 10.1351/PAC-CON-10-09-11.

Zhang, S. G. *et al.* (2013) 'Recovery of waste rare earth fluorescent powders by two steps acid leaching', *Rare Metals*, 32(6), pp. 609–615. doi: 10.1007/s12598-013-0170-6.

Zhang, W. (2012) 'The development report of China lighting industry in 2011', *China Light.Light*, 7(14.3).

Appendix A: Reagents Used For Leaching and Material Characterisation

Table A.1: Calculations for the volume of sulphuric acid recquired to make desired acid concentration

Density of acid [g/L]	1840
Molar Mass [g/mol]	98.079
Weight percentage	98%

Desired concentration [M]	2	3	5
Desired final volume [mL]	500	500	500
Volume of stock required [mL]	54.392	81.588	135.980

Table A.2: Calculations for the volume of nitric acid recquired to make desired acid concentration.

Density of acid [g/L]	1339.30
Molar Mass [g/mol]	63.01
Weight percentage[%]	55
Desired concentration [M]	5
Desired final volume [mL]	500
Volume of stock required [[mL]	213.850

Table A.3: Calculations for the volume of hydrochloric acid recquired to make desired acid concentration.

Density of acid [g/L]	1159.3
Molar Mass [g/mol]	36.46
Weight percentage	32

Desired concentration [M]	1	3	5
Desired final volume [mL]	300	300	300
Volume of stock required [[mL]	29.484	88.453	147.422

Table A. 4: Calculation of the required volumes of acids to make 200 mL of aqua regia

Substance	Concentration [wt%]	Mw [g/mol]	Molar Ratio	Density [g/L]	Required [mL]	Volume Ratio
HNO3	55	63.01	1	1339.30	44.98	1
HCl	32	36.46	3	1159.30	155.02	3.45

Appendix B: Waste Phosphor Characterisation

Table B.1 shows the amount of metals leached during aqua regia leaching of 25 g of the received sample.

Table B.1: Results of aqua regia leaching of the received sample

Aqua regia test	Mass (g)					
	Ca	Al	Y	Eu	Ce	Tb
1	4.133	0.296	1.044	0.073	0.101	0.045
2	4.362	0.299	1.069	0.075	0.101	0.047
3	4.275	0.318	1.057	0.074	0.105	0.046
4	4.186	0.306	1.034	0.071	0.104	0.044
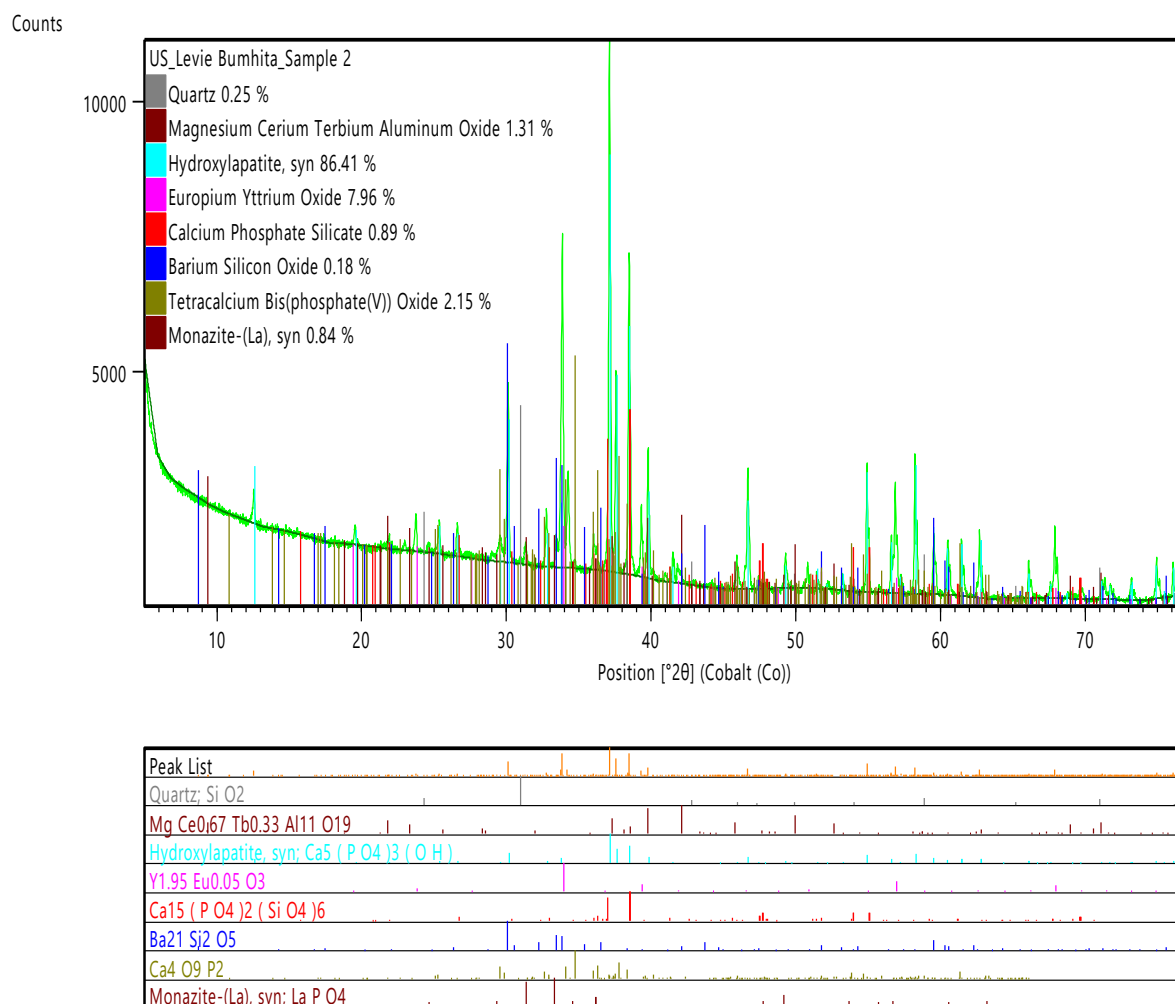
Figure B.1: XRD plot of waste fluorescent powders for phase identification

Appendix C: Experimental Data

C.1 Y and Eu Leach Tests

Table C.1.1: ICP results for leaching at 2 M and 30 ºC

Time (min)	Mass (ppm)					
	Y	Eu	Ce	Tb	Al	Ca
15	696.4	44.7	0	0	163.4	1014.4
30	1116.6	72.5	0	0	187.0	1037.0
45	1385.2	90.2	0	0	170.2	963.0
60	1513.4	98.8	0	0	164.6	820.2
120	2524.0	165.1	4.4	2.8	218.4	893.4
240	2746.2	215.2	2.9	1.0	230.0	960.0
360	2774.2	182.4	2.9	1.7	202.4	765.8

Table C.1.2: ICP results for leaching at 2 M and 60 ºC

Time (min)	Mass (ppm)					
	Y	Eu	Ce	Tb	Al	Ca
15	2541.4	165.8	0	0	230.2	1845.8
30	3091.0	214.0	0	0	355.6	2161.2
45	2873.2	189.2	0	0	302.4	1604.4
60	3360.8	221.4	15.6	0	398.4	1859.6
120	3329.0	219.8	14.4	9.6	487.8	1708.0
240	3202.6	209.4	21.4	15.8	566.4	1454.6
360	3032.4	201.4	28.4	21.4	595.4	1557.8

Table C.1.3: ICP results for leaching at 2 M and 90 ºC

Time (min)	Mass (ppm)					
	Y	Eu	Ce	Tb	Al	Ca
15	2581.8	136.0	4.2	7.8	429.8	2853.6
30	3215.4	333.8	12.4	14.8	638.4	3290.2
45	3264.0	336.0	15.0	16.8	690.4	3489.0
60	2821.0	289.4	9.0	15.8	626.6	2965.0
120	2935.0	294.0	7.2	15.2	688.0	3098.6
240	3271.8	320.6	23.8	17.4	791.0	3126.2
360	3105.6	293.0	12.6	16.0	769.6	3355.8

Table C.1.4: ICP results for leaching at 3.5 M and 30 ºC

Time (min)	Mass (ppm)					
	Y	Eu	Ce	Tb	Al	Ca
15	545.8	32.6	0	0	146.2	632.0
30	784.6	48.0	0	0	143.0	545.2
45	957.8	61.0	0	0	150.8	468.4
60	1309.8	82.0	1.16	0	164.2	603.4
120	1730.0	110.0	0	0.3	144.4	485.0
240	2053.2	162.8	0	0.2	133.2	412.2
360	2006.4	149.2	3.6	3.5	225.0	633.0

Table C.1.5: ICP results for leaching at 3.5 M and 60 ºC

Time (min)	Mass (ppm)					
	Y	Eu	Ce	Tb	Al	Ca
15	3309.8	207.6	0	0	22.4	1151.4
30	4103.4	259.4	0	0	96.2	1007.8
45	4149.8	267.6	0	0	129.6	1400.0
60	3811.4	244.4	0	3.8	92.0	895.6
120	3648.4	234.8	0	10.4	115.0	898.6
240	3780.0	245.8	5.1	19.4	140.6	1289.2
360	3992.6	257.6	10.5	20.6	132.2	1137.2

Table C.1.6: ICP results for leaching at 3.5 M and 90 ºC

Time (min)	Mass (ppm)					
	Y	Eu	Ce	Tb	Al	Ca
15	2874.6	97.706	0	0	429.5	1853.4
30	2696.8	87.6	6.7	13.4	572.8	2607.8
45	2791.0	73.2	5.8	13.6	626.2	2444.0
60	3264.4	76.2	8.0	13.8	753.4	2994.4
120	2552.0	51.6	0	11.4	607.8	2230.6
240	2958.6	54.4	3.3	12.8	691.6	2436.6
360	2876	50.6	0	10.6	657.4	2301.6

Table C.1.7: ICP results for leaching at 5 M and 30 ºC

Time (min)	Mass (ppm)					
	Y	Eu	Ce	Tb	Al	Ca
15	391.4	23.0	0	0	113.4	188.2
30	494.6	29.4	0	0	102.6	156.6
45	801.8	48.2	3.3	0	135.8	174.2
60	938.4	57.8	0	1.1	136.0	188.0
120	1691.8	106.2	7.8	0	169.8	220.8
240	2032.0	132.0	3.2	0.3	151.6	164.2
360	1760.0	109.2	0.7	0	121.8	117.2

Table C.1.8: ICP results for leaching at 5 M and 60 ºC

Time (min)	Mass (ppm)					
	Y	Eu	Ce	Tb	Al	Ca
15	2450.0	104.4	0	4.2	231.2	787.8
30	2514.2	97.2	0	7.6	246.2	728.4
45	2703.6	95.8	0	8.0	314.8	812.0
60	2729.0	92.8	0	3.4	337.2	648.8
120	2193.6	68.8	0	8.8	324.2	779.8
240	1979.8	55.4	0	6.9	364.8	445.2
360	2406.2	74.4	0	6.4	562.0	338.6

Table C.1.9: ICP results for leaching at 5 M and 90 ºC

Time (min)	Mass (ppm)					
	Y	Eu	Ce	Tb	Al	Ca
15	1691.0	50.0	0	0	338.4	787.8
30	1772.6	51.2	0	7.6	406.6	728.4
45	1931.2	67.6	0	8.0	470.4	812.0
60	1815.4	66.8	0	3.4	453.2	648.8
120	1951.0	84.8	0	8.8	522.4	779.8
240	1809.8	64.6	0	6.9	557.8	445.2
360	1866.6	67.4	0	6.4	583.8	338.6

C.2 Ce and Tb Leach Tests

Table C.2.1: ICP results for leaching at 1 M and 30 ºC

Time (min)	Mass (ppm)					
	Ce	**Tb**	**Y**	**Eu**	**Al**	**Ca**
15	31.7	223.0	110.3	19.3	790.7	7911.3
30	27.7	211.7	107.7	19.3	904.7	8780.7
45	26.3	211.3	111.7	19.3	868.3	8694.3
60	23.7	206.3	107.0	19.0	794.0	9019.0
90	28.0	217.0	108.3	19.3	851.7	8864.7
120	29.7	220.0	109.0	19.3	844.0	9159.0

Table C.2.2: ICP results for leaching at 1 M and 60 ºC

Time (min)	Mass (ppm)					
	Ce	**Tb**	**Y**	**Eu**	**Al**	**Ca**
15	51.0	250.0	118.0	35.0	920.3	8693.0
30	51.0	263.3	115.0	35.3	911.0	7746.3
45	52.3	255.7	114.0	35.3	877.3	30771.3
60	42.0	227.0	124.7	33.3	826.7	8947.0
90	52.7	261.0	115.0	35.3	788.3	9149.3
120	52.7	249.7	112.7	35.3	765.0	8933.0

Table C.2.3: ICP results for leaching at 1 M and 90 ºC

Time (min)	Mass (ppm)					
	Ce	**Tb**	**Y**	**Eu**	**Al**	**Ca**
15	91.3	255.0	128.0	35.3	753.0	8653.7
30	96.0	264.7	112.3	35.7	744.7	8939.0
45	98.0	269.0	113.3	35.7	619.0	7674.7
60	95.7	264.0	112.7	35.7	746.3	8962.7
90	88.0	232.3	113.0	35.0	695.7	8916.0
120	97.7	254.3	113.3	35.3	663.0	8376.0

Table C.2.4: ICP results for leaching at 3 M and 30 ºC

Time	Mass (ppm)					
(min)	Ce	Tb	Y	Eu	Al	Ca
15	306.0	260.0	112.0	35.7	1245.7	8387.0
30	319.7	247.0	110.3	35.3	1101.0	8896.3
45	331.3	253.7	111.0	35.3	1150.7	9105.3
60	359.3	269.0	114.0	35.7	1352.3	9041.7
90	335.3	251.3	110.7	35.3	1118.3	9012.7
120	340.3	255.3	111.0	35.3	1299.0	8837.3

Table C.2.5: ICP results for leaching at 3 M and 60 ºC

Time	Mass (ppm)					
(min)	Ce	Tb	Y	Eu	Al	Ca
15	311.7	232.7	118.0	35.0	1060.3	9240.7
30	307.7	229.3	116.0	35.0	1010.7	9202.3
45	367.0	260.0	121.0	35.7	1188.3	9535.3
60	330.0	239.3	119.3	35.3	1116.0	8878.7
90	321.0	229.3	120.3	35.0	1155.0	9051.3
120	371.7	263.0	114.0	35.7	1129.7	9098.0

Table C.2.6: ICP results for leaching at 3 M and 90 ºC

Time	Mass (ppm)					
(min)	Ce	Tb	Y	Eu	Al	Ca
15	356.7	248.7	115.7	35.3	1031.3	9130.3
30	397.3	267.0	111.7	35.7	1158.7	9085.3
45	421.7	279.0	113.0	36.0	1251.0	8729.0
60	375.0	248.7	104.7	35.3	1127.7	8761.0
90	427.3	278.7	113.0	36.0	1096.0	9211.3
120	432.3	281.0	113.3	36.0	1119.7	8770.0

Table C.2.7: ICP results for leaching at 5 M and 30 ºC

Time (min)	Mass (ppm)					
	Ce	Tb	Y	Eu	Al	Ca
15	369.3	273.3	113.0	35.7	767.7	8766.7
30	382.7	281.3	113.7	36.0	810.3	9050.7
45	383.7	275.7	112.7	35.7	756.7	8705.3
60	410.7	298.0	115.3	36.0	919.0	8056.7
90	431.7	308.9	416.0	36.3	1023.0	8511.3
120	381.0	270.9	361.0	35.7	679.7	8323.7

Table C.2.8: ICP results for leaching at 5 M and 60 ºC

Time (min)	Mass (mg)					
	Ce	Tb	Y	Eu	Al	Ca
15	534.7	358.3	414.0	41.3	4334.3	9640.3
30	548.0	357.3	405.7	43.0	4250.7	9458.7
45	548.3	351.0	376.3	43.3	4091.3	9222.7
60	529.7	341.3	335.3	45.0	4269.0	9325.7
90	527.3	334.3	352.0	42.7	4246.0	9280.3
120	529.3	337.0	349.7	42.3	4215.7	9171.3

Table C.2.9: ICP results for leaching at 5 M and 90 ºC

Time (min)	Mass (ppm)					
	Ce	Tb	Y	Eu	Al	Ca
15	455.0	307.3	119.7	36.3	1357.3	9518.0
30	427.7	286.0	123.3	36.0	1198.0	8626.3
45	443.0	293.7	114.0	36.0	1263.0	9046.0
60	458.3	301.7	115.0	44.3	1189.3	9354.0
90	429.7	280.3	112.3	41.0	1153.7	8394.3
120	381.3	237.0	111.3	40.3	1202.3	9653.3

116

C.3 Y and Eu Solvent Extraction

Table C.3.1: ICP results for solvent extraction tests performed at a pH of -0.25 and an extractant concentration of 0.5 M

O/A	Aqueous Phase(ppm)								
	Al	**B**	**Ca**	**Ce**	**Eu**	**Gd**	**Mg**	**Tb**	**Y**
0.25	212.2	23.1	577.9	2.68	229.3	6.58	154.7	1.88	3166.4
0.5	214.5	23.2	603.8	3.09	231.8	6.65	152.3	1.69	2876.8
1	212.0	22.9	646.1	2.96	228.1	6.49	154.5	1.90	2554.7
1.5	207.5	22.4	688.9	2.61	222.7	6.17	154.2	1.83	2184.3
2.5	211.0	22.6	800.6	2.54	224.9	6.29	158.1	1.77	1794.3
5	215.2	23.0	757.5	3.52	226.3	6.47	163.5	1.66	1179.9
Original Aq	**209.5**	**23.8**	**533.0**	**2.68**	**226.2**	**6.53**	**155.3**	**1.97**	**3360.9**
O/A	Organic Phase (ppm)								
	Al	**B**	**Ca**	**Ce**	**Eu**	**Gd**	**Mg**	**Tb**	**Y**
0.25	0	0	0	0	0	0	0	0.35	777.7
0.5	0	0	0	0	0	0	0	0.56	968.1
1	0	0	0	0	0	0	0	0.06	806.2
1.5	0	0	0	0	0	0	0	0.09	784.4
2.5	0	0	0	0	0	0	0	0.08	626.6
5	0	0	0	0	0	0	0	0.06	436.2

117

Table C.3.2: ICP results for solvent extraction tests performed at a pH of -0.25 and an extractant concentration of 1 M.

O/A	Aqueous Phase (ppm)								
	Al	**B**	**Ca**	**Ce**	**Eu**	**Gd**	**Mg**	**Tb**	**Y**
0.25	204.5	22.0	584.4	2.12	219.7	6.18	148.6	1.99	2534.6
0.5	214.9	23.1	661.3	1.96	229.9	6.54	156.5	1.73	2159.7
1	213.1	22.7	759.3	2.62	224.8	6.31	158.9	1.75	1429.3
1.5	218.1	23.2	872.5	3.05	229.4	6.36	166.1	1.51	1083.5
2.5	217.0	23.3	785.7	2.31	224.8	6.25	169.4	1.45	785.6
5	214.8	23.0	794.7	1.95	209.1	5.77	184.0	0.78	450.0
Original Aqueous	**209.5**	**23.8**	**533.0**	**2.68**	**226.2**	**6.53**	**155.3**	**1.97**	**3360.9**
O/A	Organic Phase (ppm)								
	Al	**B**	**Ca**	**Ce**	**Eu**	**Gd**	**Mg**	**Tb**	**Y**
0.25	0	0	0	0	0	0	0	0.00	3305.1
0.5	0	0	0	0	0	0	0	0.48	2402.3
1	0	0	0	0	0	0	0	0.22	1931.5
1.5	0	0	0	0	0	0	0	0.30	1518.3
2.5	0	0	0	0	0	0	0	0.21	1030.1
5	0	0	0	0	0	0	0	0.24	582.2

Table C.3.3: ICP results for solvent extraction tests performed at a pH of 0.5 and an extractant concentration of 0.5 M

O/A	Aqueous Phase (ppm)								
	Al	**B**	**Ca**	**Ce**	**Eu**	**Gd**	**Mg**	**Tb**	**Y**
0.25	145.26	20.10	403.10	2.25	150.00	4.48	103.20	N/D	1123.13
0.5	142.86	19.63	425.76	0.91	149.84	4.29	101.11	N/D	377.74
1	138.47	18.86	461.74	1.73	116.17	2.89	99.81	N/D	52.85
1.5	138.42	18.89	519.70	1.49	91.37	2.18	101.63	N/D	24.26
2.5	129.14	18.27	585.20	1.19	51.11	1.06	100.43	N/D	8.30
5	122.34	18.01	586.77	1.78	21.53	0.45	103.09	N/D	2.84
Original Aqueous	**139.72**	**19.62**	**360.45**	**2.10**	**150.43**	**4.43**	**100.24**	**N/D**	**2300.60**
O/A	Organic Phase (ppm)								
	Al	**B**	**Ca**	**Ce**	**Eu**	**Gd**	**Mg**	**Tb**	**Y**
0.25	0	0	0	0.00	0.00	0.00	0	N/D	4709.87
0.5	0	0	0	2.36	1.18	0.27	0	N/D	3845.73
1	1.25	0.76	0	0.36	34.26	1.54	0	N/D	2247.75
1.5	0.86	0.48	0	0.40	39.37	1.50	0	N/D	1517.56
2.5	4.23	0.54	0	0.36	39.73	1.35	0	N/D	916.92
5	3.47	0.32	0	0.06	25.78	0.79	0	N/D	459.55

Table C.3.4: ICP results for solvent extraction tests performed at a pH of 0.5 and an extractant concentration of 1M

O/A	Aqueous Phase (ppm)								
	Al	**B**	**Ca**	**Ce**	**Eu**	**Gd**	**Mg**	**Tb**	**Y**
0.25	142.02	20.28	415.08	1.70	135.42	3.59	102.96	N/D	108.76
0.5	157.32	22.44	511.55	2.12	75.58	1.58	116.08	N/D	13.44
1	129.09	19.49	509.11	2.63	21.58	0.52	101.86	N/D	2.58
1.5	122.50	18.88	570.52	1.90	12.24	0.37	102.58	N/D	1.40
2.5	119.54	19.88	739.64	1.64	6.41	0.19	115.24	N/D	0.72
5	112.38	20.20	672.64	0.73	4.34	0.04	126.86	N/D	0.54
Original aqueous	**139.72**	**19.62**	**360.45**	**2.10**	**150.43**	**4.43**	**100.24**	**N/D**	**2300.60**
O/A	Organic Phase (ppm)								
	Al	**B**	**Ca**	**Ce**	**Eu**	**Gd**	**Mg**	**Tb**	**Y**
0.25	0.00	0.00	0	1.56	60.05	3.34	0	N/D	8767.37
0.5	0.00	0.00	0	0.00	149.70	5.68	0	N/D	4574.32
1	10.62	0.13	0	0.00	128.85	3.91	0	N/D	2298.02
1.5	11.48	0.49	0	0.13	92.13	2.70	0	N/D	1532.80
2.5	8.07	0.00	0	0.18	57.61	1.69	0	N/D	919.95
5	5.47	0.00	0	0.27	29.22	0.88	0	N/D	460.01

Table C.3.5: ICP results for solvent extraction tests performed at a pH of 1 and an extractant concentration of 0.5 M

O/A	Aqueous Phase (ppm)								
	Al	B	Ca	Ce	Eu	Gd	Mg	Tb	Y
0.25	133.99	18.42	375.28	N/D	138.58	N/D	95.81	N/D	578.36
0.5	113.87	13.59	366.16	N/D	56.11	N/D	90.26	N/D	14.75
1	-	-	-	-	-	-	-	-	-
1.5	117.39	14.26	476.91	N/D	24.36	N/D	97.04	N/D	3.27
2.5	111.11	13.77	533.50	N/D	10.22	N/D	94.91	N/D	1.16
5	101.98	13.75	530.53	N/D	4.52	N/D	101.08	N/D	0.50
Original Aq. 1	**132.0**	**15.37**	**366.28**	**N/D**	**94.77**	**N/D**	**109.05**	**N/D**	**1448.28**
Original Aq. 2	**133.03**	**19.39**	**341.11**	**N/D**	**142.48**	**N/D**	**97.22**	**N/D**	**2155.46**
O/A	Organic Phase (ppm)								
	Al	B	Ca	Ce	Eu	Gd	Mg	Tb	Y
0.25	0.00	3.88	0	N/D	15.62	N/D	5.65	N/D	6308.40
0.5	36.26	3.55	0	N/D	77.32	N/D	37.57	N/D	2867.06
1	-	-	0	-	-	-	-	-	-
1.5	9.74	0.74	0	N/D	46.94	N/D	8.00	N/D	963.34
2.5	8.36	0.64	0	N/D	33.82	N/D	5.65	N/D	578.85
5	6.00	0.32	0	N/D	18.05	N/D	1.59	N/D	289.56

121

Table C.3.6: ICP results for solvent extraction tests performed at a pH of 1 and an extractant concentration of 1 M

O/A	Aqueous Phase (ppm)								
	Al	B	Ca	Ce	Eu	Gd	Mg	Tb	Y
0.25	129.92	17.76	388.77	N/D	75.81	N/D	93.53	N/D	16.44
0.5	121.99	14.86	448.40	N/D	23.82	N/D	100.53	N/D	2.92
1	107.96	13.95	453.80	N/D	7.18	N/D	94.55	N/D	0.76
1.5	92.05	13.11	480.48	N/D	3.01	N/D	92.81	N/D	0.33
2.5	86.17	13.79	602.80	N/D	2.16	N/D	102.75	N/D	0.21
5	73.32	13.50	529.56	N/D	1.11	N/D	114.35	N/D	0.12
Original Aq. 1	**132.00**	**15.37**	**366.28**	**N/D**	**94.77**	**N/D**	**109.05**	**N/D**	**1448.28**
Original Aq. 2	**133.03**	**19.39**	**341.11**	**N/D**	**142.48**	**N/D**	**97.22**	**N/D**	**2155.46**
O/A	Organic Phase (ppm)								
	Al	B	Ca	Ce	Eu	Gd	Mg	Tb	Y
0.25	12.44	6.51	0	N/D	266.71	N/D	14.78	N/D	8556.08
0.5	20.02	1.03	0	N/D	141.90	N/D	17.02	N/D	2890.74
1	24.04	1.42	0	N/D	87.59	N/D	14.49	N/D	1447.52
1.5	26.63	1.51	0	N/D	61.17	N/D	10.82	N/D	965.31
2.5	18.33	0.63	0	N/D	37.04	N/D	2.52	N/D	579.23
5	11.74	0.38	0	N/D	18.73	N/D	0.00	N/D	289.63

C.4 Tb and Ce Solvent Extraction Tests

Table C.4.1: ICP results for solvent extraction tests performed at a pH of 0.25 and an extractant concentration of 0.5 M.

O/A	Aqueous Phase (ppm)					
	Al	**Ca**	**Y**	**Eu**	**Ce**	**Tb**
1	1255.7	9425.5	0	2.74	72.57	1.16
1.5	1209.2	9224.3	0	1.33	65.44	1.01
2	1216.0	8451.9	0	0.54	44.79	0.64
2.5	1064.2	8094.3	0	0.24	32.15	0.32
5	1042.0	6355.0	0	0.08	16.28	0.17
Original Aqueous	**1226.05**	**9505.69**	**126.79**	**41.98**	**205.20**	**203.72**
O/A	Organic Phase (ppm)					
	Al	**Ca**	**Y**	**Eu**	**Ce**	**Tb**
1	0	80.2	126.8	39.2	132.6	202.6
1.5	11.2	187.6	84.5	27.1	93.2	135.1
2	5.0	526.9	63.4	20.7	80.2	101.5
2.5	64.7	564.6	50.7	16.7	69.2	81.4
5	36.8	630.1	25.4	8.379	37.8	40.7

Table C.4.2: ICP results for solvent extraction tests performed at a pH of 0.25 and an extractant concentration of 1 M

O/A	Aqueous Phase (ppm)					
	Al	Ca	Y	Eu	Ce	Tb
1	1223.6	9194.8	0	0.408	54.081	0
1.5	1271.8	8900.0	0	0.334	47.306	1.171
2	1224.9	8198.6	0	0.061	35.409	1.422
2.5	1235.0	7962.9	0	0.057	27.742	0.914
5	1333.9	7014.9	0	0.048	10.721	0.457
Original aqueous	**1226.05**	**9505.69**	**126.79**	**41.98**	**205.20**	**203.72**
O/A	Organic Phase (ppm)					
	Al	Ca	Y	Eu	Ce	Tb
1	2.4	310.9	126.8	41.6	151.1	203.7
1.5	0.0	403.8	84.5	27.8	105.3	135.0
2	0.6	653.5	63.4	21.0	84.9	101.1
2.5	0.0	617.1	50.7	16.8	71.0	81.1
5	0.0	498.2	25.4	8.4	38.89	40.7

Table C.4.3: ICP results for solvent extraction tests performed at a pH of 0.5 and an extractant concentration of 0.5 M

O/A	Aqueous Phase (ppm)					
	Al	Ca	Y	Eu	Ce	Tb
1	1291.5	9710.6	0	0	48.4	0.346
1.5	1312.3	9315.8	0	0	42.0	0.753
2	1177.6	8463.7	0	0	34.8	0.921
2.5	1112.7	7621.4	0	0	16.0	1.820
5	1164.6	7152.1	0	0	5.4	1.846
Original aqueous	**1226.05**	**9505.69**	**126.79**	**41.98**	**205.20**	**203.72**
O/A	Organic Phase (ppm)					
	Al	Ca	Y	Eu	Ce	Tb
1	0	0	126.8	41.6	156.7	203.4
1.5	0.0	126.6	84.5	28.0	108.8	135.3
2	24.2	521.0	63.4	21.0	85.2	101.4
2.5	45.4	753.7	50.7	16.8	75.7	80.8
5	12.3	470.7	25.4	8.4	40.0	40.4

Table C.4.4: ICP results for solvent extraction tests performed at a pH of 0.5 and an extractant concentration of 1 M

O/A	Aqueous Phase (ppm)					
	Al	Ca	Y	Eu	Ce	Tb
1	1227.8	8224.7	0	0	11.67	1.58
1.5	1180.8	7104.2	0	0	8.96	1.32
2	1095.0	6346.5	0	0	8.19	1.95
2.5	1096.9	5397.8	0	0	5.71	0.65
5	1063.6	4104.4	0	0	4.18	1.00
Original aqueous	**1226.05**	**9505.7**	**126.79**	**41.98**	**205.20**	**203.72**
O/A	Organic Phase (ppm)					
	Al	Ca	Y	Eu	Ce	Tb
1	0	1281.0	126.8	42.0	193.5	202.1
1.5	30.2	1601.0	84.5	28.0	130.8	134.9
2	65.5	1579.6	63.4	21.0	98.5	100.9
2.5	51.7	1643.2	50.7	16.8	79.8	81.2
5	32.5	1080.2	25.4	8.4	40.2	40.5

Table C.4.5: ICP results for solvent extraction tests performed at a pH of 1 and an extractant concentration of 0.5 M

O/A	Aqueous Phase (ppm)					
	Al	Ca	Y	Eu	Ce	Tb
1	925.2	8700.54	0	0	5.56	0.55
1.5	983.4	6866.0	0	0	11.29	1.10
2	1002.5	7067.9	0	0	9.21	1.03
2.5	722.8	5948.3	0	0	8.09	0.91
5	502.2	3732.6	0	0	5.39	0.93
Original aqueous	**1226.05**	**9505.69**	**126.79**	**41.98**	**205.20**	**203.72**
O/A	Organic Phase (ppm)					
	Al	Ca	Y	Eu	Ce	Tb
1	300.8	805.1	126.8	41.98	199.6	203.2
1.5	161.7	1759.8	84.5	28.0	129.3	135.1
2	111.8	1218.9	63.4	21.0	98.0	101.3
2.5	201.3	1423.0	50.7	16.8	78.8	81.1
5	144.8	1154.6	25.4	8.4	40.0	40.6

Table C.4.6:ICP results for solvent extraction tests performed at a pH of 1 and an extractant concentration of 1 M

O/A	Aqueous Phase (ppm)					
	Al	Ca	Y	Eu	Ce	Tb
1	760.6	8131.9	0	0	3.62	0.99
1.5	876.0	6932.5	0	0	7.99	1.48
2	722.3	4334.7	0	0	6.90	1.40
2.5	545.6	4389.2	0	0	6.31	1.37
5	644.6	1321.9	0	0	2.93	0.86
Original Aqueous	**1226.05**	**9505.69**	**126.79**	**41.98**	**205.20**	**203.72**
O/A	Organic Phase (ppm)					
	Al	Ca	Y	Eu	Ce	Tb
1	465.4	1373.7	126.8	41.1	201.6	202.7
1.5	233.4	1715.4	84.5	27.8	131.5	134.8
2	251.9	2585.5	63.4	21.0	99.1	101.2
2.5	272.2	2046.6	50.7	16.8	79.6	80.9
5	116.3	1636.8	25.4	8.4	40.5	40.6

Table C.4.7: ICP results for solvent extraction tests performed at a pH of 1.5 and an extractant concentration of 0.5 M

O/A	Aqueous Phase (ppm)					
	Al	Ca	Y	Eu	Ce	Tb
1	420.7	8131.94	0	0.63	0	0.94
1.5	301.4	6932.52	0	0.14	0	0.71
2	316.8	4334.70	0	0.06	0	1.30
2.5	409.9	4389.23	0	0	0	0
5	158.1	1321.93	0	0	0	0
Original aqueous	**1226.05**	**9505.92**	**126.79**	**41.98**	**205.20**	**203.72**
O/A	Organic Phase (ppm)					
	Al	Ca	Y	Eu	Ce	Tb
1	805.4	1374.0	126.8	41.3	205.2	202.8
1.5	616.4	1715.6	84.5	27.9	136.8	135.3
2	454.6	2585.6	63.4	21.0	102.6	101.2
2.5	326.5	2046.7	50.7	16.8	82.1	81.5
5	213.6	1636.8	25.4	8.4	41.0	40.7

Table C.4.8: ICP results for solvent extraction tests performed at a pH of 1.5 and an extractant concentration of 1 M

O/A	Aqueous Phase (ppm)					
	Al	Ca	Y	Eu	Ce	Tb
1	367.5	5344.2	0	0	0	1.0
1.5	352.5	2648.4	0	0	0	0.4
2	107.0	1179.0	0	0	0	2.1
2.5	94.9	569.9	0	0	0	1.5
5	24.6	98.9	0	0	0	1.0
Original aqueous	**1226.05**	**9505.92**	**126.79**	**41.98**	**205.20**	**203.72**
O/A	Organic Phase (ppm)					
	Al	Ca	Y	Eu	Ce	Tb
1	858.5	4161.7	126.8	42.0	205.2	202.7
1.5	873.6	6857.5	84.5	28.0	136.8	135.5
2	1119.0	8326.9	63.4	21.0	102.6	100.8
2.5	1131.2	8936.0	50.7	16.8	82.1	80.9
5	1201.5	9407.0	25.4	8.4	41.04	40.6

Table C.4.9: ICP results for solvent extraction tests performed at a pH of 2 and an extractant concentration of 0.5 M

O/A	Aqueous Phase (ppm)					
	Al	Ca	Y	Eu	Ce	Tb
1	261.6	8092.5	0	0	0.0	0
1.5	465.3	6472.6	0	0	0	2.0
2	68.3	4348.6	0	0	0	1.5
2.5	51.0	3231.1	0	0	0	1.1
5	4.2	211.2	0	0	0	2.2
Original Aqueous	**1226.05**	**9505.92**	**126.79**	**41.98**	**0**	**203.72**

O/A	Organic Phase (ppm)					
	Al	Ca	Y	Eu	Ce	Tb
1	964.5	1413.4	126.8	42.0	205.2	203.7
1.5	507.2	2022.2	84.5	28.0	136.8	134.4
2	578.9	2578.7	63.4	21.0	102.6	101.1
2.5	470.0	2509.9	50.7	16.8	82.1	81.1
5	244.4	1858.9	25.4	8.4	41.0	40.3

131

Table C.4.10: ICP results for solvent extraction tests performed at a pH of 2 and an extractant concentration of 1 M

O/A	Aqueous Phase (ppm)					
	Al	Ca	Y	Eu	Ce	Tb
1	175.9	4970.1	0	0	0	1.4
1.5	38.6	1678.5	0	0	0	0.8
2	8.3	356.5	0	0	0	0.8
2.5	1.9	75.1	0	0	0	0.8
5	4.1	6.4	0	0	0	2.3
Original Aqueous	**1226.049**	**9505.919**	**126.8**	**42.0**	**205.2**	**203.7**
O/A	Organic Phase (ppm)					
	Al	Ca	Y	Eu	Ce	Tb
1	1050.2	4535.9	126.8	41.9	205.2	202.3
1.5	1187.5	5218.3	84.5	28.0	136.8	135.3
2	1217.7	4574.7	63.4	21.0	102.6	101.5
2.5	1224.1	3772.3	50.7	16.8	82.1	81.2
5	1222.0	1899.9	25.4	8.4	41.0	40.3

Table C.4.11: Separation factors of Tb and Ce relative to other elements at an extractant concentration of 1 M

| pH	O/A	Tb/Ce	Tb/Al	Ce/Al	Tb/Ca	Ce/Ca	Tb/Y. Ce/Y	Tb/Eu	Ce/Eu
0.25	1	-	-	-	-	82.6	-	-	0.03
	1.5	51.8	-	-	2541.2	49.0	-	1.4	0.03
	2	29.7	-	-	892.4	30.1	-	0.2	0.01
	2.5	34.7	-	-	1144.7	33.0	-	0.3	0.01
	5	24.5	-	-	1253.2	51.1	-	0.5	0.02
0.5	1	6.7	-	-	819.9	121.9	-	-	-
	1.5	7.0	3991.4	571.0	452.7	64.8	-	-	-
	2	4.3	863.0	201.1	207.5	48.3	-	-	-
	2.5	9.0	2666.9	296.6	412.7	45.9	-	-	-
	5	4.2	1325.2	314.4	153.9	36.5	-	-	-
1	1	3.7	333.3	91.0	354.2	96.7	-	-	-
	1.5	5.5	342.0	61.7	143.1	25.8	-	-	-
	2	5.0	207.2	41.2	74.2	14.8	-	-	-
	2.5	4.7	118.8	25.3	42.1	9.0	-	-	-
	5	3.4	260.4	76.4	20.6	6.0	-	-	-
1.5	1	-	88.1	-	264.3	-	-	-	-
	1.5	-	126.6	-	121.2	-	-	-	-
	2	-	4.6	-	6.8	-	-	-	-
	2.5	-	4.6	-	3.5	-	-	-	-
	5	-	0.9	-	0.4	-	-	-	-
2	1	-	23.7	-	155.4	-	-	-	-
	1.5	-	5.4	-	52.9	-	-	-	-
	2	-	0.9	-	10.0	-	-	-	-
	2.5	-	0.2	-	2.1	-	-	-	-
	5	-	0.1	-	0.1	-	-	-	-

133
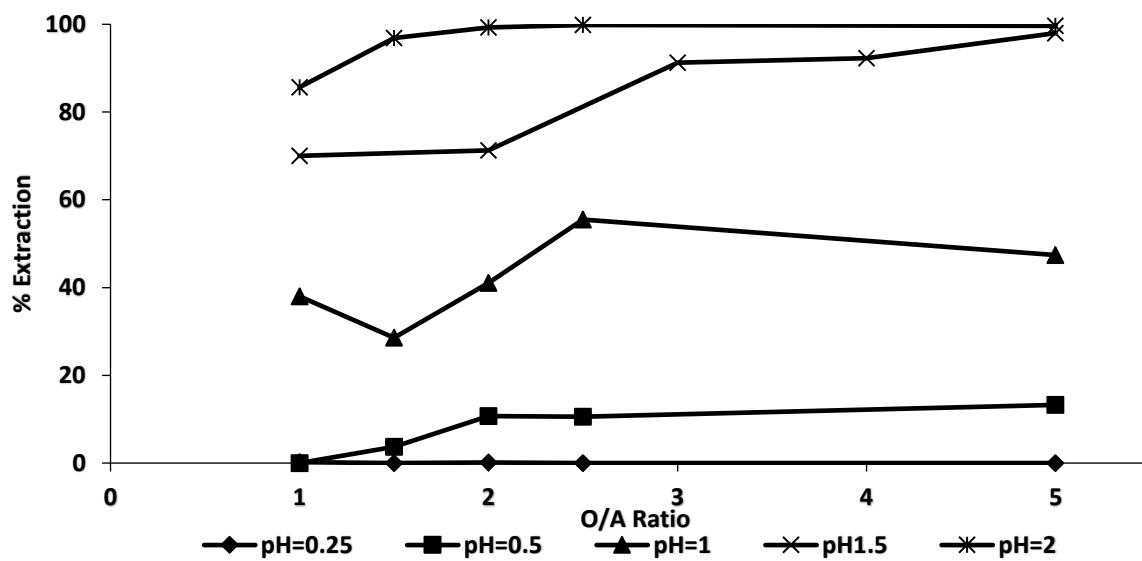
Figure C.4.1: Percentage extraction of Al at an extractant concentration of 1 M

Appendix D: Thermodynamic Properties of Rare Earths Leaching with H_2SO_4

Table D.1: Thermodynamic properties for leaching of yttrium with H_2SO_4

T [°C]	ΔH [kJ]	ΔS [J/K]	ΔG [kJ]	k
0	-381.706	-388.233	-275.642	5.23E+052
10	-382.501	-391.037	-271.751	1.37E+050
20	-382.627	-391.581	-267.86	5.37E+047
30	-382.459	-391.037	-263.927	3.03E+045
40	-382.208	-390.116	-260.036	2.38E+043
50	-381.916	-389.238	-256.144	2.54E+041
60	-381.664	-388.484	-252.253	3.57E+039
70	-381.497	-387.94	-248.362	6.44E+037
80	-381.413	-387.773	-244.471	1.46E+036
90	-381.497	-387.982	-240.622	4.08E+034
100	-381.79	-388.735	-236.731	1.38E+033

Table D.2: Thermodynamic properties for leaching of europium with H_2SO_4

T [°C]	ΔH [kJ]	ΔS [J/K]	ΔG [kJ]	k
0	-398.317	-345.18	-304.051	1.40E+058
10	-402.124	-358.82	-300.537	2.77E+055
20	-404.76	-368.025	-296.897	8.01E+052
30	-406.81	-374.845	-293.173	3.30E+050
40	-408.526	-380.409	-289.407	1.88E+048
50	-410.074	-385.346	-285.558	1.45E+046
60	-411.58	-389.949	-281.667	1.47E+044
70	-413.086	-394.342	-277.776	1.93E+042
80	-414.634	-398.735	-273.801	3.17E+040
90	-416.266	-403.296	-269.784	6.43E+038
100	-418.023	-408.107	-265.726	1.59E+037

Table D.3: Thermodynamic properties for leaching of cerium with HCl

T [°C]	ΔH [kJ]	ΔS [J/K]	ΔG [kJ]	k
0	-59.3291	-347.983	35.73136	1.48E-007
10	-58.7015	-345.64	39.20408	5.90E-008
20	-57.8647	-342.711	42.63496	2.53E-008
30	-56.9442	-339.699	46.024	1.17E-008
40	-56.0656	-336.854	49.41304	5.69E-009
50	-55.2706	-334.302	52.76024	2.94E-009
60	-54.5175	-332.042	56.10744	1.59E-009
70	-53.8481	-330.118	59.4128	9.00E-010
80	-53.346	-328.611	62.71816	5.29E-010
90	-52.9276	-327.482	65.98168	3.21E-010
100	-52.6766	-326.812	69.2452	2.01E-010

Table D.4: Thermodynamic properties for leaching of terbium with HCl

T [°C]	ΔH [kJ]	ΔS [J/K]	ΔG [kJ]	k
0	-401.873	-439.697	-281.792	7.74E+053
10	-387.899	-388.275	-277.943	1.91E+051
20	-390.744	-398.149	-274.01	6.78E+048
30	-392.919	-405.43	-269.994	3.37E+046
40	-394.76	-411.413	-265.935	2.29E+044
50	-396.476	-416.768	-261.793	2.08E+042
60	-398.066	-421.705	-257.609	2.46E+040
70	-399.698	-426.433	-253.341	3.70E+038
80	-401.329	-431.203	-249.074	6.95E+036
90	-403.087	-436.098	-244.722	1.60E+035
100	-404.969	-441.245	-240.329	4.43E+033

Appendix E: Repeatability Data

Table E.1: Y leaching repeatability tests results

Time (min)	Y (%)				Std Dev
	Test 1	Test 2	Test 3	Average	
15	78.3	79.50	83.2	81.4	2.574
30	97.1	92.92	96.6	94.7	2.271
45	98.2	98.31	97.9	98.1	0.240
60	90.2	85.92	89.7	87.8	2.334
120	86.3	86.09	88.6	87.4	1.392
240	89.4	93.42	82.7	88.0	5.442
360	94.5	94.79	94.7	94.8	0.169

Table E.2: Eu leaching repeatability tests results

Time (min)	Eu (%)				Std Dev
	Test 1	Test 2	Test 3	Average	
15	71.0	68.39	76.8	72.6	4.33
30	88.6	85.34	88.5	86.9	2.22
45	91.4	88.10	90.1	89.1	1.42
60	83.5	80.71	82.5	81.6	1.29
120	80.2	77.24	81.8	79.5	3.23
240	84.0	87.62	77.3	82.5	5.25
360	88.0	85.17	87.5	86.3	1.65

Table E.3: Ce leaching repeatability tests results

Time (min)	Ce (%)				Std Dev
	Test 1	Test 2	Test 3	Average %	
15	93.9	95.575	97.55	95.69	1.80
30	96.3	96.158	98.12	96.87	1.09
45	96.353	90.945	92.32	93.21	2.81
60	93.077	93.288	96.96	94.44	2.18
90	92.677	95.450	96.60	94.91	2.01
120	93.024	90.429	94.67	92.71	2.14

Table E.4: Tb leaching repeatability tests results

Time (min)	Tb (%)				Std Dev
	Test 1	Test 2	Test 3	Average	
0	0	0	0	0	0
15	99.94	98.59	95.63	98.1	2.21
30	99.66	98.61	96.69	98.3	1.51
45	97.86	97.12	96.98	97.3	0.469
60	95.12	94.37	98.58	96.0	2.25
90	93.22	97.64	98.85	96.6	2.96
120	93.97	97.11	96.59	95.9	1.69

Table E.5: Ce leaching results for the ANOVA analysis

SUMMARY

Groups	Count	Sum	Average	Variance
1.0	3	148.2	49.4	3.2
1.5	3	117.8	39.3	22.8
2.0	3	88.9	29.6	29.9
2.5	3	51.1	17.0	41.1
5	3	10.8	3.6	2.5

ANOVA

Source of Variation	SS	df	MS	F	P-value	F crit
Between Groups	3909.35	4	977.3375	49.12693	1.53E-06	3.47805
Within Groups	198.9413	10	19.89413			
Total	4108.291	14				

Table E.6: Tb leaching for the ANOVA analysis

SUMMARY

Groups	Count	Sum	Average	Variance
1.0	3	1.447318	0.482439	0.022575
1.5	3	2.160909	0.720303	0.007677
2.0	3	3.233383	1.077794	0.026514
2.5	3	5.318264	1.772755	0.030664
5	3	5.635056	1.878352	0.000995

ANOVA

Source of Variation	SS	df	MS	F	P-value	F crit
Between Groups	4.641634	4	1.160409	65.6155	3.87E-07	3.47805
Within Groups	0.17685	10	0.017685			
Total	4.818484	14				

Appendix F: Statistical Analysis

Table F.1: ANOVA table for a 3^2 full factorial design for Y leaching

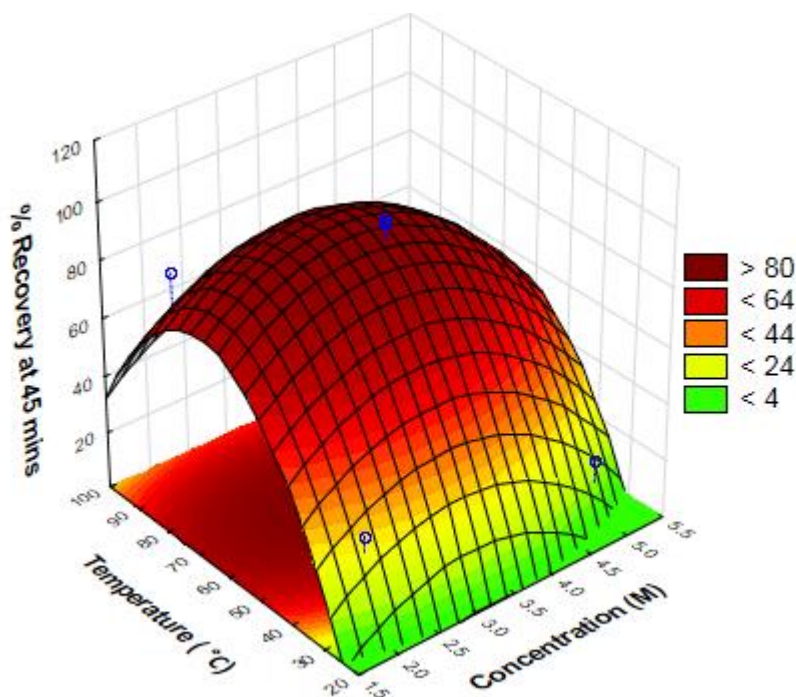|	Factor	SS	df	MS	F	p
	(1)Concentration (L)	405.082	1	405.082	3.05145	0.131263
	Concentration(Q)	718.320	1	718.320	5.41106	0.047654
r^2=0.911	Temperature (L)	2181.227	1	2181.227	16.43104	0.006699
Adjusted r^2 = 0.861	Temperature (Q)	3863.344	1	3863.344	29.10233	0.001672
	1L by 2L	78.322	1	78.322	0.59000	0.471559
	Error	796.502	6	132.750		
	Total SS	9864.907	11			

Figure F.1: Surface plot for Y leaching after 45 minutes

Table F.2: ANOVA table for a 3^2 full factorial design for Tb leaching

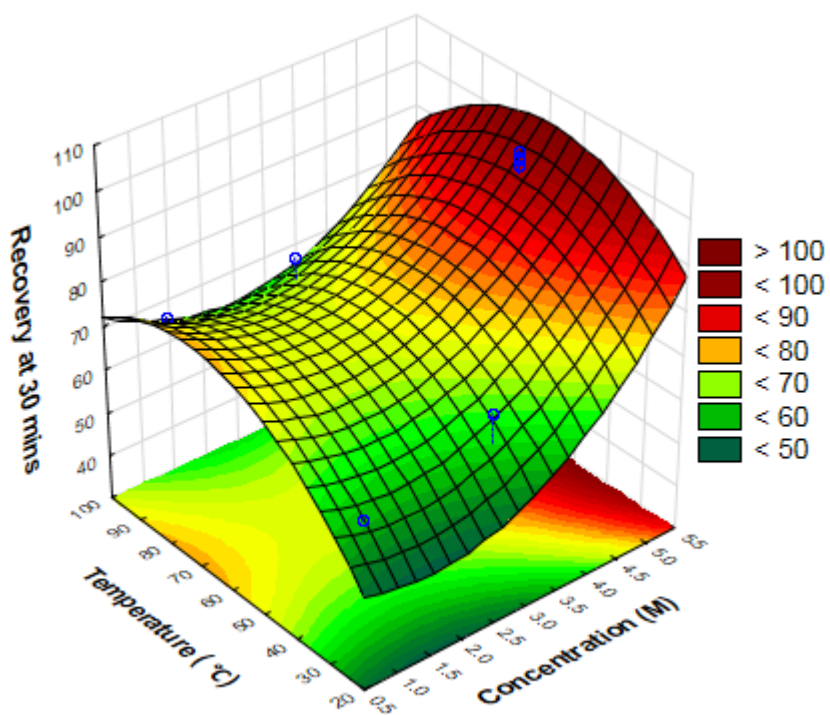|	Factor	SS	df	MS	F	p
	(1)Concentration (L)	754.370	1	745.3699	12.86936	0.011540
	Concentration(Q)	208.244	1	208.2441	3.59549	0.106734
r^2 = 0.84864	Temperature (L)	78.428	1	78.4817	1.35504	0.288588
Adjusted r^2 = 0.7225	Temperature (Q)	226.198	1	226.1976	3.90547	0.095522
	1L by 2L	45.563	1	45.5625	0.78667	0.409250
	Error	347.509	6	57.9182		
	Total SS	2295.852	11			

140

Figure F.2: Surface plot for Tb leaching after 30 min